

SANDIA REPORT

SAND2012-4483
Unlimited Release
Printed June 2012

Development and Testing of a Photometric Method to Identify Non-Operating Solar Hot Water Systems in Field Settings

Jeff Carlson, Hongbo He, Andrea Mammoli, David Menicucci, and Peter Vorobief

Prepared by
Sandia National Laboratories
Albuquerque, New Mexico 87185 and Livermore, California 94550

Sandia National Laboratories is a multi-program laboratory managed and operated by Sandia Corporation, a wholly owned subsidiary of Lockheed Martin Corporation, for the U.S. Department of Energy's National Nuclear Security Administration under contract DE-AC04-94AL85000.

Approved for public release; further dissemination unlimited.



Sandia National Laboratories

Issued by Sandia National Laboratories, operated for the United States Department of Energy by Sandia Corporation.

NOTICE: This report was prepared as an account of work sponsored by an agency of the United States Government. Neither the United States Government, nor any agency thereof, nor any of their employees, nor any of their contractors, subcontractors, or their employees, make any warranty, express or implied, or assume any legal liability or responsibility for the accuracy, completeness, or usefulness of any information, apparatus, product, or process disclosed, or represent that its use would not infringe privately owned rights. Reference herein to any specific commercial product, process, or service by trade name, trademark, manufacturer, or otherwise, does not necessarily constitute or imply its endorsement, recommendation, or favoring by the United States Government, any agency thereof, or any of their contractors or subcontractors. The views and opinions expressed herein do not necessarily state or reflect those of the United States Government, any agency thereof, or any of their contractors.

Printed in the United States of America. This report has been reproduced directly from the best available copy.

Available to DOE and DOE contractors from
U.S. Department of Energy
Office of Scientific and Technical Information
P.O. Box 62
Oak Ridge, TN 37831

Telephone: (865) 576-8401
Facsimile: (865) 576-5728
E-Mail: reports@adonis.osti.gov
Online ordering: <http://www.osti.gov/bridge>

Available to the public from
U.S. Department of Commerce
National Technical Information Service
5285 Port Royal Rd.
Springfield, VA 22161

Telephone: (800) 553-6847
Facsimile: (703) 605-6900
E-Mail: orders@ntis.fedworld.gov
Online order: <http://www.ntis.gov/help/ordermethods.asp?loc=74-0#online>



Development and Testing of a Photometric Method to Identify Non-Operating Solar Hot Water Systems in Field Settings

Jeff Carlson
Energy Surety Engineering and Analysis
Sandia National Laboratories
P.O. Box 5800
Albuquerque, New Mexico 87185-1108

Hongbo He, Andrea Mammoli, David Menicucci, and Peter Vorobief
University of New Mexico
Albuquerque, NM 87131

Abstract

This report presents the results of experimental tests of a concept for using infrared (IR) photos to identify non-operational systems based on their glazing temperatures; operating systems have lower glazing temperatures than those in stagnation. In recent years thousands of new solar hot water (SHW) systems have been installed in some utility districts. As these numbers increase, concern is growing about the systems' dependability because installation rebates are often based on the assumption that all of the SHW systems will perform flawlessly for a 20-year period. If SHW systems routinely fail prematurely, then the utilities will have overpaid for grid-energy reduction performance that is unrealized. Moreover, utilities are responsible for replacing energy for loads that failed SHW system were supplying. Thus, utilities are seeking data to quantify the reliability of SHW systems. The work described herein is intended to help meet this need. The details of the experiment are presented, including a description of the SHW collectors that were examined, the testbed that was used to control the system and record data, the IR camera that was employed, and the conditions in which testing was completed. The details of the associated analysis are presented, including direct examination of the video records of operational and stagnant collectors, as well as the development of a model to predict glazing temperatures and an analysis of temporal intermittency of the images, both of which are critical to properly adjusting the IR camera for optimal performance. Many IR images and a video are presented to show the contrast between operating and stagnant collectors. The major conclusion is that the technique has potential to be applied by using an aircraft fitted with an IR camera that can fly over an area with installed SHW systems, thus recording the images. Subsequent analysis of the images can determine the operational condition of the fielded collectors. Specific recommendations are presented relative to the application of the technique, including ways to mitigate and manage potential sources of error.

CONTENTS

SECTION 1. INTRODUCTION	11
SECTION 2. HARDWARE CONFIGURATION FOR THE EXPERIMENT	13
SECTION 3. EXPERIMENTAL DESIGN	17
Approach.....	17
Technical Issues	18
SECTION 4. DESCRIPTION OF EXPERIMENTAL TESTS	21
SECTION 5. EXPERIMENTAL RESULTS.....	23
Initial Tests and Adjustments	23
Directional Emissivity	26
Video Optimization Process	29
Significant Results	31
SECTION 6. ANALYSIS OF TEMPORAL INTERMITTENCY AND IMAGE RESOLUTION	35
Temporal Intermittency	35
Image Resolution	36
SECTION 7. DEVELOPMENT AND TESTING OF THE GLAZING MODEL.....	39
Background Information.....	39
Test Results With an Unglazed Polymer Collector	40
Test Results With the Painted Fin Single-Glazed Collector.....	45
Test Results With the Chrome Double- and Single-Glazed Collectors.....	50
Sensitivity Analysis	58
Summary of the Glazing Model Development Work.....	60
SECTION 8. CONCLUSIONS AND RECOMMENDATIONS	61
APPENDIX A. Matlab Code	65
APPENDIX B. Single-Glaze Collector TYPE 244–Fortran Code	69
APPENDIX C. Double-Glaze Collector TYPE 242–Fortran Code.....	89

FIGURES

Figure 1. Telescoping mast.....	13
Figure 2. Roofing surfaces next to collectors.	14
Figure 3. Mast and collectors.....	14
Figure 4. Test bed and controls.....	14
Figure 5. Photon 320 camera.	15
Figure 6. Spectral response of the Photon 320 camera.....	16
Figure 7. Experimental test matrixes.	19
Figure 8. Matrixes showing tests that were actually applied.	21
Figure 9. Photos showing collectors in near-field and far-field positions — AGC on.....	23
Figure 10. Thermal emissivity of glazed collectors showing angular dependence.	25
Figure 11. Directional emissivity of a dielectric material predicted by electromagnetic theory.	26
Figure 12. Directional emissivity values for the four collectors.....	28
Figure 13. Thermal emissivity of collectors under stagnation and flowing conditions.....	29
Figure 14. Data used to optimize contrast and brightness settings.....	30
Figure 15. Results of the experiments corresponding to Figure 14.	32
Figure 16. Representative image from sequence of analysis of temporal intermittency.....	35
Figure 17. Complementary plots, temporal intermittency.	36
Figure 18. Visual effect of manually simulating the loss of resolution in an image by downsampling.....	37
Figure 19. Results of downsizing shown graphically.....	38
Figure 20. Unglazed collector plate temperature.....	43
Figure 21. Water tank top temperature.....	43
Figure 22. Water tank node 6 temperature.....	44
Figure 23. Useful energy gain by the solar collector.....	44
Figure 24. Thermal network for a single-glazed collector.....	46
Figure 25. Paint single-glazed collector plate temperature.....	48
Figure 26. Paint single-glazed glazing temperature.....	48
Figure 27. Water tank top temperature.....	49
Figure 28. Water tank node 6 temperature.....	49
Figure 29. Useful energy gain by the collector.....	49
Figure 30. Thermal network for a double-glazed collector.....	51
Figure 31. Chrome double-glazed plate temperature.....	54
Figure 32. Chrome single-glazed plate temperature.....	54
Figure 33. Glazing temperature comparison of the chrome double-glazed collector.....	55
Figure 34. Glazing temperature of the chrome single-glazed collector.....	55
Figure 35. Water tank top temperature.....	57
Figure 36. Water tank node 6 temperature.....	57
Figure 37. Water tank node 8 temperature.....	57
Figure 38. Useful energy gain by the collectors.....	58
Figure 39. Sensitivity analysis for the collector plate temperature.....	59
Figure 40. Sensitivity analysis for the collector glazing temperature.....	59
Figure 41. Sensitivity analysis for the useful energy gain.....	60

TABLES

Table 1. Temperature Data From Collector Surfaces Using an IR Thermometer.	27
Table 2. Unglazed Collector TYPE 559 User-Supplied Input Parameters.	40
Table 3. TRNSYS Model Water Tank TYPE 534 Parameters.	41
Table 4. TRNSYS Solar Loop Pump Parameters.	42
Table 5. TRNSYS Water Draw Profile Used in the Simulations.	42
Table 6. Paint Single-Glazed Collector TYPE 244 User-Supplied Input Parameters.	47
Table 7. Chrome Double-Glazed Collector TYPE 242 User-Supplied Input Parameters.	52
Table 8. Chrome Single-Glazed Collector TYPE 244 User-Supplied Input Parameters.	53
Table 9. Water Tank TYPE 1237 Parameters.	56

ACRONYMS

AGC	Automatic Gain Control
IR	infrared
LWIR	Long-Wave Infrared
NREL	National Renewable Energy Laboratory
NSRDB	National Solar Radiation Data Base
SHW	solar hot water
SNL	Sandia National Laboratories
TESS	TRNSYS Thermal Energy System Specialists
TMY	Typical Meteorological Year
TRNSYS	Transient System Simulation Program
UNM	University of New Mexico

SECTION 1. INTRODUCTION

In recent years utility rebate programs have greatly piqued consumer interest in solar hot water (SHW) systems. Thousands of new systems have been installed in some utility districts, and as these numbers increase concern is growing about the systems' dependability. Planners in both electric and gas utilities are concerned because if SHW systems fail in the field, the applicable utility must supply customer loads. Moreover, often installation rebates are based on the assumption that all of the SHW systems will perform flawlessly for a 20-year period. If systems routinely fail prematurely, then the utilities will have overpaid for grid-energy reduction performance that is unrealized.

Sandia National Laboratories (SNL) has addressed this SHW reliability issue. Two studies have been conducted over the past two years to quantify SHW reliability. The most recent research effort found that insufficient data exist to properly characterize the reliability of fielded systems.¹

The SNL report documents a number of recommendations for generating reliability data and information. One idea is to use infrared (IR) aerial photography to identify collectors that are non-operational and exhibiting hotter glazing temperature than ones that are being cooled with liquids flowing through their collector tubes. Quoting from the SNL report:

“Infrared photos of homes with solar collectors may be a significant source of reliability information that can help to define failure rates of SHW systems. These efforts should be planned and executed in cooperation of utilities who are involved with SHW installations and who hold critical information—such as SHW system installation dates and locations. These data are keys to the success of these collection methodologies because they provide a time to failure, an essential element in estimating failure rates for the life periods beyond startup.”

The concept of using IR photos to identify non-operational systems has some appeal to various parties. First, the utilities could direct these photographs to be taken of areas where many SHW systems have been installed. Thousands of installations could be assessed in a single aerial flyover event, generating much data without intrusive and extremely expensive field surveys. Second, once non-operating systems are identified, they could be traced back to their dates of installation based on a record of rebates. Thus, a meaningful reliability database could be developed that could lead to the computation of statistics that the utilities are seeking. Such statistical measures include the mean time to failure, a key engineering reliability metric. Third, the database could be useful to the SHW industry to improve products.

SNL has teamed with the University of New Mexico (UNM) to assess the effectiveness and applicability of this idea. An experiment has been designed to test whether differences in SHW collector glazing temperatures can be discerned by IR camera imaging. In addition, an analytical model was developed for the Transient System Simulation Program (TRNSYS) that can be used to predict the expected glazing temperature as a function of ambient conditions. The expected glazing temperature range is needed to properly configure the operational parameters of the IR camera before aerial photographing of an area containing SHW systems.

¹ D. Menicucci, *Report on the Analysis of Field Data Relating to the Reliability of Solar Hot Water Systems*, SAND2011-4759. Sandia National Laboratories, Albuquerque, NM, July 2011.

The experiment is limited only to understanding whether the basic photometric concept is sound and does not address detailed application issues, which will follow later if the experiment shows that the photometric process has reasonable potential and if resources and interest are available and sufficient.

This report documents the results of this photometric experiment and is arranged in the following sections as numbered below:

1. A description of the hardware configuration that was used.
2. A discussion of the experimental design.
3. A description of the experiments that were conducted.
4. A description of results of the experiments including the data that were gathered, observations, and some web links to actual videos taken during experimentation.
5. A presentation of detailed analysis of the temporal intermittency of the images and image resolution.
6. The results of the glazing model development.
7. The conclusions and recommendations for this work, including possible applications.

Appendix A contains Matlab code and Appendices B and C contain the working version of the glazing model Fortran codes used in this effort. (This code is not applicable for commercialization at this time.)

SECTION 2. HARDWARE CONFIGURATION FOR THE EXPERIMENT

The experimental effort was conducted on the SHW Reliability Test Bed located in the mechanical engineering building at UNM. The creation of the test bed was co-funded by SNL and UNM and consists of a highly instrumented SHW system with four different SHW collectors representing the most popular ones that are on the market. The collectors included the following collectors:

1. A Lennox LSC-18 with a steel fin collector, copper riser tubes coated with black chrome selective coating and double glazing on the front surface.
2. A Lennox LSC-18 with a steel fin collector, copper riser tubes coated with black chrome selective coating and single glazing on the front surface.
3. A Fafco Sun Saver unglazed polymer collector, nominally 39 square feet of aperture area.
4. A Sun Earth SB-32 single-glazed collector panel with a copper fin collector and coated with a nonselective paint.

The test bed is arranged to be able to operate with any single collector or groups of collectors as its solar heat source.

The test configuration included an IR camera that is mounted on a telescoping mast (Figure 1). The mast's height is adjustable up to 5.3 meters, as is its location relative to the collectors. The mast can be located directly above the collectors, which is referred to as the near-field location, or 16.3 meters to the south and east of them, which is referred to as the far-field location.

Additionally, two types of roofing surfaces were included on a platform next to the collectors (Figure 2). These surfaces included concrete barrel tiles and standard 90-lb three-tab roofing shingles. These represent the most common roofing systems upon which collectors are likely to be mounted and they served as a temperature reference during the testing.

Figure 2 shows from right to left the pseudo roof surfaces, the glazed painted fin collector, the unglazed collector, the single-glazed selective surface (black chrome) collector, and the double-glazed selective surface collector. Figure 1 shows the mast/camera positioned in the near-field location with the collectors below it.



Figure 1. Telescoping mast.



Figure 2. Roofing surfaces next to collectors.

Figure 3 shows the mast/camera in the far-field location with the collectors pertinent to this project visible in the background, as annotated in the picture.

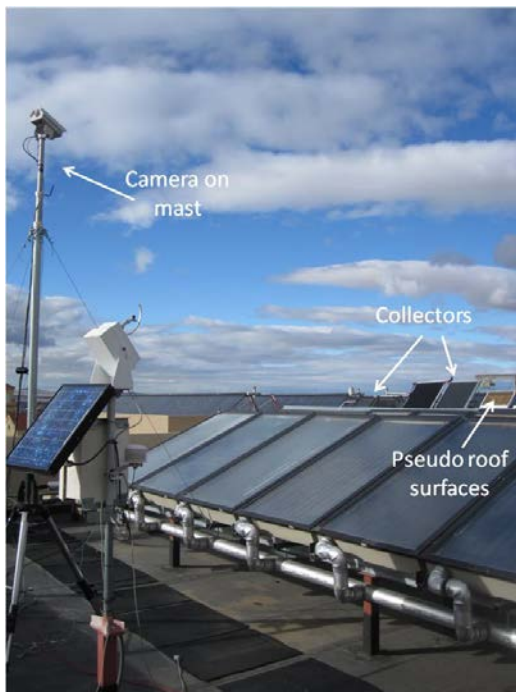


Figure 3. Mast and collectors.

The selective surface collectors are high-performance ones that are relatively expensive and not commonly in use today. The other collectors are relatively low cost and constitute the vast majority of collectors currently in use today.

Software and algorithms were developed to collect, process, and log thermal images over the duration of each experiment. In addition, the test bed's data collection system includes numerous thermocouples that sense temperatures of various components, such as the glazing and collector-fin temperatures of all the collectors and the fluid temperatures inside the piping and storage tanks. Other sensors are used to record solar-loop line-temperatures, flow rates, and ambient temperature conditions both inside the lab where the tanks, pumps, and controls are located, as well as the conditions near the collectors.

The information from the IR camera is recorded by a separate computer that was supplied by SNL.

Figure 4 is a picture of the test bed and controls.



Figure 4. Test bed and controls.

The camera used for the experiments was the small, lightweight, Photon 320 from FLIR (Figure 5, courtesy of the manufacturer's website). It is a commercially developed, military qualified, 320×240 , long-wave (7 to 13 micron) infrared (LWIR) thermal imager. The experimental hypothesis was that solar-thermal collectors emit measurable amounts of energy in this band. The Photon 320 achieves superior LWIR image quality using an uncooled, 320×240 , vanadium-oxide micro-bolometer array that operates over a temperature range of -40 to 80 °C. For this experiment, the camera was used with a fixed 14.25mm lens that provided a 46-degree horizontal field of view and a 36-degree vertical field of view. The Photon 320 acquires images at 30 frames per second and camera settings (including Automatic Gain Control [AGC] modes) can be controlled and set through a standard RS-232 serial communication interface. The vanadium-oxide micro-bolometer array has a broad spectral response. A short-wave blocking filter incorporated within the lens blocks wavelengths less than 7.0 microns. Figure 6 illustrates the spectral response of the Photon 320 camera.

The camera was mounted within a standard security camera enclosure with the glass faceplate removed to enable imaging of thermal wavelengths (glass effectively blocks thermal wavelengths in the 7 to 13 micron range). The camera and enclosure were mounted on a telescoping mast that was designed to meet the requirements of the experiments.



Figure 5. Photon 320 camera.

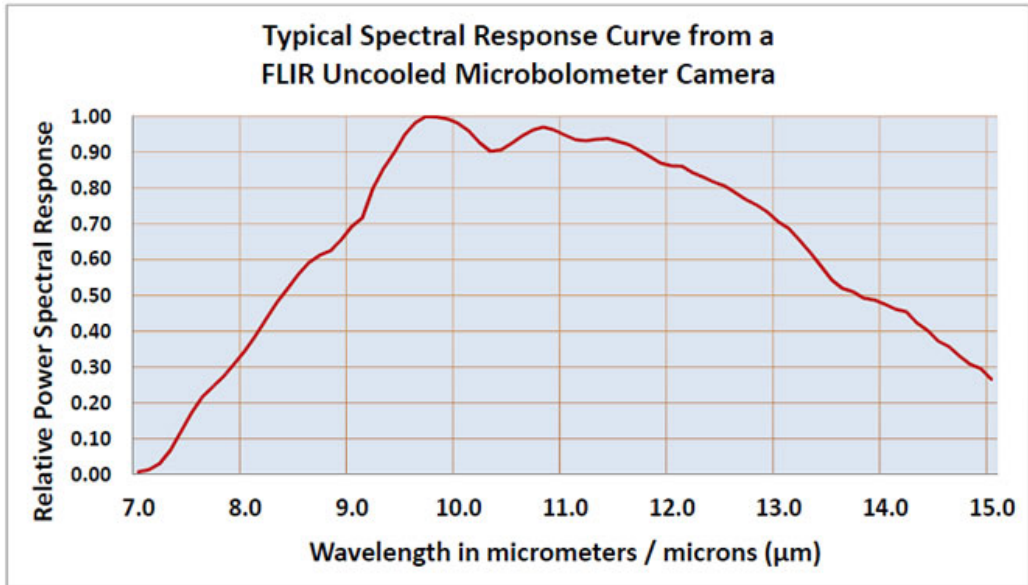


Figure 6. Spectral response of the Photon 320 camera.

SECTION 3. EXPERIMENTAL DESIGN

Approach

The purpose of this project was to assess the capability of using long-wave (7 to 13 micron) thermal imagers (cameras) to distinguish between functional and non-functional, roof-top-mounted, solar-thermal collectors. The intent is to establish the viability of using these cameras onboard low-flying aircraft to both quickly and cost-effectively provide an estimate of the failure rates of solar-thermal systems that are currently in use.

Since the unglazed and painted fin collectors are relatively low cost and are most commonly applied in the area of first application of this photometric technique (Arizona), they were the focus of the experimental efforts.

Experiments were designed and conducted to assess the capability of using a thermal camera, under different environmental conditions, to distinguish between functional and non-functional collector systems.

The underlying experimental design is quite simple. Each solar system would be run in two modes of operation (functional and non-functional) and images of the collectors would be captured in each mode. The images would be analyzed to assess the ability to distinguish between functional and non-functional modes of operation and also to assess ease of interpretation.

In the functional mode, the collectors would be run near thermal steady-state conditions with glycol flowing through the collectors. In this state the collector is relatively cool. In the non-functional mode, the collectors are set in stagnation with no glycol flowing through the collectors. In this state the collector is relatively hot.

The hypothesis, backed by both physical laws and empirical evidence, is that functional collectors will appear in the images as being cooler (darker) than non-functional collectors when viewed with a thermal camera. In the intended application, using a thermal camera onboard a low-flying aircraft, flyovers and data collections would be conducted in the morning after the sun has risen to an altitude that allows sufficient heating of the collectors. The morning is also assumed to be the time when the collectors are most likely to be operating to replace heat in the storage tank that had been lost overnight and during the morning hot-water draws. A stagnant collector observed at this time would be assumed to be non-functional, although there could still be false positives.

No data currently exist to determine the significance of the issue of false positives. An initial application of this technique with appropriate ground truth verification of the findings will produce data that can be used to estimate the statistical significance of this potential error.

Technical Issues

There are several technical issues that were considered and addressed including choice of camera, optimal camera settings, best time of day for data collection, and ease of interpretation of thermal images, as well as the impacts of different physical characteristics of collectors commonly in use.

One of these issues involves the operational characteristics of the camera itself. (e.g., pixels on target, field of view, AGC settings, etc.). Other issues regard the physical properties (e.g., angular thermal emissivity, thermal emissivity versus temperature) of the different collectors to be imaged (e.g., polymer versus single-glazed, copper fin with nonselective paint versus steel fin with selective coating).

To simplify operation and data interpretation, a goal was to operate a single camera with fixed settings and record visual images of the collectors in various operational modes ranging from stagnation to fully wetted operation. The setting of the camera would be adjusted for maximum photo contrast between operation, a cool state that will appear dark, and stagnation, a hot state that will appear light or white. Thus, at these camera settings the difference between functional and nonfunctional modes of operation should be easily distinguished by observing whether the collectors appear black or white.

Figure 7 is the experimental test matrixes that were designed as a guide for the testing. They were designed to address the issues noted above.

Each numbered yellow cell represents a single test conducted in clear or nearly clear sky conditions (up to about 25% cloudiness). The numbering in each of the yellow cells shows the logical sequence of the tests. Hot ambient is defined as ambient temperatures above 30 °C (86 °F).

The notes after the matrixes give additional details that were imposed upon the test team before implementation.

Chrome Double Glaze			
Near field		hot ambient	cool ambient
	Stagnant	1	9
	Flowing	2	10
Far field		hot ambient	cool ambient
	Stagnant	17	25
	Flowing	18	26

Chrome Single Glaze			
Near field		hot ambient	cool ambient
	Stagnant	3	11
	Flowing	4	12
Far field		hot ambient	cool ambient
	Stagnant	19	27
	Flowing	20	28

Unglazed			
Near field		hot ambient	cool ambient
	Stagnant	5	13
	Flowing	6	14
Far field		hot ambient	cool ambient
	Stagnant	21	29
	Flowing	22	30

Painted Single Glaze			
Near field		hot ambient	cool ambient
	Stagnant	7	15
	Flowing	8	16
Far field		hot ambient	cool ambient
	Stagnant	23	31
	Flowing	24	32

Figure 7. Experimental test matrixes.

Addendum notes to the testing plan:

1. If time permits, all of the tests would be repeated under partly cloudy conditions.
2. Tests will precede the testing to determine whether the AGC camera setting should be applied in the testing.
3. The near field is a camera location about 5.3 meters above the collectors and directly in front of them.
4. The far field is a camera location about 5.3 meters above the collectors and about 16.7 meters from them.
5. Sequencing of tests would be altered as needed for convenience.
6. If time or resource availability become an issue during the testing, priority is given to testing the unglazed and painted fin collector.

SECTION 4. DESCRIPTION OF EXPERIMENTAL TESTS

The matrixes in Figure 8 are duplicated from the previous section with cross hatching to show the tests that were actually conducted.

Chrome Single Glaze				Chrome Double Glaze			
Near field		hot ambient	cool ambient	Near field		hot ambient	cool ambient
	Stagnant	3	11		Stagnant	1	9
	Flowing	4	12		Flowing	2	10
Far field		hot ambient	cool ambient	Far field		hot ambient	cool ambient
	Stagnant	19	27		Stagnant	17	25
	Flowing	20	28		Flowing	18	26

Unglazed				Painted Single Glaze			
Near field		hot ambient	cool ambient	Near field		hot ambient	cool ambient
	Stagnant	5	13		Stagnant	7	15
	Flowing	6	14		Flowing	8	16
Far field		hot ambient	cool ambient	Far field		hot ambient	cool ambient
	Stagnant	21	29		Stagnant	23	31
	Flowing	22	30		Flowing	24	32

Figure 8. Matrixes showing tests that were actually applied.

As the available experimental time became short, it became clear that not all could be completed. Thus, the research team concentrated on completing the tests on the collectors that are most likely to be found in the field. As a consequence, all of the tests on the unglazed and painted fin collector were completed, but only 50% of the tests on the chrome-coated collectors were performed. This shortcoming is considered inconsequential to the results of the project because the test that did occur was focused on the most popular collectors, ones most likely to be found in the field. All of the tests were conducted in either clear or partly cloudy conditions with up to 25% cloud cover.

SECTION 5. EXPERIMENTAL RESULTS

Data collection took place under the conditions noted in the test matrixes discussed in the previous two sections.

Initial Tests and Adjustments

In the default mode of operation, the camera uses internal algorithms for automatic contrast and brightness control. This is referred to as AGC. Although these algorithms effectively balance contrast and brightness throughout the entire scene to produce aesthetically pleasing images, they unfortunately do not produce thermal images that can easily be discerned by a human observer as being a functional or nonfunctional SHW system.

The use of AGC makes quantitative assessments difficult. This is illustrated in Figure 9 showing the collectors in both the near-field and far-field positions taken with AGC on.

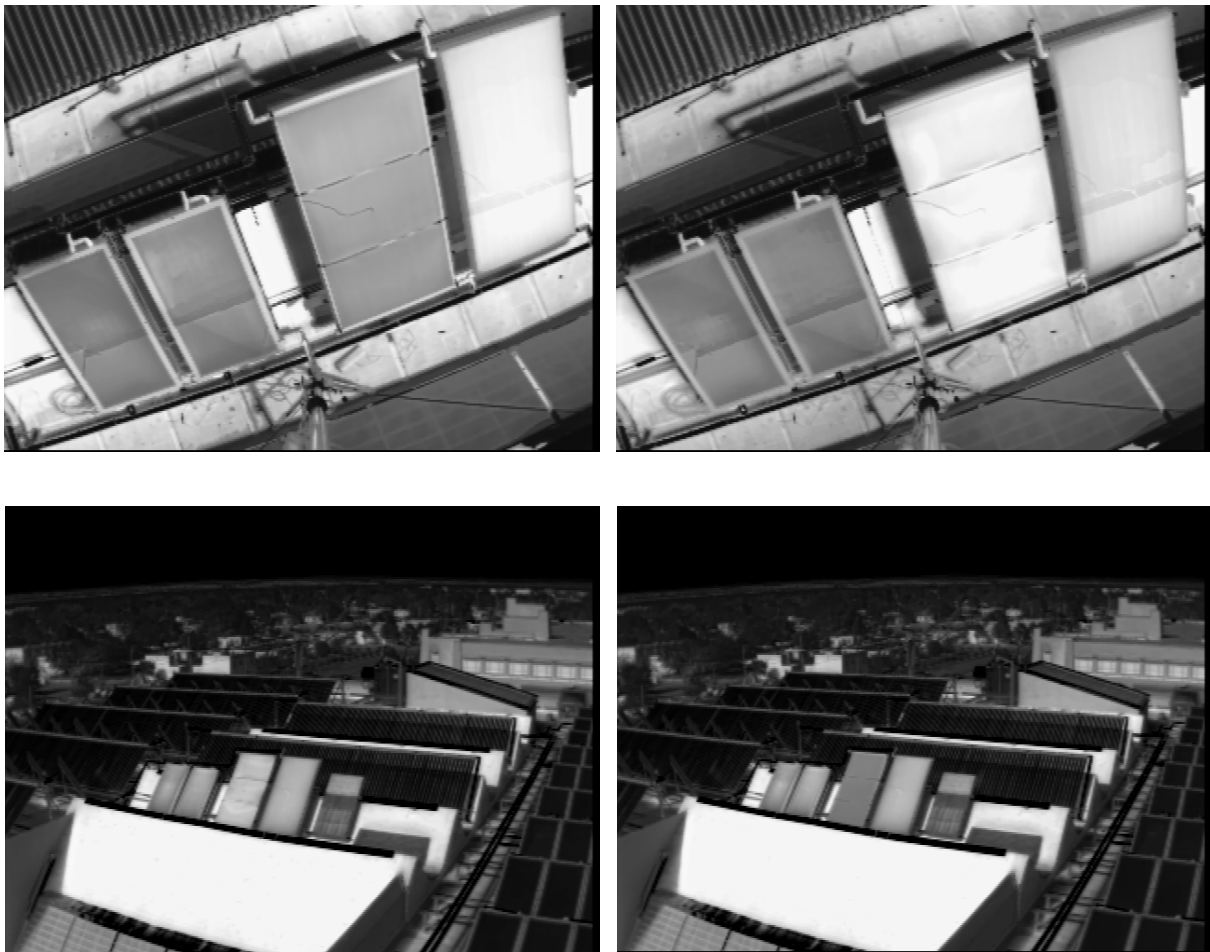


Figure 9. Photos showing collectors in near-field and far-field positions — AGC on.

The left-side pictures, both top and bottom, show all of the collectors in stagnation. The right-side pictures are identical with the exception that glycol solution is flowing through the unglazed polymer collector (third collector from the left). Although it is rather easy to visually determine the difference between stagnation and flowing states of operation with the two pictures side by side, it is much more difficult to make an assessment of the state of operation when viewing just one of the pictures on its own, especially from the far field (lower right picture).²

The problem is confounded when the type of collector being viewed is not known. For example, compare the unglazed polymer collector with glycol flowing through it (right-side pictures) to the glazed, copper fin collectors with black chrome selective coatings (the smaller two collectors on the left side). With AGC operational, the LWIR emissions from the polymer collector with glycol flowing appear to be nearly identical to the emissions observed from the copper fin collectors in stagnation. Effectively, the visual indication of glazing temperature is equal in both cases. Using AGC, and not knowing the type of collector being observed, it is clear that it is not readily apparent whether the collector is functional or not.

The bottom two pictures (far field) also indicate the state of the collectors relative to the thermal emissions observed from two reference materials (asphalt shingles and barrel tiles) that would commonly be found in the vicinity of rooftop-mounted, solar-thermal collectors. The reference roofing materials, mounted on a small plywood platform in the same geometric planes of the panels, are visible in the bottom two pictures (far field view). The platform is located just to the right of the single-glazed, painted fin collector (right-most collector), the fifth position from the left. The asphalt shingles are mounted on the top third of the plywood sheet and the barrel tiles are mounted on the bottom third of the sheet.

The thermal emissions from the shingles are noticeably greater than the emissions from the barrel tiles, indicating that the temperatures are different. With respect to the collectors, several properties of the reference materials are desirable. First, regardless of the operational state of the collectors, the collectors should be easily distinguished from the background roofing material, which is represented by the reference samples. This would facilitate a human observer's ability to review the aerial thermal imagery to recognize and identify collectors on rooftops. Most important, it is desirable that the operational state of the collectors can be assessed by comparing their thermal emissions relative to those of the reference material.

Even with the aid of reference materials, the operation of the camera AGC-on mode degrades the ability to make accurate assessments of the operational state of the collectors. In the bottom right picture, the thermal emissions observed from the polymer collector with glycol flowing through it appear to be very similar to the emissions observed from the barrel tiles, while the emissions from the stagnant collectors appear similar to the emissions observed from the asphalt shingles.

As a result of these findings, the use of the camera with AGC on was not investigated further. Instead, the fixed manual gain (contrast) and offset (brightness) settings were used.

² Note: When these near-field pictures were taken, the reference roofing materials had not yet been installed.

Manual fixed contrast and brightness settings were found to produce superior results. Since the settings are fixed, they facilitate quantitative assessments of results. As explained previously, experiments were conducted with different reference materials (asphalt shingles and barrel tiles) that are commonly found adjacent to rooftop-mounted, solar-thermal collectors. An ideal reference would be a collector in stagnation that is physically close to the operational collectors, but that is an unlikely occurrence in a real application. It is desirable that the reference material can aid an interpreter in assessing the operational state of observed collectors. This is the case when a functional collector appears cool (darker) relative to the reference material and when a stagnant collector appears warm (whiter) relative to the reference material.

Since the collectors will typically be mounted on roofs, the most common roofing materials—concrete barrel tiles and 90-lb asphalt shingles—were selected and used as thermal references. The exact configuration and location of these reference materials is described in Section 2.

One of the issues was the difference in thermal emissivity between glazed and unglazed collectors. The thermal emissivity of glazed collectors also showed angular dependence. That is, they appear cooler than they actually are when the viewing angle is not perpendicular to the face of the collector. This is illustrated in Figure 10. The left-side picture shows the unglazed polymer collector (third from the left) with glycol flowing through it (all other collectors in stagnation) while the right-side picture shows the single-glazed, painted fin collector (fourth from the left) with glycol flowing through it (all other collectors in stagnation).

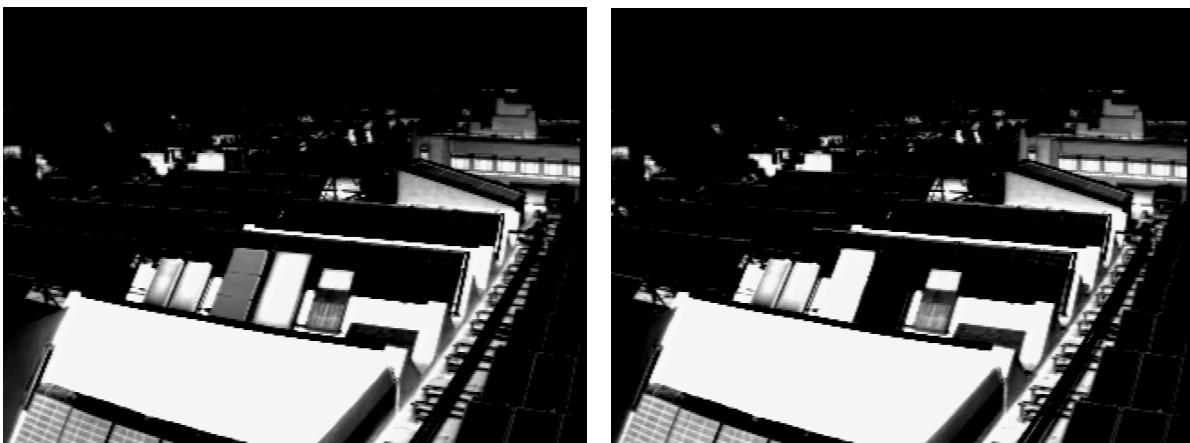


Figure 10. Thermal emissivity of glazed collectors showing angular dependence.

The surface temperature of both the unglazed polymer collector (left-side picture, third from left) and the painted fin, single-glazed collector (right-side picture, fourth from left), as measured by thermocouples on the collector surfaces, are nearly identical. Yet the observed thermal emissions are significantly different. The glazed collector appears significantly cooler than the polymer collector primarily because of the differences in angular emissivity between the two materials. Temperature measurements of the unglazed and glazed collectors were taken at different incidence angles. The unglazed polymer collector demonstrated no angular dependence but the glazed collectors showed a significant angular dependence. It is possible that this issue could

present some application problems, but the full extent of the impact cannot be determined based on this experiment and would have to be assessed in the initial field tests.

Directional Emissivity

The observed phenomenon can be explained as follows. Glass is a dielectric material, with a refractive index of approximately 1.5 for the case of low-iron glass, and is opaque in the IR spectrum. Electromagnetic theory can therefore be used to predict its radiative properties.³ The theoretical emissivity for various refractive index ratios is shown in Figure 11, which shows the directional emissivity of a dielectric material predicted by electromagnetic theory (taken from Siegel et al.). For the case of $n_2/n_1=1.5$ (glass), the emissivity drops relatively slowly for angles up to 40 degrees from the normal direction, and increasingly fast for larger angles.

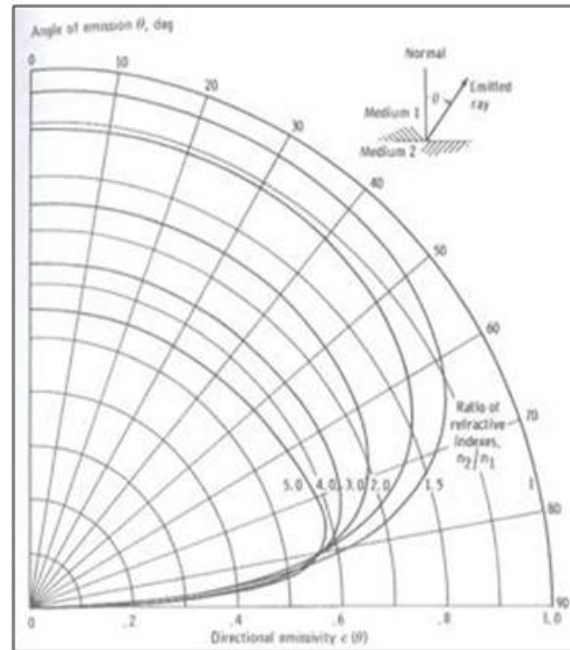


Figure 11. Directional emissivity of a dielectric material predicted by electromagnetic theory.

³ R. Siegel and J. Howell, *Thermal Radiation Heat Transfer* (4th ed.). Taylor & Francis, New York, 2002.

Apparent temperatures of the collector surfaces were measured using an IR thermometer (Extech EX830). The data were obtained on a sunny day in November, at 2:15 p.m.. The data are listed in Table 1. It is simple to show that the relationship between directional and normal emissivity (indicated by the ratio $\varepsilon/\varepsilon_n$) and apparent temperature measured θ degrees away from the normal and in the direction normal to the plate (indicated by the ratio T/T_n) is given by:

$$\frac{\varepsilon}{\varepsilon_n} = \frac{T}{T_n}$$

Table 1. Temperature Data From Collector Surfaces Using an IR Thermometer.

Collector	Angle from normal (degrees)				Angle from normal (degrees)			
	60	45	30	0	60	45	30	0
	Apparent temperature (degrees C)				Apparent temperature (degrees C)			
chrome DG	36.00	42.00	46.00	48.00	0.86	0.93	0.98	1.00
chrome SG	36.00	40.00	43.00	47.00	0.87	0.92	0.95	1.00
unglazed	57.00	59.00	59.00	60.00	0.96	0.99	0.99	1.00
paint SG	40.00	43.00	47.00	54.00	0.84	0.87	0.92	1.00

The directional emissivity for the four collectors based on the data in Table 1 and the equation is presented in graph form in Figure 12. These graphs display the calculated directional emissivity values for the four collectors. Note that the glazed collectors all show a marked decrease in emissivity with increasing angle from the normal, while the emissivity of the unglazed surface is approximately constant. While the calculated emissivity ratio from the measurements drops off with angle somewhat faster than what is predicted theoretically, there is good agreement. Moreover, the unglazed collector does not exhibit a significant variation in emissivity, probably as a consequence of its large-scale surface roughness (the parallel tube structure).

The directional radiative properties of the glazing means that care should be taken when interpreting IR images taken at very shallow angles from the collector surfaces. In such cases, collectors may appear cooler than they really are, and a stagnation condition may be missed. To correct this problem, the gain in the camera could be adjusted, but may result in false positives.

A balance between the two requirements should be carefully identified. It should be noted that in an application of this technique where the camera is mounted on an aircraft flying over a field of installed collectors mounted in various orientations relative to the direction of flight, it is likely that the issue of angular dependence will be in play. However, the direction of flight could be determined based on minimal overall angle of view, thus minimizing the effect of the angular emissivity characteristics.

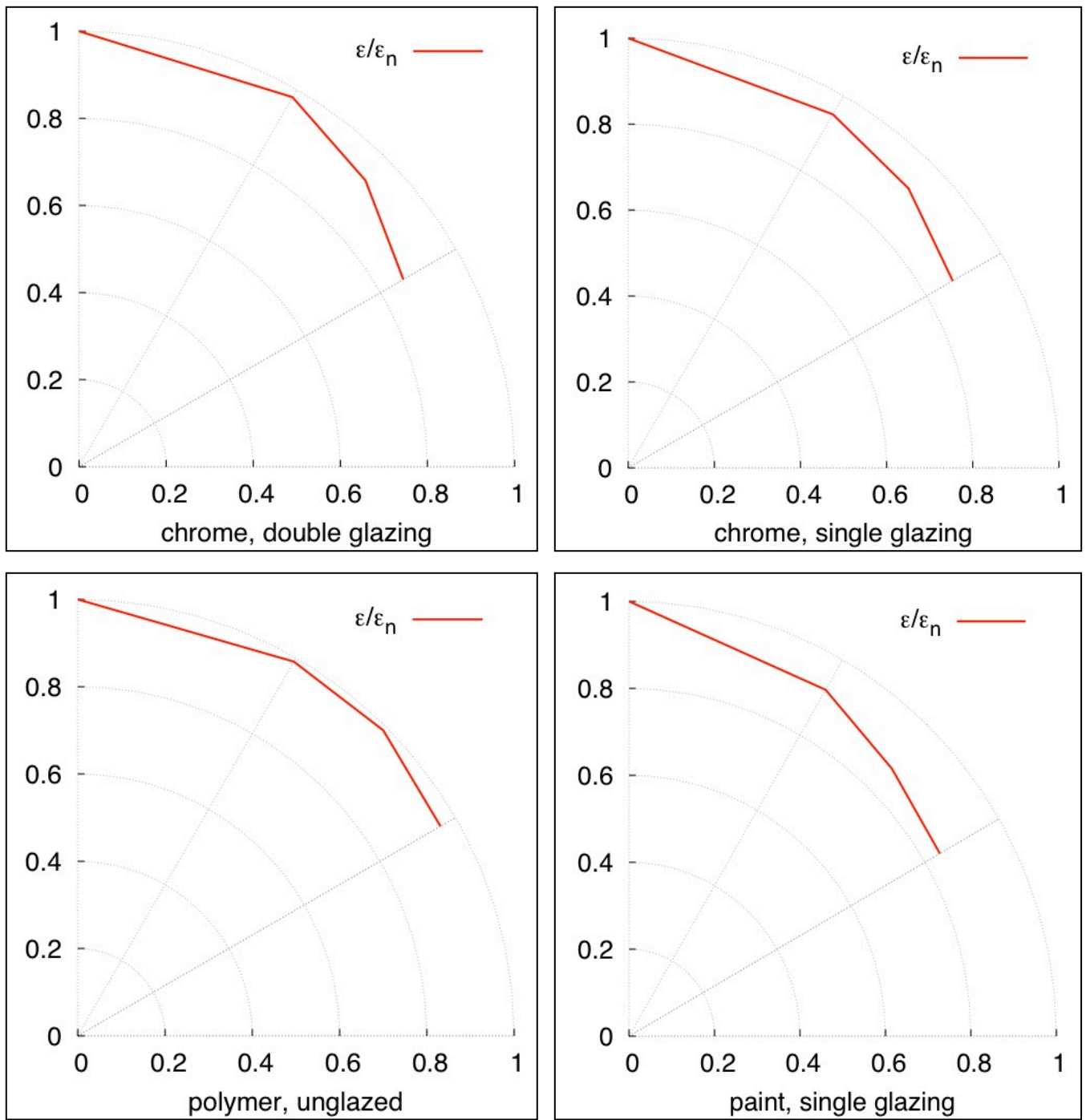


Figure 12. Directional emissivity values for the four collectors.

Video Optimization Process

A significant part of the experimental work involved optimizing the gain (contrast) and offset (brightness) settings of the thermal camera. These settings impact observed pixel intensities. Increasing contrast makes dark pixels (relative to an average intensity) darker and bright pixels (relative to the same average intensity) brighter. Adjusting brightness either increases or decreases all of the image's pixel intensities by an equal amount. The variations in thermal emissivity of the different collectors used in the experiment as well as moderate differences in environmental conditions (hot ambient and cool ambient) were accommodated with a single set of camera settings. More extreme rooftop temperature conditions might require modification of the brightness setting. The contrast setting is not expected to require any modification. The process of optimizing contrast and brightness settings involved repeating the following sequence of steps for different camera settings and different operating temperatures.

1. Adjust camera settings (Contrast, Brightness),
2. Cycle each collector between stagnation and flowing,
3. Record results and operating conditions,
4. Assess results, and
5. Repeat process with new camera settings until desired results are achieved.

The objective of this part of the research was to achieve a single set of camera settings that would accommodate both hot ambient conditions (temperatures above 30 °C) and cool ambient conditions (temperatures below 30 °C) and still allow accurate assessment of the operational state of observed collectors (both glazed and unglazed).

Figure 13 shows some intermediate results that illustrate the situation. The photos show the thermal emissivity of the collectors under stagnation and flowing conditions. In the photo on the left, all of the collectors are in stagnation. In the photo on the right, only the unglazed polymer collector (third collector from left) is operational with glycol flowing through it. These contrast and brightness settings were deemed unsatisfactory because the polymer collector in the photo on the right showed little difference with respect to the barrel tile reference.

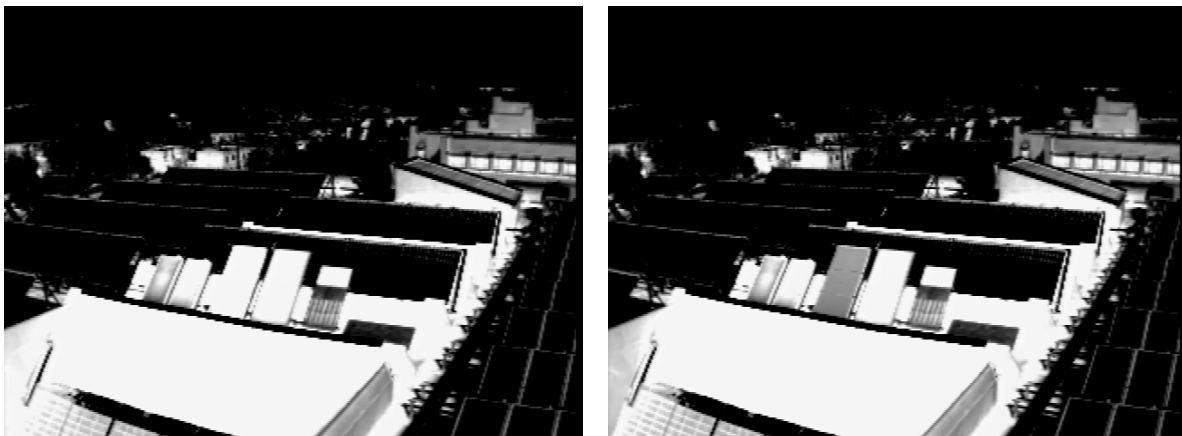


Figure 13. Thermal emissivity of collectors under stagnation and flowing conditions.

Relative to the asphalt shingles, the collectors and shingles are impossible to distinguish when the collectors are in stagnation. This would make it impossible for a human image analyst to identify collectors mounted on rooftops with asphalt shingle roofing material based solely on IR photos or videos. Barrel tiles are a better reference material because they allow easy identification of collectors on rooftops and also allow assessment of the operational state of the installed SHW system. Barrel tiles constitute the majority of roof surfaces in the area of potential first application of this technology, southern Arizona and southern California. Therefore, another visual reference (i.e., from another visual camera) may be needed in a real application of this method to identify collectors on asphalt shingled roofs.

Through trial and error the contrast and brightness settings were optimized, and the results are discussed below. Figure 14 shows the data collected during one of the experiments that helped to provide guidance on the optimization; radiation (kW) is plotted on the right axis and temperatures (degrees C) are plotted on the left axis.

The green line indicates global irradiance measured with a pyranometer mounted next to and in the same geometric plane as the collectors. For most of the experiment, the irradiance hovered around 1 kilowatt/m² except for a dip about 75% through the experiment where an aircraft contrail momentarily partially obscured the sun. The black line indicates ambient air temperature close to the collectors. The ambient temperature was close to 15 °C for the entire experiment. The purple line indicates the temperature of glycol solution flowing to the collectors. The blue curve indicates the surface temperature of the unglazed polymer collector. The red curve indicates the surface (glazing) temperature of the single-glazed, painted fin collector.

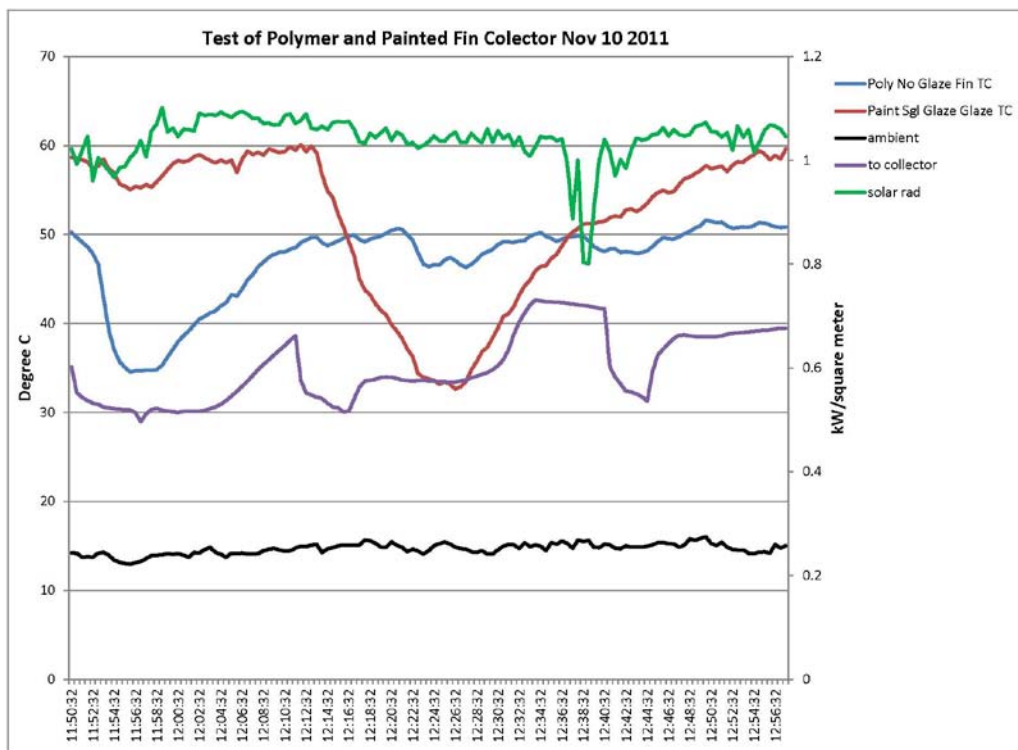


Figure 14. Data used to optimize contrast and brightness settings.

The experiment began with all collectors in stagnation on the morning of November 10, 2011, at approximately 11:50 a.m. It is interesting to note that the surface temperature of the unglazed and glazed collectors differed significantly in stagnation. The surface temperature of the unglazed polymer collector in stagnation hovered around 50 °C. The single-glazed, painted fin collector's surface temperature in stagnation was about 60 °C. The reason for this difference is that the glazing insulates the absorber material inside the collector, which in turn heats the glazing. Any breeze blowing does not impact the absorber temperature for glazed collectors. However, for unglazed collectors, even a light breeze can cause significant cooling of the surface temperature. This led to a concern about temporal intermittency, which was addressed by the analysis described in Section 6.

Shortly into the experiment, glycol was pumped into the unglazed, polymer collector. Data and thermal images were collected (once every 5 seconds). Pumping continued until it reached thermal steady-state conditions, which, as can be seen in the graph (blue line at 11:55), were reached in a few minutes. The thermal inertia of the unglazed polymer collector was much lower than the thermal inertia of any of the glazed collectors. For this collector, under the conditions present, it took approximately 10 minutes to reach thermal steady-state conditions. Note that the steady-state surface temperature of the unglazed polymer collector with glycol flowing was close to 35 °C (blue line at 11:55). Shortly after steady state had been reached, glycol was allowed to drain out of the collector to the drainback storage tank. During this time the collector's surface temperature slowly returned to its stagnation temperature of about 50 °C (blue line, 11:58-12:12).

The red line shows the glazing temperature of the painted fin, single-glazed collector as it moves from stagnation (red line, 12:12) and into full operation with glycol flowing to a thermally steady state (red line, about 12:24).

Note that for both collectors the time to achieve thermal steady-state conditions while transitioning from a flowing condition to a stagnation one was longer than the time required to achieve steady state when transitioning from stagnation to flowing. The apparent reason is that glycol is not actively being pumped out of the collector when the flow stops, but is draining only under the influence of gravity, and that latent pipe-line pressure resists the draining process. The time needed for the unglazed collector to return to stagnant steady-state conditions after flowing was approximately 15 minutes (blue line, 11:58-12:13). The time needed for the glazed collector to achieve steady state after flowing was approximately 30 minutes (red line, 12:26-12:56).

Significant Results

The pictures in Figure 15, all taken from the far field, illustrate the results of the experiment corresponding to Figure 14. The top left picture shows all the collectors in stagnation. Note that relative to the barrel tiles (located on the fifth pane from left),⁴ all four of the stagnant collectors to the left of the tiles appear much whiter. The top right picture shows the unglazed polymer collector (third from left) in thermal steady-state with glycol flowing through it. Note that it appears uniformly darker than the barrel-tile reference material.

⁴ The barrel tiles are at the bottom half of this panel while the asphalt shingles are on the top half.



Figure 15. Results of the experiments corresponding to Figure 14.

Shortly after the polymer collector returned to stagnant steady-state conditions, glycol was pumped into the single-glazed, painted fin collector, shown in the lower left picture (fourth collector from left). In stagnation, the surface temperature of the painted fin collector glazing was approximately 60 °C (10 degrees warmer than the unglazed polymer collector). Because of the insulation properties of the glazing material, the thermal inertia of this collector is significantly greater than the inertia of an unglazed collector. As noted above, the transition time to thermal steady state (stagnation to flowing) for the painted fin collector was approximately 15 minutes.

Again, the bottom left picture shows the painted-fin collector (fourth from left) in steady state with glycol flowing through it. From the previous graph, it can be seen that the glazing temperature dropped from 60 °C to about 33 °C. Recall that the operational steady-state surface temperature of the unglazed polymer collector reached 35 °C – nearly identical to the glazing temperature of the single-glazed, painted fin collector in operational steady-state conditions. However, the appearance of the glazed collector in the LWIR thermal image is much darker than the unglazed polymer collector with glycol flowing through it (compare the upper right photo with the lower left photo). This, as was previously explained, is because of the differences in angular emissivity of the two collectors.

Shortly after achieving steady state with glycol flowing, the glycol was allowed to drain back. Drain back was much faster for the painted fin collector because the copper tubing within the collector had a significantly larger diameter than the polymer tubing in the unglazed collector. From the bottom left picture, the appearance of the painted fin collector with glycol flowing through it is significantly darker than both of the reference materials. This makes it extremely easy to discern the operational state of the collector with glycol flowing through the collector.

The bottom right-hand picture shows both of the chrome fin collectors in thermal steady-state conditions with glycol flowing through the collectors (the double-glazed chrome collector is farthest left and the single-glazed collector is to its right). They both appear very dark with respect to the reference materials making it easy to assess the operational state of these collectors as well. The effect of double glazing on thermal inertia and overall system performance was significant. However, as discussed earlier, because of increased cost, this type of collector is not commonly used.

The following link is to a movie showing the results of the experiments described using the optimized contrast and brightness settings. Clicking on the link should download the file and, depending on the media software on the destination computer, should start playing. It is a large file and may take several seconds to download.

http://energy.sandia.gov/?page_id=2499

The video begins with all of the collectors in dry stagnation. Then the unglazed collector (third from left) is shown filling with glycol and reaching steady state. The unglazed collector then drains and re-establishes dry stagnation. The glazed, painted fin collector (fourth from left) is then subjected to the same sequence. After the collector has returned to dry stagnation, the two selective surface collectors (the two left-most collectors) are shown being operated in parallel, with the single-glazed collector (second from left) achieving steady operational state before the double-glazed collector (left-most collector).

This video indicates the ease of assessing the operational state of installed SHW systems using LWIR thermal imagery. Assessment of the operational state of installed systems is possible with either asphalt shingles or barrel tiles as a background reference. Barrel tiles have the advantage that collectors can easily be distinguished from tiles in either state of operation (stagnant or flowing).

With asphalt shingles, and using the optimized contrast and brightness settings that were used in the experiment, it would not be possible to identify collectors from aerial imagery if the collectors are stagnant. However, this deficiency can be overcome by using a color camera that is sensitive in the visible portion of the electromagnetic spectrum in conjunction with the LWIR camera. The color camera would be bore-sighted with the thermal camera and might even have a wider field of view. This would increase a human image-analyst's situational awareness of observed conditions and is expected to aid in the identification of rooftop-mounted, solar-thermal collectors.

SECTION 6. ANALYSIS OF TEMPORAL INTERMITTENCY AND IMAGE RESOLUTION

One of the concerns in considering the application of this method in the field is the stability of the images and whether wind or intermittent cloud cover could alter sufficiently the glazing temperature and thus distort the image contrast to a degree that could confuse an interpretation about operational status. To assess the image stability, an analysis of the intermittency was conducted.

Another concern is the resolution of the images as taken during a flyover. The field of view can be controlled to some extent with different camera lens optics, but in all cases the greater the distance between the subjects on the ground and the camera aboard an aircraft the greater the areal coverage of the view and the lower the resolution of the image. If the resolution becomes too low then it will be difficult to visually distinguish collectors from other items, such as architectural roof features. An analysis was conducted to assess the potential loss of resolution and the results are presented in this section.

Temporal Intermittency

For one of the image sequences, a simple analysis of short-term intermittency in the intensity of the panel images was conducted. The analysis was performed using data from a test that was conducted with some cloud cover, thus producing potential intermittency of glazing temperatures. Figure 16 shows a representative image from the sequence, with the square highlighting the panel area over which the averaging was conducted. The image sequence comprises 602 images acquired on September 27, 2011, starting at 11:08 a.m., and covering approximately 20 minutes of time. The weather on that day was mostly sunny (about 25% cloud cover), with cumulous clouds passing by at random intervals.

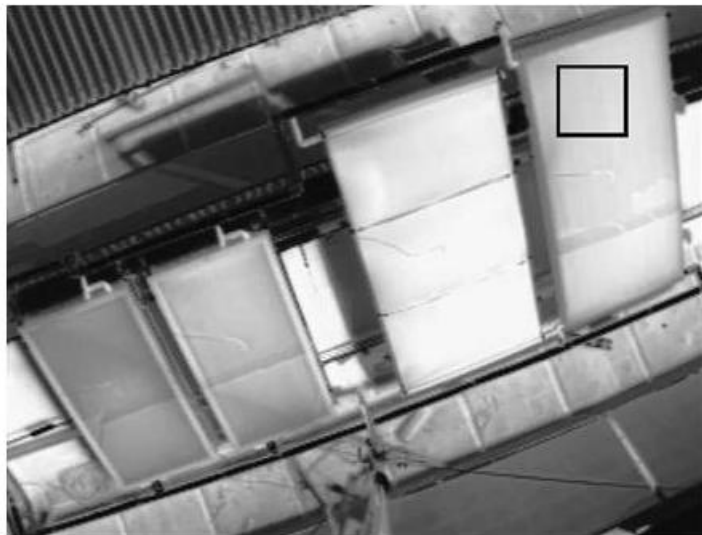


Figure 16. Representative image from sequence of analysis of temporal intermittency.

Figure 17 shows complementary plots. The left plot graphs two parameters, the average pixel intensity of a 64×64 pixel patch (a solid line plotted against the left vertical axis) and standard deviation over this patch (plotted as a dashed line against the right vertical axis). The horizontal axis represents time, with intermittency because of passage of clouds over the panels. Interestingly, there appears to be a negative correlation between the two, indicating that under cloud-free conditions, the pixel intensity is reasonably uniform.

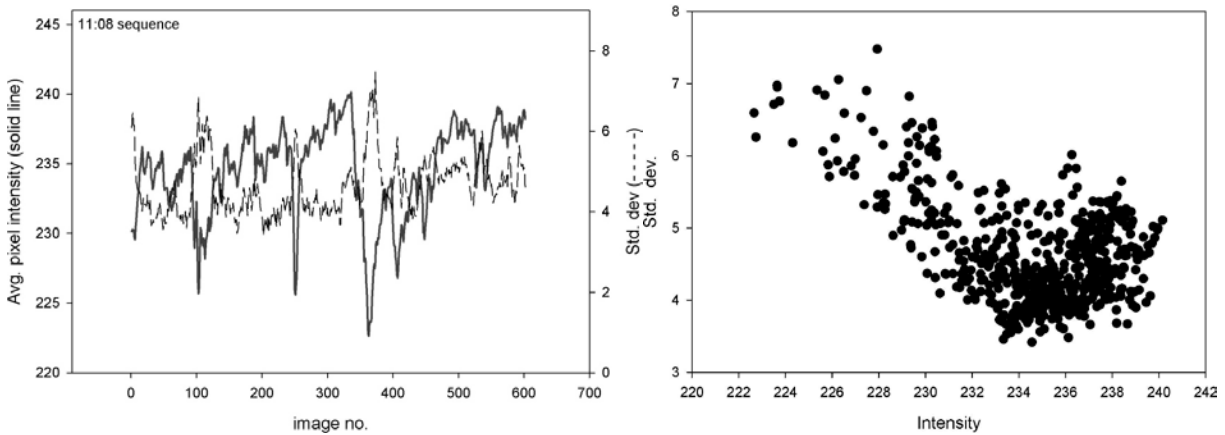


Figure 17. Complementary plots, temporal intermittency.

The right image of the pair shows a scattergram derived from the previous plot that presents the relationship between average pixel intensity (horizontal axis) and standard deviation (left axis). A high linear correlation coefficient of -0.9 confirms the existence of this correlation.

Thus, neither the intermittency of the average nor the variation of individual pixel intensities on the panel appear high enough to prevent correct identification of the panel state as working (i.e., fluid flowing through it).

It is also noteworthy that deparallaxing the images before analysis (to make the panels appear as rectangles with a geometrically correct aspect ratio) did not have a statistically discernible effect on the data behavior.

Image Resolution

The analysis of the resolution issues involved averaging of a selected square panel sample of a fixed size and was conducted upon the image sequence data linearly downsampled by 4 (resulting in 16 times fewer pixels in the sample) and by 16 (resulting in 256 times fewer pixels available).

Downsampling is defined as the effect of reducing the sample rate of a signal. In the case of digital photographs associated with this project, the downsampling effect is to manually reduce the resolution of the image to approximate the loss of resolution of the image because of increased distance between the camera and the subject. In effect, the downsampling process simulates the loss of resolution that might occur if the camera that was used in this project were

placed in an aircraft that is flown over the subjects at a height many times that of the experimental setup.

The visual effect of manually simulating the loss of resolution in an image by downsampling is illustrated in set of five images shown in Figure 18, with three images in the top row and two images in the bottom row. The single image of the collectors in the left-most position shows the original image. The center images, the top one and smaller bottom one, shows the effect of downsampling by 4 in each direction, effectively moving the camera to four times the height of the original test setup and then magnifying to the same size as the left-most image. The small image below the larger one in this middle pair shows how that downsampled image would be displayed without magnification. A slight amount of resolution loss can be seen with a slight image blur in the middle-top image. The right-most set of images shows the effect of downsampling by an additional factor of 16 in each direction. The loss of resolution is clearly seen with considerable image blur.



Figure 18. Visual effect of manually simulating the loss of resolution in an image by downsampling.

Figure 19 shows the results of downsizing by superimposing the graphs of matching panel sample averages upon the original and downsampled data. There is considerable overlap between the three lines, indicating that the signal deterioration because of downsampling is quite modest, even for the linear downsampling by a factor of 16, which would correspond to the camera being 16 times farther away from the panels. This suggests that the camera location of up to 16 times the distance used in the test setup, approximately 89 meters, will produce satisfactory results. Helicopters typically fly at less than 91 meters above the ground.

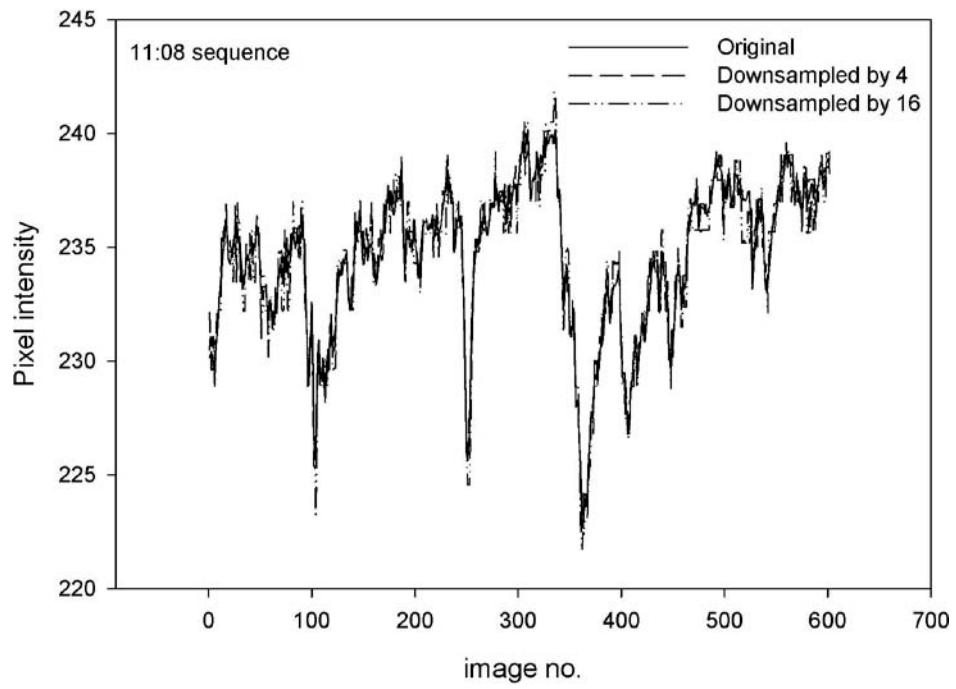


Figure 19. Results of downsizing shown graphically.

SECTION 7. DEVELOPMENT AND TESTING OF THE GLAZING MODEL

Background Information

The glazing model is an important part of the photometric system. For optimal results, the IR camera must be configured for the expected range of temperatures of the glazing temperatures to be expected on the fielded SHW systems. The camera configuration allows the recording of images with the maximum gray level contrast to represent temperature differences between the glazing and the surrounding areas.

In this experiment the temperature of the outermost glazing panel is measured, but estimating this temperature is complex because the heat transfer mechanisms between the absorber plate and the exterior of the collector are themselves complex. Both convective and radiative processes are in the calculation. Accurate estimates of material/surface parameters may be needed to obtain accurate glazing temperature predictions. In developing the model, the sensitivity of the predictions relative to changes in these fundamental parameters is of interest because that information would assist in focusing the effort on properly estimating those parameters that have the most impact on the accuracy of the final prediction.

TRNSYS Version 16 contains a basic glazing model. However, the inputs to the model must be adjusted for the actual systems that are simulated. In this case, the TRNSYS model must be configured for each of the four types of collectors that were under test. In the field, the most common collectors that will be encountered include the glazed painted fin collector and the unglazed polymer collector.

To validate the accuracy of the glazing model, the standard TRNSYS model for flat plate collectors was modified to match closely the ones that were under test in this effort.

In the SHW test bed, two sensors, the outside ambient temperature sensor (located very close to the collectors) and incident solar radiation in the plane of the collectors, comprise weather information relative to the collectors. Typical weather data for the TRNSYS model come from Typical Meteorological Year (TMY 2) weather data, which include wind velocity, relative humidity, total radiation on horizontal, horizontal diffuse radiation, solar azimuth, etc.⁵ Some of these, such as wind speed, can affect the glazing temperature.

Thus, using the glazing collector components from the TRNSYS Thermal Energy System Specialists (TESS) library without a full set of weather data is expected to produce some error. For example, TYPE 944 is a double glazing collector component in TRNSYS 17. Using this model with user-defined inputs to match the test bed collector and with TMY2 weather data produced predictions with no error. However, if the weather data are limited to only those recorded by the test bed and inputted to the TRNSYS model, run-type errors were encountered. (This is an expected situation in which the TRNSYS model was expecting a full set of data that

⁵ The weather data are typical meteorological year (TMY) data sets which are derived from decades of hourly data in the National Solar Radiation Data Base (NSRDB) archives. More information can be obtained at the NREL.gov website.

do not exist in the test bed configuration.) Thus, a glazing collector model was needed that would execute with the limited data measured by the test bed. This implied that some estimates of certain parameters were needed, as will be explained later.

Test Results With an Unglazed Polymer Collector

The TRNSYS SHW test bed model includes the solar collector, storage tank, pump, and control system. The collector module from the TRNSYS TESS library that matches the test bed's unglazed polymer collector is TYPE 559 (model: Sunsaver, Certification # 2007051A, by Fafco, Inc.). Using this model requires a number of input parameters to be defined so that the modeled collector is an accurate representation of the real one. Some of these parameters, such as physical dimension, are measured directly. Others, such as the back and edge heat loss coefficients, are not known precisely and are estimated based on engineering judgment, some of which may or may not be consistent with estimates made by others. The parameters used for the TYPE 559 module are listed in Table 2. The edge width was assumed to be negligible relative to the collector aperture.

Table 2. Unglazed Collector TYPE 559 User-Supplied Input Parameters.

Parameter	Value	Unit
Collector length	2.18	m
Collector width	1.219	m
Fluid specific heat	3.747	kJ/kg.k
Plate absorptance	0.55	Fraction
Emissivity of the absorber plate	0.45	Fraction
Atmospheric pressure	0.809	atm
Collector efficiency factor	0.7	
Heat loss coefficient–back and edges	5	kJ/hr.m ² .k

The test bed's water tank components were identical to those that were used in the experiments described in SAND2011-5528.⁶ TYPE 534 matches the test bed's tank most closely. The heat exchanger of TYPE 534 is immersed in the water tank, but the heat exchanger in the test bed's tank consists of a copper tube coiled around the outside of the water tank.⁷ The input parameters for the TYPE 534 are shown in Table 3. The simulation results of the water tank matches the measured values well using the TYPE 534, and it was used for the unglazed collector model. For the single- and double-glazed collector model, the TYPE 1237 water tank model from TRNSYS 17 was used. TYPE 1237 is a water tank with wraparound heat exchanger that most closely matches the water tank in the test bed.

⁶ D. Menicucci, H. He, A. Mammoli, T. Caudell, and J. Burch, *Testing and Evaluation for Solar Hot Water Reliability*, SAND2011-5528. Sandia National Laboratories, Albuquerque, NM, 2011.

⁷ Although a wraparound tank heat exchanger model exists in TRNSYS, limited resources led the team to use one that already existed and was proven to be adequate for the test bed and for this application.

Table 3. TRNSYS Model Water Tank TYPE 534 Parameters.

Parameter	Value	Units
# of tank nodes	8	
Number of ports	1	
Number of immersed heat exchangers	1	
Number of miscellaneous heat flows	0	
Tank volume	0.297	m ³
Tank height	1.4	M
Top-loss coefficient	15	kJ/hr.m ² .k
Bottom-loss coefficient	5	kJ/hr.m ² .k
Additional thermal conductivity	0	kJ/hr.m ² .k
Edge-loss node #1	5	kJ/hr.m ² .k
Edge-loss node #2	5	kJ/hr.m ² .k
Edge-loss node #3	2	kJ/hr.m ² .k
Edge-loss node #4	2	kJ/hr.m ² .k
Edge-loss node #5	10	kJ/hr.m ² .k
Edge-loss node #6	30	kJ/hr.m ² .k
Edge-loss node #7	15	kJ/hr.m ² .k
Edge-loss node #8	5	kJ/hr.m ² .k
Top-loss temperature	22	C
Bottom-loss temperature	22	C
Inversion mixing flow rate	-10	Kg/hr
Number of miscellaneous heat gains	0	

No sky temperature measurements are recorded by the test bed. An empirically derived equation was used to estimate the sky temperature based on outside ambient temperature.⁸

$$T_{sky} = 0.0552 \cdot T_a^{-1.5}, \quad (1)$$

where T_{sky} = sky temperature (C) and T_a = outside ambient temperature (C).⁹

⁸ W. C. Swinbank, Long-waver radiation from clear skies, *Quarterly Journal of the Royal Meteorological Society*, vol. 89(381), pp. 339-348, 1963.

⁹ The martin-berdahl relationships may be superior to this correlation and account for moisture content through use of *Tdewpoint*. However, limits on resources dictated that the team applied the simple relationship noted in the text.

The pump controller is modeled using a Matlab module (listed in full in Appendix A). The parameters of the pump are shown in Table 4. The pump is controlled using the differences between the tank and the collector, as is typical of a commercial SHW controller. The water draw profile used in the simulation is shown in Table 8.¹⁰

Table 4. TRNSYS Solar Loop Pump Parameters.

Parameter	Value	Unit
Rated flow rate	380	Kg/hr
Fluid specific heat	3.747	Kj/kg.k
Rated power	864	kJ/hr

Table 5. TRNSYS Water Draw Profile Used in the Simulations.

Hour	Watt Hours	Hour	Watt Hours
0	150	12	430
1	0	13	300
2	0	14	180
3	0	15	300
4	0	16	450
5	150	17	450
6	900	18	625
7	1100	19	750
8	900	20	625
9	625	21	750
10	625	22	450
11	430	23	300

A validation experiment was conducted from 1 p.m. on September 29, 2011 (hour 6517), to 1 p.m. on October 3, 2011 (hour 6613). As shown in Figure 20, the collector plate temperature of the TRNSYS model is consistent with the measured data, except at night. In the TRNSYS model the sky temperature is calculated from Equation (1), which is a function of only outside ambient temperature. In reality, sky temperature is also influenced by other factors, such as relative humidity and cloud conditions. However, this is not of concern because the photometric technique is only expected to be applied during daylight hours.

¹⁰ Draws in the test bed are based on energy. During a draw the mass of water drawn and the delta T are measured. At small periodic intervals the energy is computed and added to any previous calculations in that draw period, effectively accumulating the total energy being drawn. The accumulated total energy is compared against the energy draw goal for that period and the draw is terminated when the cumulative total equals or exceeds the draw goal. The method was verified with simple stopwatch and volume in a bucket and was determined to be accurate.

The water tank top temperature is shown in Figure 21 and water tank node 6 temperatures are shown in Figure 22. Comparing Figure 21 with Figure 22, it can be seen that the temperature predicted by the TRNSYS model coincides well with the measured data in the upper part of the water tank, but there are some differences in the bottom half of the water tank. These differences occur because the heat exchanger is located at the bottom portion of the tank and the heat exchanger in the TRNSYS model is different from those in the test bed. However, the differences were deemed acceptable for the purposes of this experiment, which are focused on the glazing temperatures.

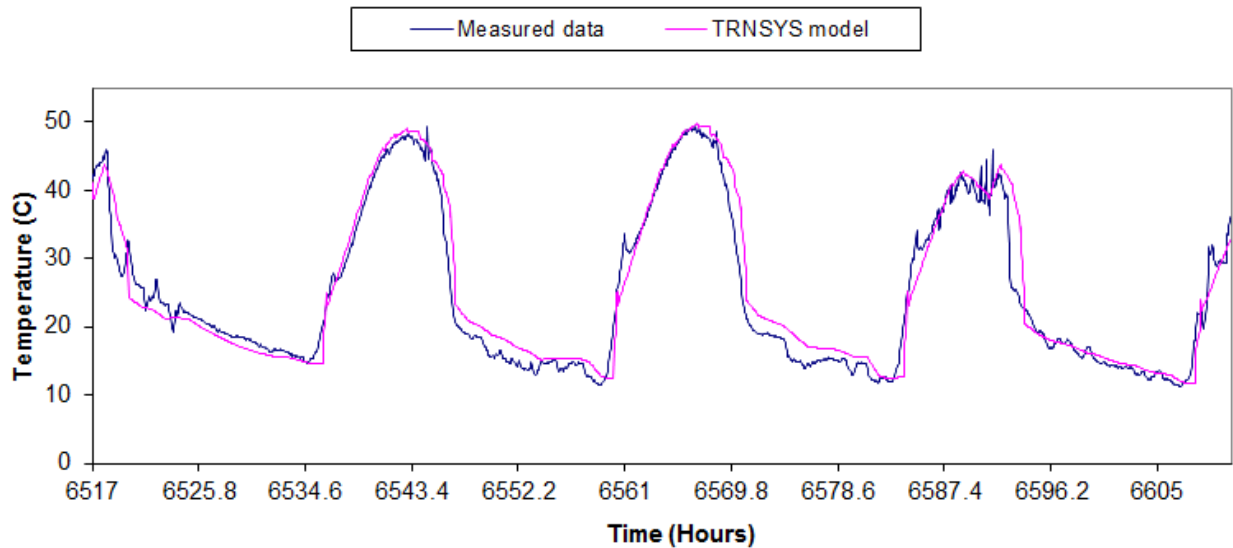


Figure 20. Unglazed collector plate temperature.

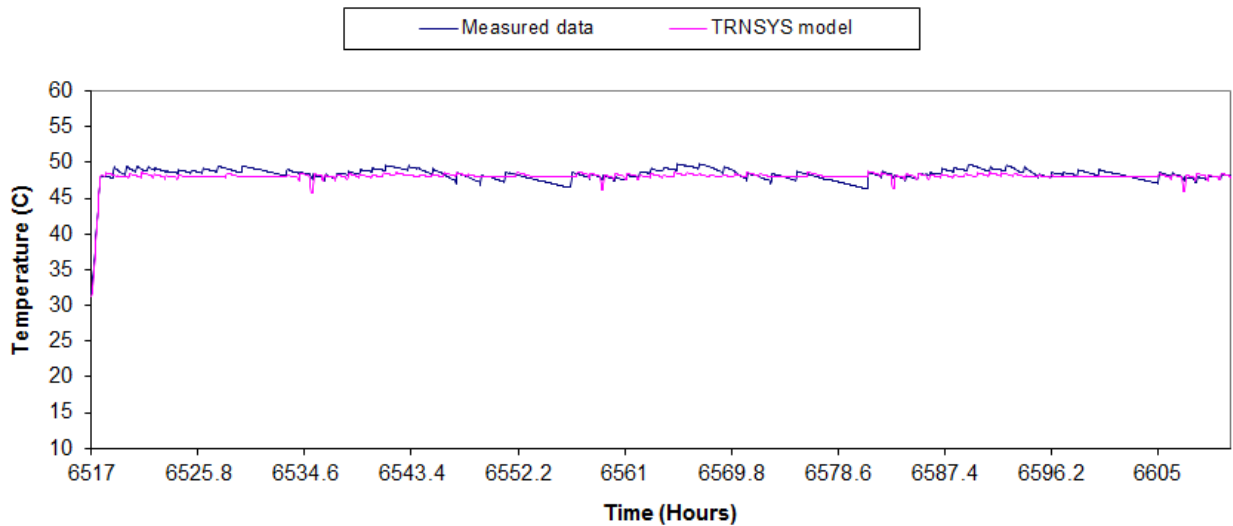


Figure 21. Water tank top temperature.

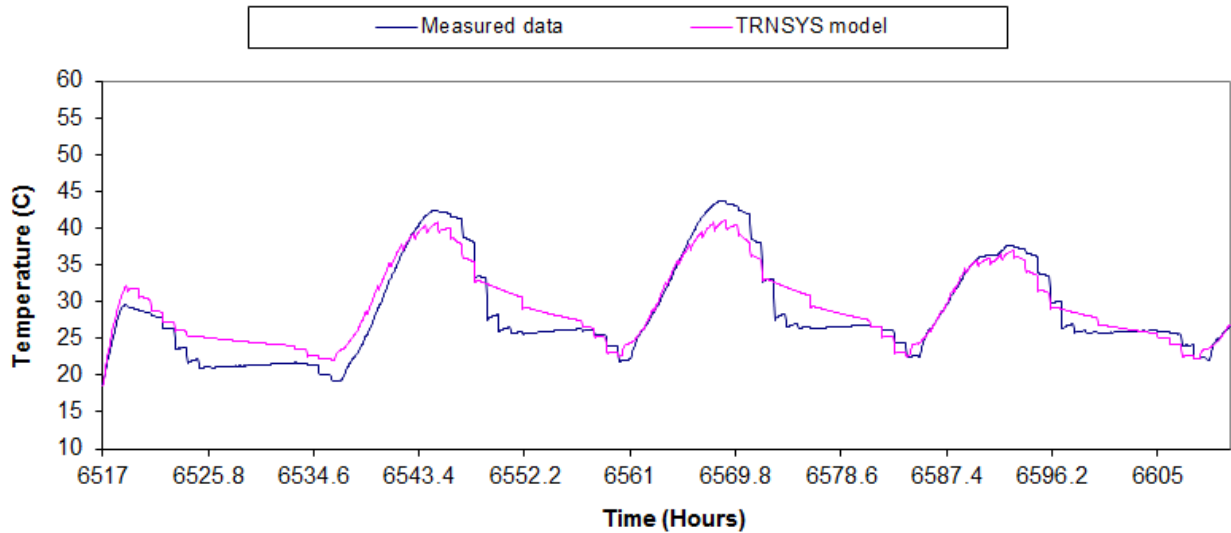


Figure 22. Water tank node 6 temperature.

Figure 23 presents a comparison of the predicted and measured useful energy gain by the unglazed collector. As can be seen, the overall trends are reasonably accurately predicted with a slight time lag, with differences between the total measured and simulation energy at less than 5%. The first two days are clear and the third day is partly cloudy. In the TRNSYS model, the radiation data are averaged one-hour values that were needed to conform to the required input format based on the TMY hourly averages. Although TRNSYS is capable of running at smaller time step intervals than one hour, it is senseless to do so if the weather data are based on hourly averages. As a consequence, the simulated results are much smoother than measured data, which are presented in the graph at the much higher recording interval employed by the test bed.

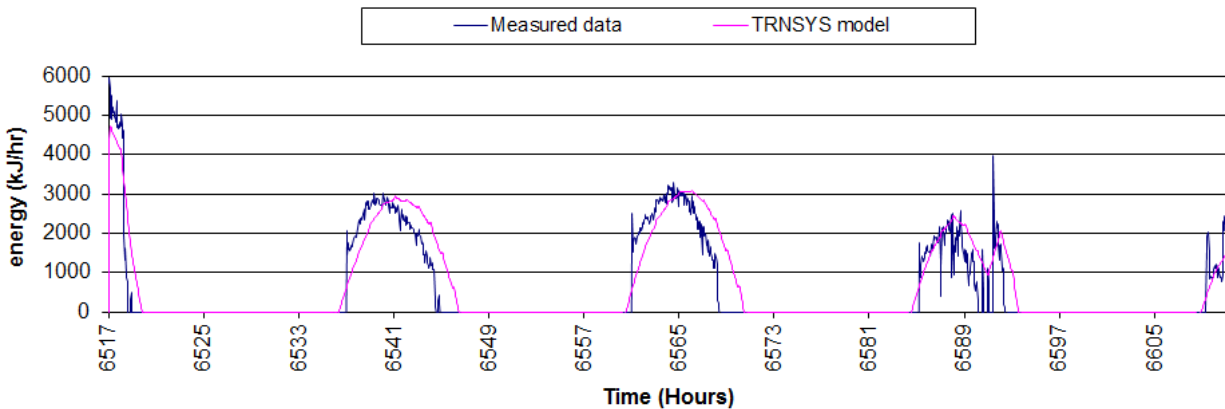


Figure 23. Useful energy gain by the solar collector.

The curve at the left-most part of the graph reflected an initial startup data calibration effort and should be ignored. The time mismatch between the actual and predicted values is sufficiently large for concern had total energy gain been one of the focuses of the study. However, for the purposes of this study with a focus on the glazing temperature, these differences were declared inconsequential.

Test Results With the Painted Fin Single-Glazed Collector

The TRNSYS TYPE 244 collector model supplied by TRNSYS was selected to model the SunBelt SB-32-0.75, by SunEarth, Inc., which was installed in the test bed. However, it requires definition of the collector components. The Fortran code of TYPE 244 is listed in Appendix B. The thermal network for a single-cover collector is shown in Figure 24. The definition of the collector components is discussed below.

The collector energy top-loss is influenced by convection and radiation between parallel plates. The energy transfer between the plate at T_p and the cover at T_c is equal to the energy loss to the surroundings from the top cover:¹¹

$$q_{loss,top} = h_{p-c}(T_p - T_c) + \frac{\sigma(T_p^4 - T_c^4)}{\frac{1}{\epsilon_p} + \frac{1}{\epsilon_c} - 1} \quad (2)$$

where h_{p-c} is the heat transfer coefficient for convection between the collector plate and the cover.

Equation (2) can be written as

$$q_{loss,top} = (h_{p-c} + h_{r,p-c})(T_p - T_c) \quad (3)$$

where

$$h_{r,p-c} = \frac{\sigma(T_p + T_c)(T_p^2 + T_c^2)}{\frac{1}{\epsilon_p} + \frac{1}{\epsilon_c} - 1}. \quad (4)$$

The resistance R_1 and R_2 can be expressed a

$$R_1 = \frac{1}{h_{c-a} + h_{r,c-a}} \quad (5)$$

$$R_2 = \frac{1}{h_{p-c} + h_{r,p-c}}. \quad (6)$$

¹¹ J. A. Duffie and W. A. Beckman, *Solar Engineering of Thermal Processes* (2nd ed.). John Wiley & Sons, New York, 1991.

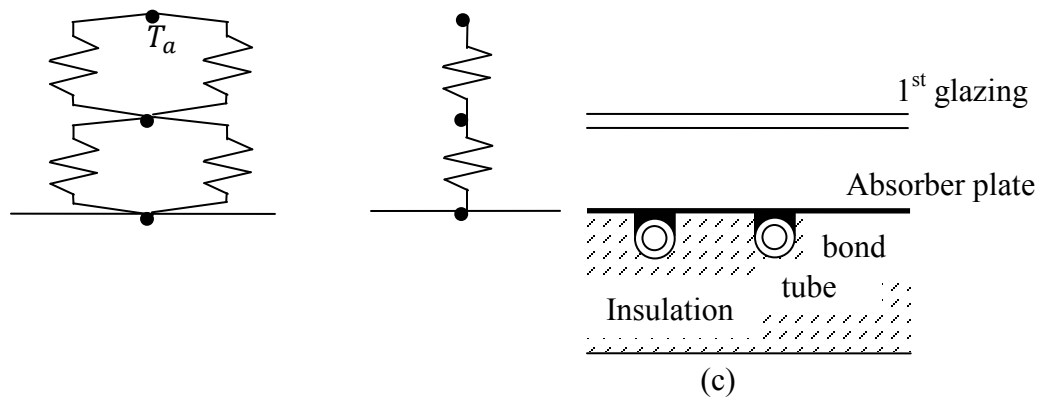


Figure 24. Thermal network for a single-glazed collector.
 (a) In terms of conduction, convection and radiation resistances,
 (b) In terms of combined effective resistances between plates,
 (c) Schematic for single glazing flat plate collector. In this case the assumption is that the radiative losses off of the glazing are to a single ambient temperature, T_a , with no sky temperature depression.

For this single-glazed collector, the top-loss coefficient from the collector plate to the ambient is

$$U_t = \frac{1}{R_1 + R_2}. \quad (7)$$

The glazing temperature is

$$T_c = T_p - \frac{U_t(T_p - T_a)}{h_{p-c} + h_{r,p-c}}. \quad (8)$$

The parameters used for the collector TYPE 244 module are listed in Table 6. Again, these values were based on engineering judgments.

Table 6. Paint Single-Glazed Collector TYPE 244 User-Supplied Input Parameters.

Parameter	Value	Unit
Collector length	2.44	m
Collector width	1.14	m
Absorber plate thickness	0.0012	m
Conductivity of absorber material	194	Kj/hr.m.k
Number of tubes	10	
Inner tube diameter	0.0044	m
Outer tube diameter	0.0064	m
Bond resistance	0.05	h.m ² .k/kJ
Fluid specific heat	3.747	kJ/kg.k
Absorptance of the absorber plate	0.95	Fraction
Emissivity of the absorber plate	0.9	Fraction
Top-loss mode	1	
Number of identical covers	1	
Index of refraction of cover material	1.526	
Extinction coefficient, thickness product	0.005	
Emissivity of the glass	0.9	Fraction
Plate spacing	0.025	m
Glass spacing	0.01	m

A validation experiment was conducted from 2 p.m. on October 3, 2011 (hour 6614), to 9 a.m. on October 12, 2011 (hour 6825). As shown in Figure 25, the collector plate temperature of the TRNSYS model is consistent with measured data, except at night. As with the polymer collector, the nighttime problem was traced to the equation used to estimate sky temperature. Figure 26 shows the paint single-glazed glazing temperature.

The water tank top temperature is shown in Figure 27 and water tank node 6 temperature is shown in Figure 28. Comparing Figure 21 with Figure 22, it is apparent that the temperature in TRNSYS model coincides well with measured data in the upper part of the water tank, but with some differences in the bottom half of the water tank, as discussed earlier. The errors were acceptable for this application.

Figure 29 presents a comparison of the predicted and measured useful energy gain by the painted fin glazed collector. As can be seen, the overall predictions are reasonably accurate with a slight time lag; the cumulative error between the total measured and simulation energy is less than 5%.

The first five days are partly cloudy or cloudy; the others are clear. In the TRNSYS model, the radiation data are presented in one-hour time steps, so the simulation results are much smoother than the measured data in Figures 25, 26, and 29.

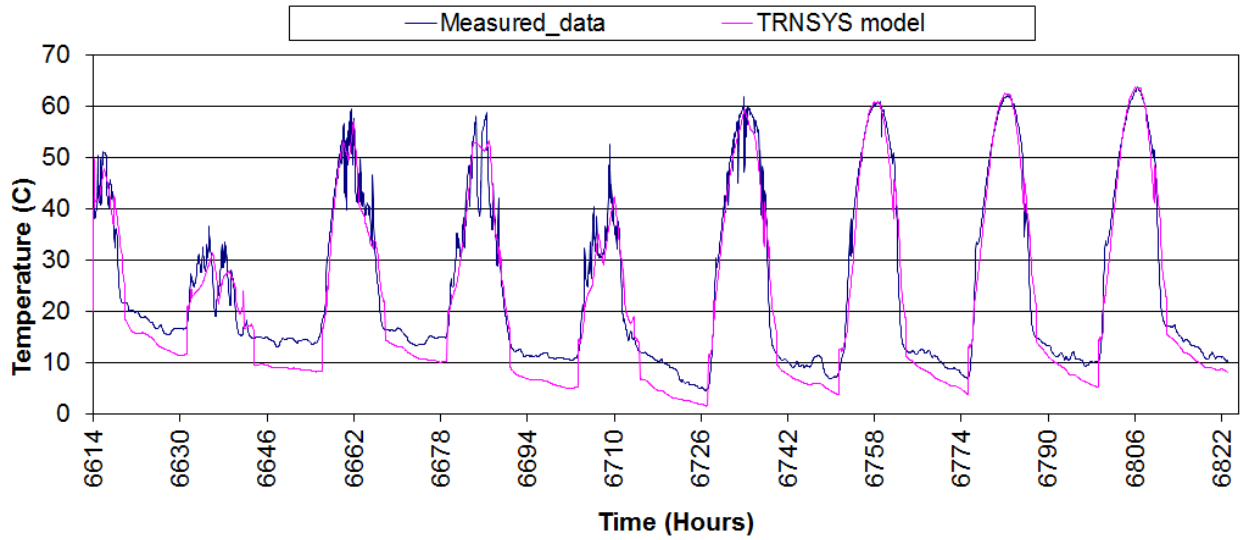


Figure 25. Paint single-glazed collector plate temperature.

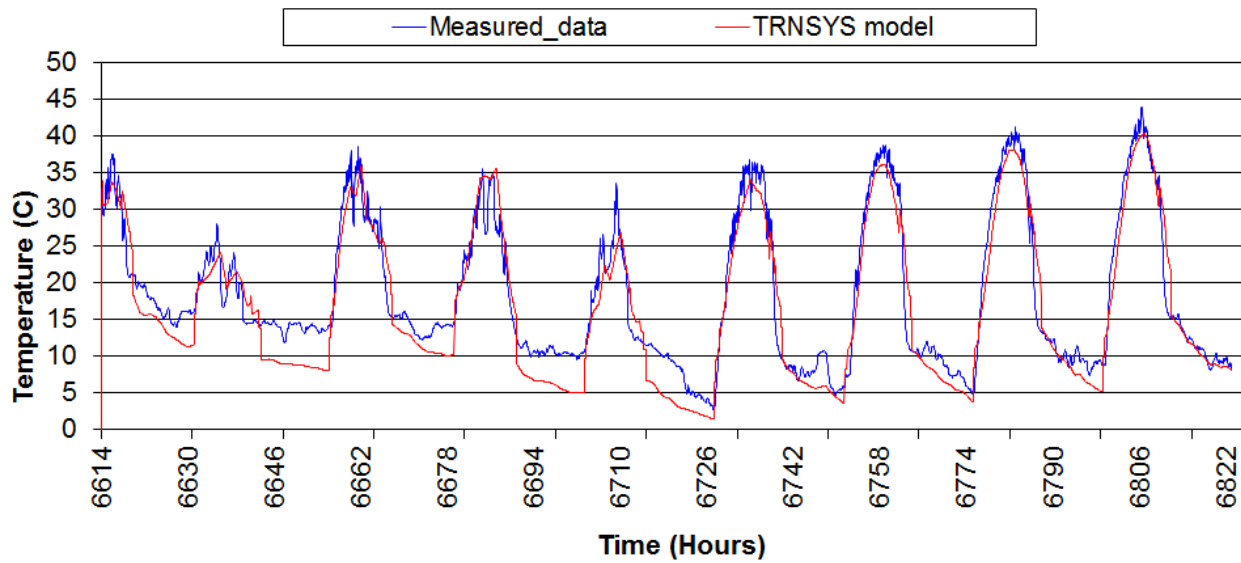


Figure 26. Paint single-glazed glazing temperature.

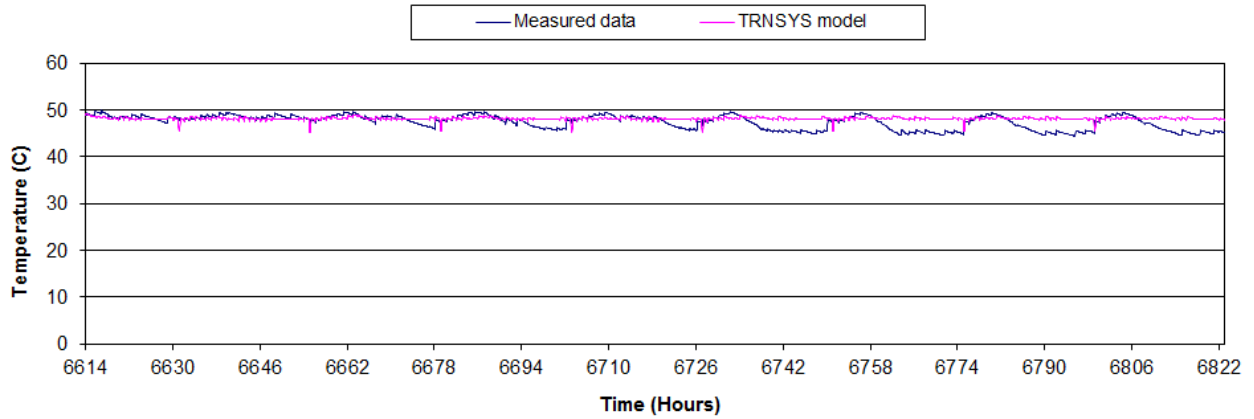


Figure 27. Water tank top temperature.

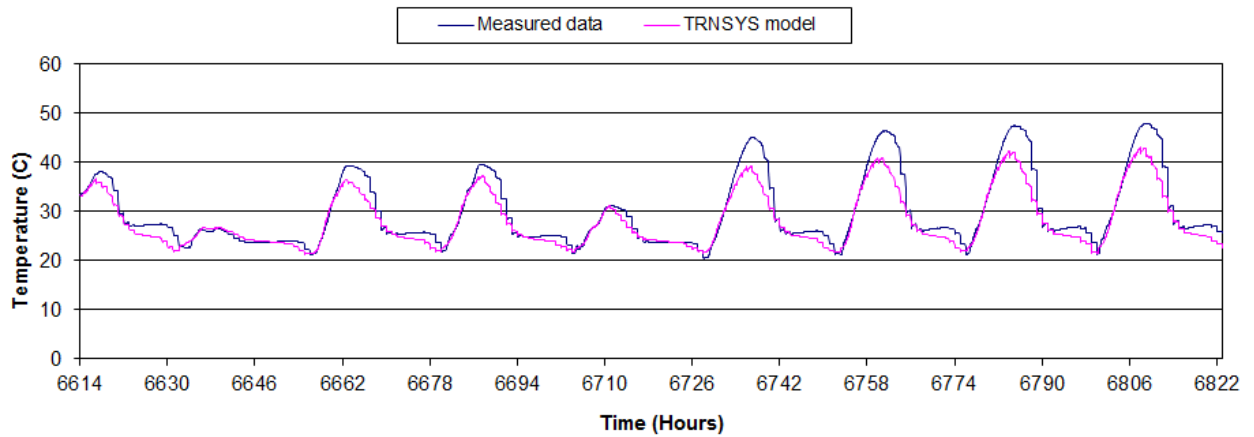


Figure 28. Water tank node 6 temperature.

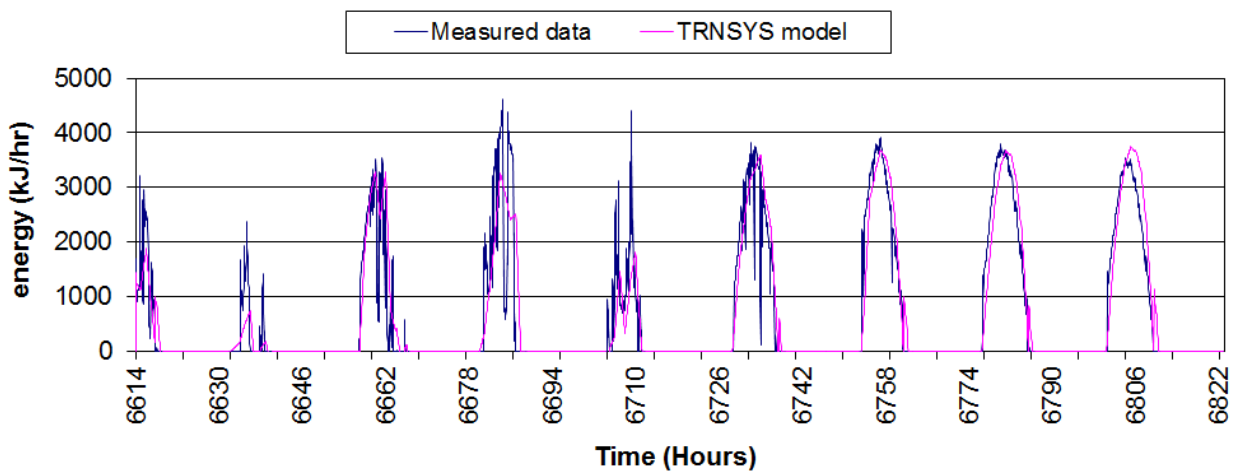


Figure 29. Useful energy gain by the collector.

Test Results With the Chrome Double- and Single-Glazed Collectors

The parameters input to the TRNSYS models for the chrome fin double- and single-glazed collectors (model: SC3-32S, by Lennox Industries, Inc.) are equivalent to those used in the previous tests, except that the collector component for the chrome double-glazed collector is replaced by a user-defined collector TYPE 242. The Fortran code of TYPE 242 is in Appendix C. The thermal network for a double-cover collector is shown in Figure 30, which displays the thermal network for a double-glazed collector with the following features: (a) in terms of conduction, convection, and radiation resistances, (b) in terms of combined effective resistances between plates, and (c) schematic for double-glazing flat plate collector.

The collector energy top-loss is the result of convection and radiation between parallel plates. The energy transfer between the plate at T_p and the first cover at T_{c1} is the same as between any other two adjacent covers and is also equal to the energy loss to the surroundings from the top cover:

$$q_{loss,top} = h_{p-c1}(T_p - T_{c1}) + \frac{\sigma(T_p^4 - T_{c1}^4)}{\frac{1}{\varepsilon_p} + \frac{1}{\varepsilon_c} - 1} \quad (9)$$

where h_{p-c1} is the heat transfer coefficient between collector plate and the first cover. Equation (9) can be written as

$$q_{loss,top} = (h_{p-c1} + h_{r,p-c1})(T_p - T_{c1}) \quad (10)$$

where

$$h_{r,p-c1} = \frac{\sigma(T_p + T_{c1})(T_p^2 + T_{c1}^2)}{\frac{1}{\varepsilon_p} + \frac{1}{\varepsilon_c} - 1}. \quad (11)$$

The resistance R_1 and R_2 can be expressed as

$$R_1 = \frac{1}{h_{c2-a} + h_{r,c2-a}} \quad (12)$$

$$R_2 = \frac{1}{h_{c1-c2} + h_{r,c1-c2}} \quad (13)$$

$$R_3 = \frac{1}{h_{p-c1} + h_{r,p-c1}}. \quad (14)$$

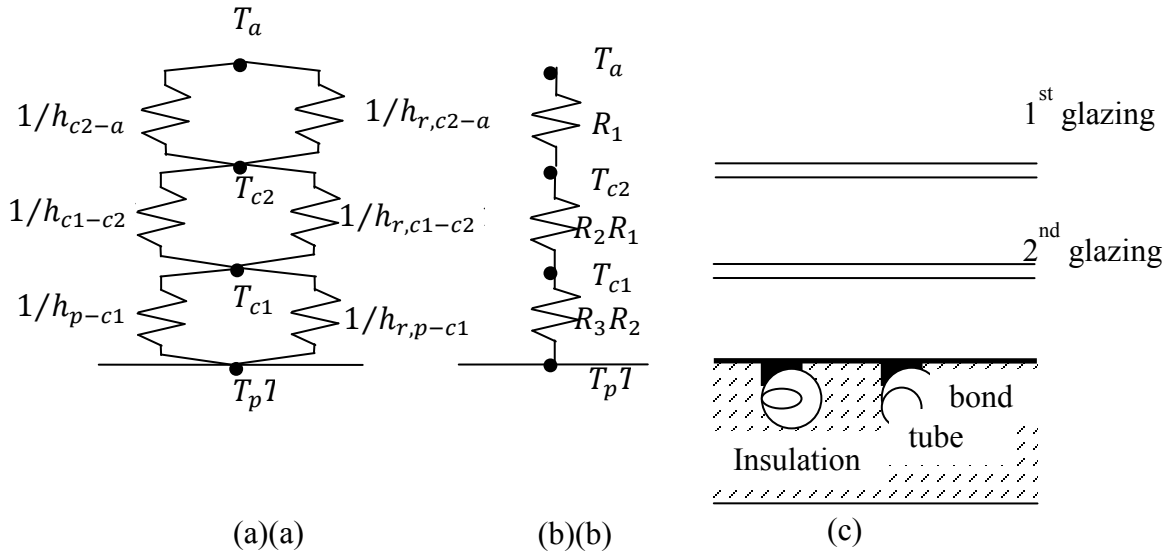


Figure 30. Thermal network for a double-glazed collector.

For the double-glazed collector, the top-loss coefficient from the collector plate to the ambient is

$$U_t = \frac{1}{R_1 + R_2 + R_3} \quad (15)$$

The new temperature of plate j can be expressed by the temperature of plate i as

$$T_j = T_i - \frac{U_t(T_p - T_a)}{h_{i-j} + h_{r,i-j}} \quad (16)$$

The parameters used for the collector TYPE 242 module are listed in Table 7. Again, many of these values were selected based on engineering judgment.

Table 7. Chrome Double-Glazed Collector TYPE 242 User-Supplied Input Parameters.

Parameter	Value	Unit
Collector length	1.71	m
Collector width	0.805	m
Absorber plate thickness	0.0012	m
Conductivity of steel absorber material	194	Kj/hr.m.k
Number of tubes	10	
Inner tube diameter	0.0044	m
Outer tube diameter	0.0064	m
Bond resistance	0.05	$\text{h.m}^2.\text{k/kJ}$
Fluid specific heat	3.747	kJ/kg.k
Absorptance of the absorber plate	0.55	Fraction
Emissivity of the absorber plate	0.5	Fraction
Top-loss mode	1	
Number of identical covers	2	
Index of refraction of cover material	1.53	
Extinction coefficient, thickness product	0.005	Unitless
Emissivity of the glass	0.15	Fraction
Plate spacing	0.025	m
Glass spacing	0.01	m

The chrome single-glazed collector uses the same TYPE 242 as the previous test, and the parameters are listed in Table 8.

Table 8. Chrome Single-Glazed Collector TYPE 244 User-Supplied Input Parameters.

Parameter	Value	Unit
Collector length	1.71	m
Collector width	0.805	m
Absorber plate thickness	0.0012	m
Conductivity of absorber material	194	Kj/hr.m.k
Number of tubes	10	
Inner tube diameter	0.0044	m
Outer tube diameter	0.0064	m
Bond resistance	0.05	$\text{h.m}^2.\text{k/kJ}$
Fluid specific heat	3.747	kJ/kg.k
Absorptance of the absorber plate	0.5	Fraction
Emissivity of the absorber plate	0.2	Fraction
Top-loss mode	1	
Number of identical covers	1	
Index of refraction of cover material	1.53	
Extinction coefficient, thickness product	0.005	
Emissivity of the glass	0.2	Fraction
Plate spacing	0.035	m
Glass spacing	0.01	m

The validation experiment was conducted from 2 p.m. on November 15, 2011 (hour 7646), to 9a.m. on November 19, 2011 (hour 7737). The double-glazed chrome-plated collector and the single-glazed chrome-plated collector were run in parallel. As shown in Figure 31 and Figure 32, the collector plate temperatures of the TRNSYS model are consistent with measured data, except at night. The nighttime estimation errors occur because the sky temperature is estimated from Equation (1), which is based only on the outside ambient temperature. In reality, other factors, such as humidity, sunny day or cloudy day, affect the sky temperature.

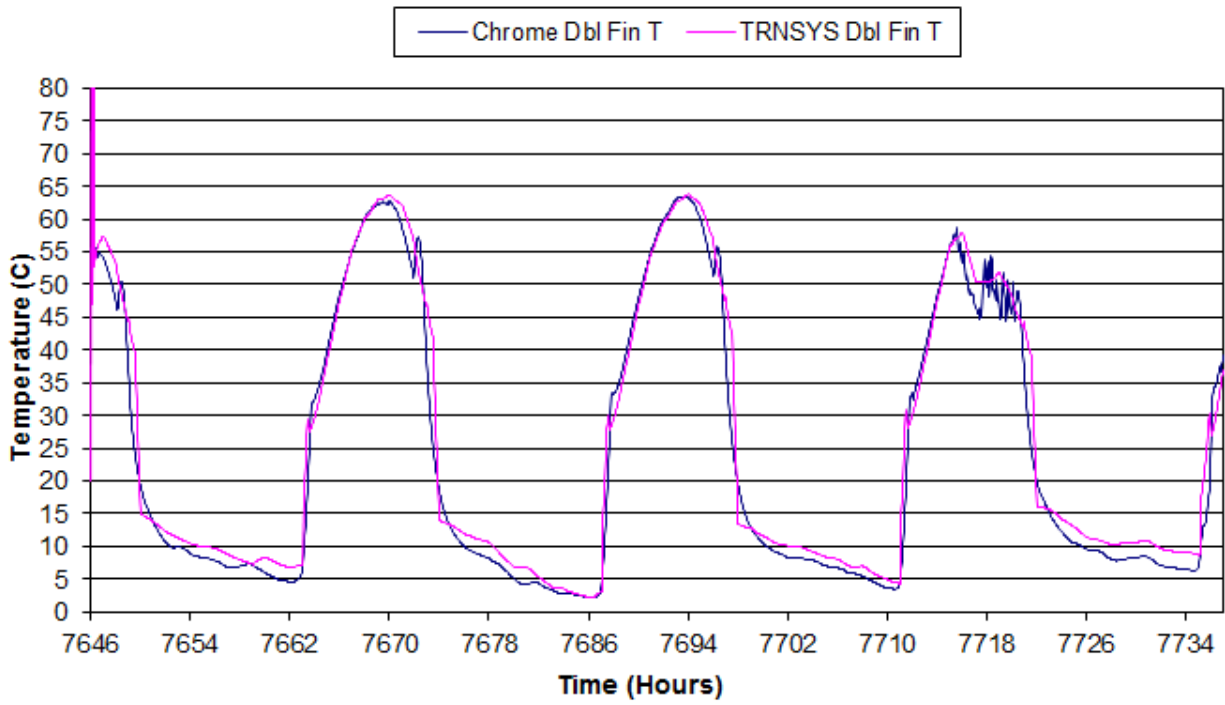


Figure 31. Chrome double-glazed plate temperature.

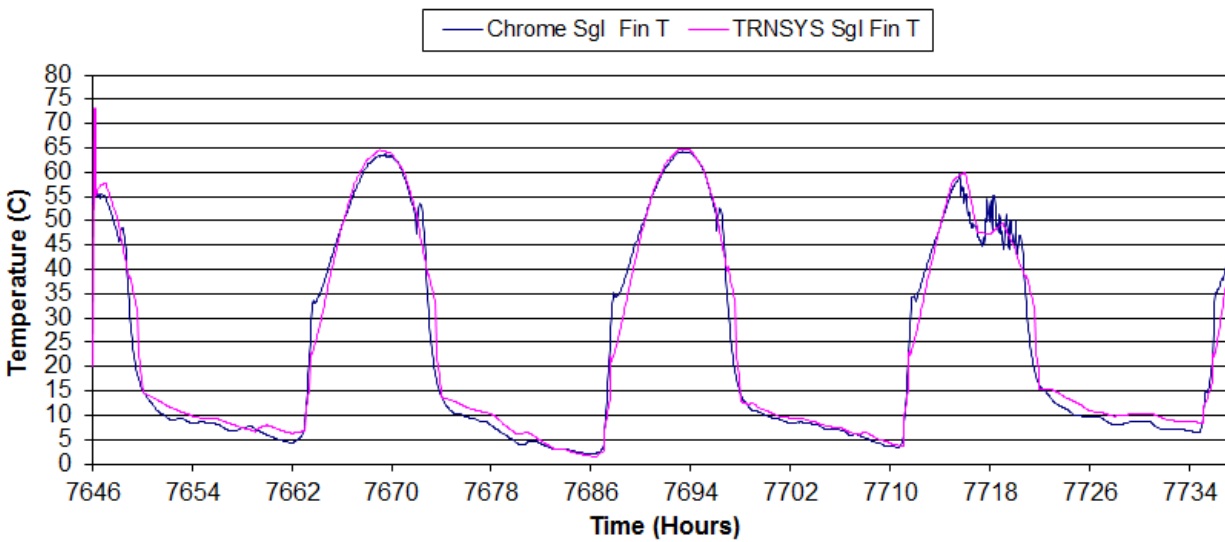


Figure 32. Chrome single-glazed plate temperature.

Figure 33 and Figure 34 present the comparisons of the predicted and measured glazing temperatures of the single- and double-glazed collectors. As can be seen, and which was seen with the tests of the other collectors, the nighttime sky temperature estimation errors produce some errors that are not of consequence to this application. Overall the predictions are reasonably accurate, with a slight time lag.

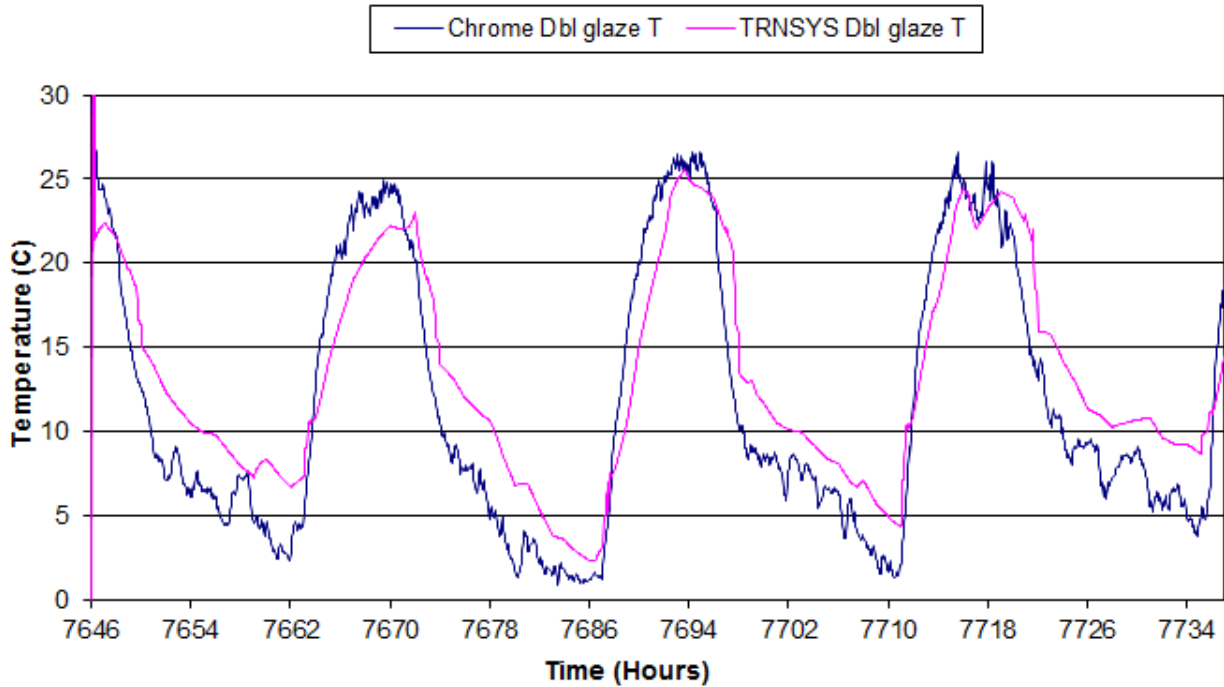


Figure 33. Glazing temperature comparison of the chrome double-glazed collector.

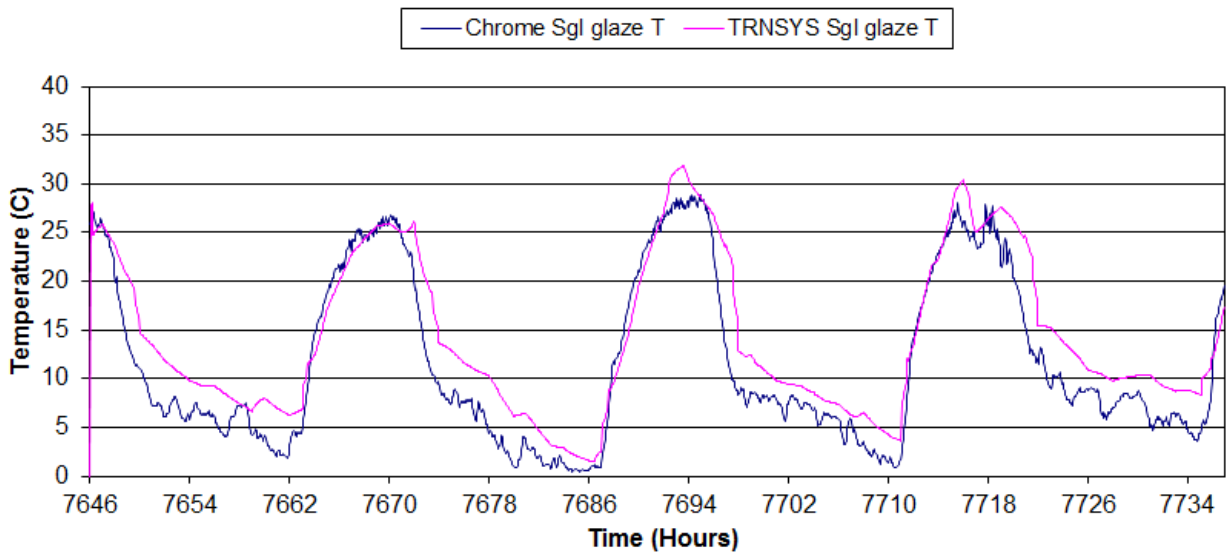


Figure 34. Glazing temperature of the chrome single-glazed collector.

A TYPE 1237 water tank model from TRNSYS 17 was used in the model. TYPE 1237 is a water tank with a wraparound heat exchanger that is identical to the one in the test bed. The parameters of the TYPE 1237 are listed in Table 9. The water tank top temperature is shown in Figure 35, the water tank node 6 temperature is shown in Figure 36, and the water tank node 8 temperature is shown in Figure 37. Comparing measured water tank temperatures with those predicted by TRNSYS, the error is small and acceptable.

Table 9. Water Tank TYPE 1237 Parameters.

Parameter	Value	Unit
Number of tank nodes	8	
Number of ports	1	
Number of miscellaneous heat flows	0	
Tank volume	0.297	M ³
Tank height	1.4	M
Fluid specific heat	4.19	kJ/kg.K
Fluid density	1000	Kg/m ³
Fluid thermal conductivity	2.14	kJ/hr.m.K
Fluid viscosity	3.21	Kg/m.hr
Fluid thermal expansion coefficient	0.00026	1/K
HX fluid specific heat	3.747	kJ/kg.K
HX fluid density	1041	Kg/m ³
HX fluid thermal conductivity	1.224	kJ/hr.m.K
HX fluid viscosity	8.21	Kg/m.hr
Top-loss coefficient	2	kJ/hr.m ² .K
Edge-loss coefficient for node-1	2	kJ/hr.m ² .K
Edge-loss coefficient for node-2	2	kJ/hr.m ² .K
Edge-loss coefficient for node-3	2	kJ/hr.m ² .K
Edge-loss coefficient for node-4	2	kJ/hr.m ² .K
Edge-loss coefficient for node-5	2	kJ/hr.m ² .K
Edge-loss coefficient for node-6	2	kJ/hr.m ² .K
Edge-loss coefficient for node-7	2	kJ/hr.m ² .K
Edge-loss coefficient for node-8	2	kJ/hr.m ² .K
Bottom-loss coefficient	2	kJ/hr.m ² .K
HX loss coefficient	2	kJ/hr.m ² .K
Additional thermal conductivity	0	kJ/hr.m ² .K

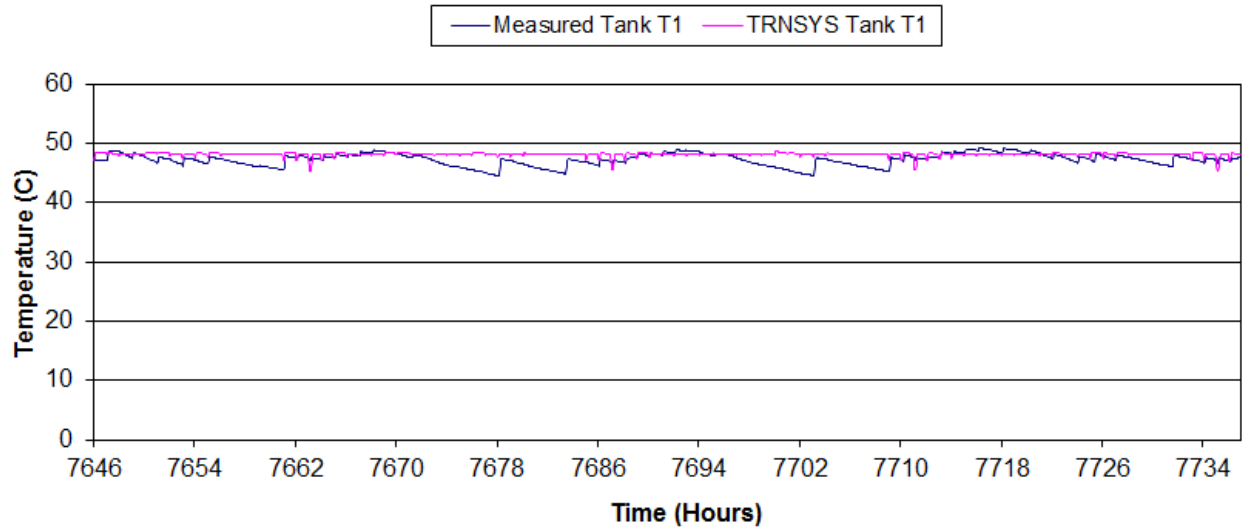


Figure 35. Water tank top temperature.

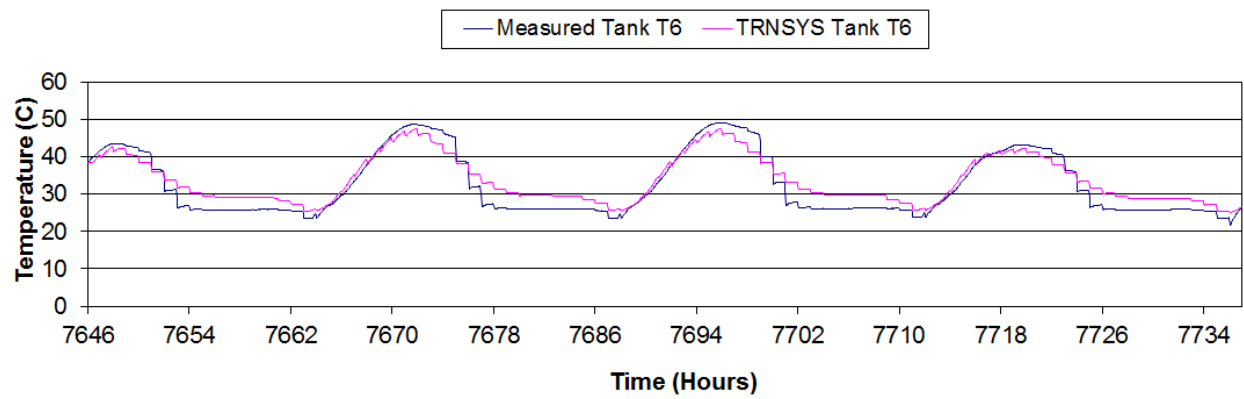


Figure 36. Water tank node 6 temperature.

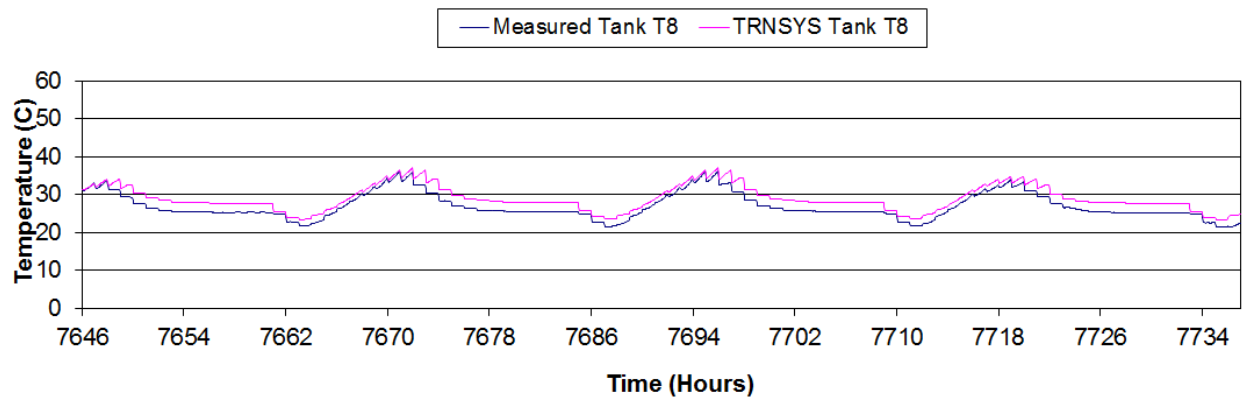


Figure 37. Water tank node 8 temperature.

Figure 38 presents a comparison of the predicted and measured useful energy gain by the double-glazed collector. As can be seen, the overall trends are reasonably accurate, with a slight time lag. Since the two collectors were run in parallel for this experiment, there are heat losses at the point at which the two collector outlets are mixed before they return to the tank in a single pipe. Thus, the simulation value is slightly higher than the measured value.

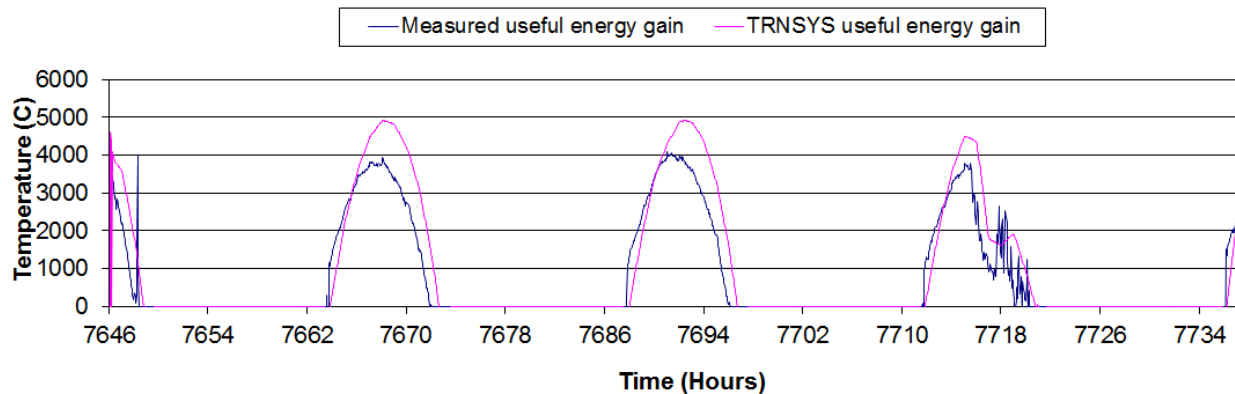


Figure 38. Useful energy gain by the collectors.

Sensitivity Analysis

An analysis was conducted to determine the sensitivity of the TRNSYS model output predictions to various collector parameters. This information is useful to determine which parameters are most significant relative to the accuracy of the overall prediction of energy performance of the system, which is a key parameter in accurately estimating glazing temperatures. The analysis focused on the painted fin single-glazed collector model. The results are assumed to apply to the other collector types.

Five parameters were considered for this analysis: plate emissivity, plate absorptance, glass emissivity, index of refraction of cover material influence the solar irradiance transmission, and absorptance by the plate and cover. The overall heat loss coefficient (a lumped parameter) incorporates the top, bottom, and edge-loss coefficient. The back and edge heat loss coefficient influence the overall heat loss by the collector to the environment. The influence of these five parameters on the collector plate temperature, collector glazing temperature, and collector useful energy gain is shown in Figures 39, 40, and 41 respectively.

Sensitivity studies were conducted for predictions of the plate temperature, which is a major driver of the glazing temperature. As shown in Figure 39, the plate temperature is most sensitive to the plate absorptance. Changes in the plate absorptance from 0.95 to 0.75 produce 15% increases in the plate peak temperatures (0.75 and 0.95 are in what would be an extended range of the plate absorptance). The plate temperature is less affected by changes in the plate or glass emissivity, the back or edge heat loss coefficient, or the index of refraction of cover material.

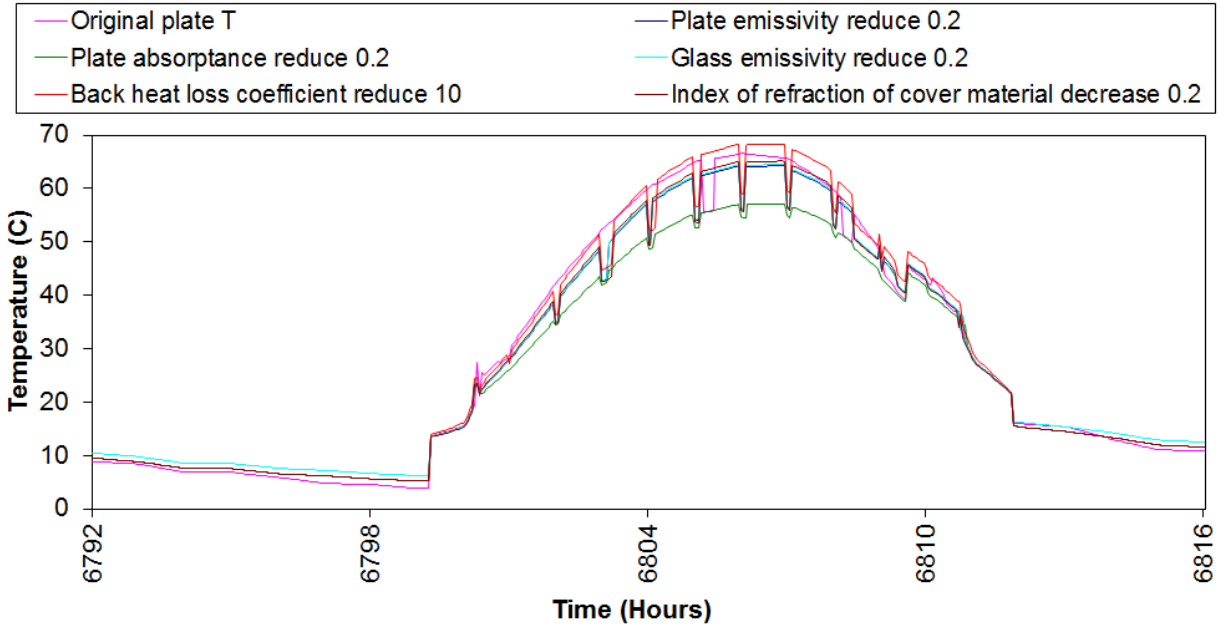


Figure 39. Sensitivity analysis for the collector plate temperature.

As shown in Figure 40, the glazing temperature is most sensitive to the index of refraction of cover material and back or edge heat loss coefficient. A change in the index of refraction of the cover material from 1.526 to 1.326 will force 10% increases in the predicted glazing temperature (1.526 and 1.326 are typical values for the glazing material refractive index). A change in the back heat loss coefficients from 15 kJ/hr.m².K to 5 kJ/hr.m².K will create 15% increases in the predicted plate temperature. The original edge heat loss coefficient is 18 kJ/hr.m².K and the top heat loss coefficient is calculated by empirical equations, which are included in Appendix B. The glazing temperatures are only slightly affected by plate emissivity, plate absorptance, and glass emissivity.

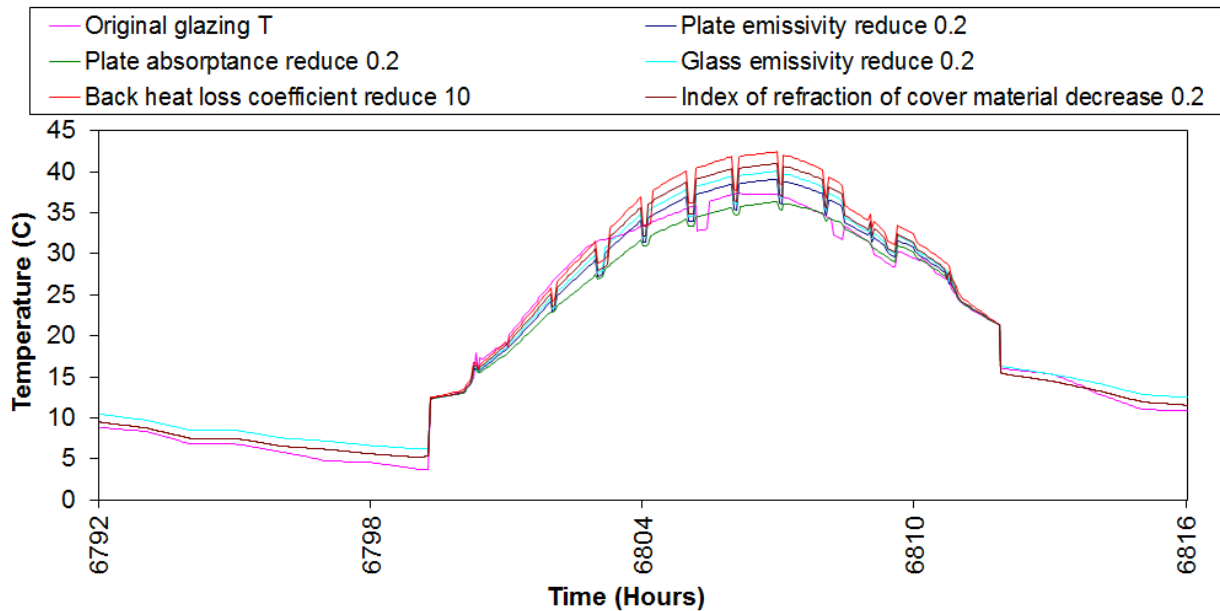


Figure 40. Sensitivity analysis for the collector glazing temperature.

Figure 41 shows the results of the tests for the collector's useful energy gain and it shows that it is most sensitive to the index of refraction of glazing material and back heat loss coefficient. Changes in the back loss coefficient from 15 kJ/hr.m².K to 5 kJ/hr.m².K produces increases in the predicted total energy by about 20%. Changes in the refraction of the glazing material, plate emissivity, plate absorptance, or glass emissivity will influence the useful energy gain by about 9% to 14%.

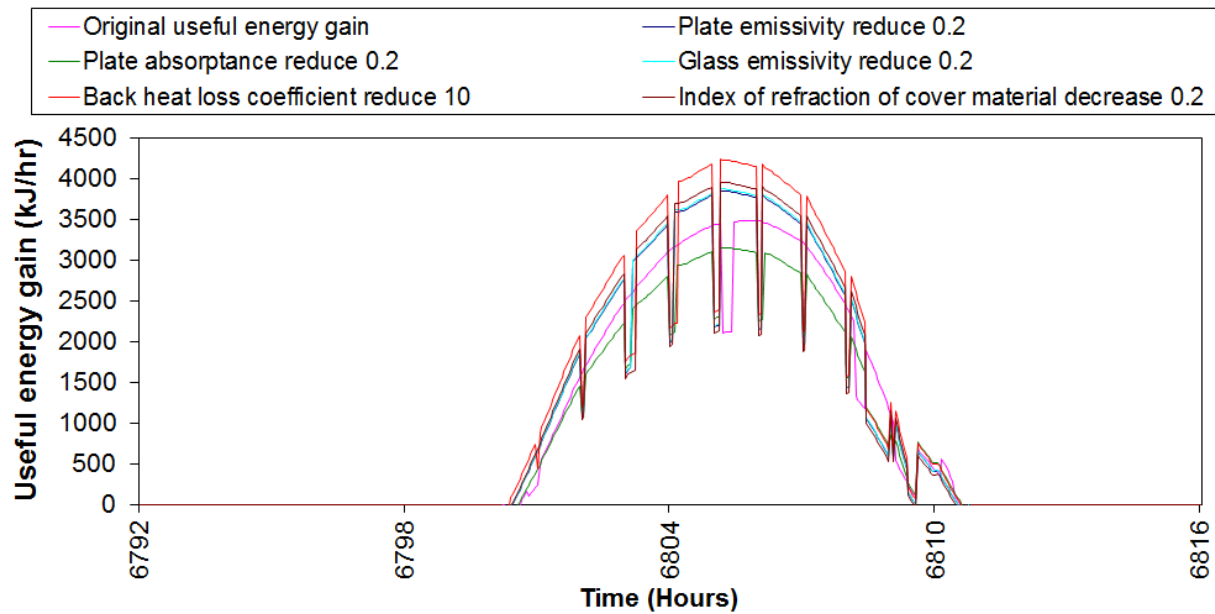


Figure 41. Sensitivity analysis for the useful energy gain.

Summary of the Glazing Model Development Work

The TRNSYS models developed in this work were verified to predict with reasonable accuracy the collector plate and glazing temperatures of the four collectors under test. On the day of a flyover of a collector area the glazing model can be run given the actual and expected ambient conditions. The range of glazing temperatures can be predicted for the expected types of collectors and these predictions can be used to fix the operational parameters of the IR camera.

Based on the sensitivity analysis, the most important parameter affecting accuracy of predictions relating to this work include the glazing index of refraction, the edge and back loss coefficients, and the glazing emissivity. Thus, in modeling the glazing temperature, these parameters are most important to be estimated accurately.

SECTION 8. CONCLUSIONS AND RECOMMENDATIONS

The following conclusions are drawn from the experiments.

1. The experiments confirm the applicability of using photometric methods to identify non-operating SHW collectors in the field. Applying techniques that are similar to the ones used in the experiment will likely identify non-operating collectors with a low rate of error, perhaps less than 15% (a qualitative estimate based on consensus of the experimental team). There are, however, technical challenges remaining in the implementation of the methodology and some field experimentation will be required before it can be routinely applied with confidence. Some of the technical challenges include the selection of the appropriate camera lens, mounting and adjusting the camera on the aircraft used in a flyover, adjustments of the camera recording parameters, and the selection of the aircraft height for overflying an area.
2. Distinguishing collectors from other architectural features could be especially difficult in field application because customary details that appear in the visible spectral range are lost in the IR range. Roof windows, for example, might be easily identified in a visible light photo but could be difficult to identify in an IR record. It is likely that a pair of cameras—one to record visible images and one to record the IR information— will be needed to accomplish the two-fold task of identifying collectors and subsequently determining their operational states.
3. False positive indications could be a confounding factor in applying the technique, but their rate of occurrence can be mitigated by collecting image data in the mid-morning time period. A false positive indication is one in which a normally non-operating collector is presumed to be in a non-operational state because fluid was not flowing in it when the photos were recorded. For example, it is possible that a collector is not operating because the storage tank was saturated with heat, a normal condition that can occur when a home is not occupied for some reason. However, a large majority of collectors will normally be operating in the morning, shortly after the solar radiation levels in the plane of the collectors are sufficiently high to heat the panel. In the morning period most SHW systems will have been cooling during the night and the associated storage tank will have experienced draws from the normal morning loads in the home. Therefore, it is likely that the controller will have activated the solar loop pump. This is especially true in cool weather conditions because many solar storage tanks are in unheated garages.

Integral collector systems will represent another confounding factor because these systems have no pump or solar loop. The collector itself is the storage medium for these systems; thus the collectors are normally in a warm to hot condition, especially when there have been no draws or small draws. However, in the area of likely application for this technique, such as the Phoenix, Arizona, area, few of these collectors have been installed relative to the number of pumped systems.

4. There is sufficient thermal inertia in the collectors so that variation in the glazing temperature, the parameter that is most critical to the technique, will not vary sufficiently to affect the accuracy of the methodology. Thus, the photometric technique will be applicable in both sunny conditions (100% clear) and mostly sunny conditions ($\leq 25\%$ cloud cover).
5. Camera resolution is not expected to be an issue in the application of the photometric technique, especially if the overflights are conducted at a height of less than 91 meters, which is typical for a helicopter, the most likely conveyance for the recording cameras. However, a higher quality camera might produce acceptable results from flights at higher altitudes, which would allow more data to be collected per flyover event.
6. The experimental results show that the collector plate and glazing temperatures can be predicted with accuracy sufficient for photometric applications. The model can be run given the ambient conditions on the day that a flyover of an area is planned. The range of glazing temperatures can be predicted for the expected types of collectors and these predictions can be used to fix the operational parameters of the IR camera.
7. Based on the sensitivity analysis conducted as part of the modeling effort, the most important parameter affecting accuracy of predictions relating to this work include the glazing index of refraction, the edge and back loss coefficients, and the glazing emissivity. Thus, in modeling the glazing temperature, these parameters are most important to be estimated accurately.

The following are recommendations and considerations regarding the application of the photometric methodology in the field.

1. An IR camera with a resolution higher than the one used in the experiments is suggested because it would provide more flexibility in selecting the overflight altitudes.
2. Experiments should be conducted to determine the best optical and recording settings to achieve optimal results. Other experiments will be needed to determine the optimal speed of the flyover craft for recording images.
3. The glazing model should be used to predict the expected range of glazing temperatures for the ambient conditions during a flyover. These predictions should be used as guidance in setting the operational parameters of the IR camera.
4. The directional emissivity of collector glazing materials must be considered when applying this methodology, especially when interpreting IR images that were taken at very shallow angles from the collector surfaces. In such cases, collectors may appear cooler than they really are, and a stagnation condition may be missed. To correct this problem, the gain in the camera could be adjusted, but may result in false positives. A balance between the two requirements should be carefully identified.
5. The initial application of the technique should incorporate a manual identification technique to distinguish the operational status of collector systems. The records of both the visible and IR images can be reviewed simultaneously by a human analyst and non-operating collectors identified. Using this approach, costs can be minimized while determining the efficacy of the methodology. Later, more advanced automated techniques can be developed and applied, if warranted.

6. The first application for the technique should focus on determining the accuracy of the method based on ground truth information. This will involve identifying the specific address for a suspected non-operating collector so that a physical inspection of the site can be conducted to confirm the determination. Methods developed by UNM's Earth Data Analysis Center may be most applicable to this problem.
7. After the technique has been verified, then it can be applied as a sampling method in which a statistically relevant number of systems will be photographed and the results used to determine the operational status of many others that were not sampled. If the error rate is calculated based on ground truth tests, statistical sampling methodology can be subsequently applied to future sampling procedures to ensure that the resulting failure estimates can be used to predict the failure rates in the population of fielded collectors with a fixed level of error.

APPENDIX A. Matlab Code

```
% SolarCollector.m
% -----
%
% Simple first-order solar collector model (M-file called by TRNSYS type 155)
%
% Data passed from / to TRNSYS
% -----
%
% trnTime (1x1)      : simulation time
% trnInfo (15x1)    : TRNSYS info array
% trnInputs (n1x1)  : TRNSYS inputs
% trnStartTime (1x1) : TRNSYS Simulation Start time
% trnStopTime (1x1) : TRNSYS Simulation Stop time
% trnTimeStep (1x1) : TRNSYS Simulation time step
% mFileErrorCode (1x1) : Error code for this m-file. It is set to 1 by TRNSYS and the m-file should set it to 0 at the
%                       end to indicate that the call was successful. Any non-zero value will stop the simulation
% trnOutputs (nOx1) : TRNSYS outputs
%
%
% Notes:
% -----
%
% You can use the values of trnInfo(7), trnInfo(8) and trnInfo(13) to identify the call (e.g. first iteration, etc.)
% Real-time controllers (callingMode = 10) will only be called once per time step with trnInfo(13) = 1 (after
% convergence)
%
% The number of inputs is given by the size of trnInputs and by trnInfo(3)
% The number of expected outputs is given by trnInfo(6)
% -----
% This example implements a very simple solar collector model. The component is iterative (should be called at
% each
% TRNSYS call)
%
% trnInputs
% -----
%
% trnInputs(1) : T, collector outlet temperature
% trnInputs(2) : T, water tank top temperature
% trnInputs(3) : T, water tank bottom temperature
% trnInputs(4) : forcing function
% trnInputs(5) : T, outside ambient temperature
%
% trnOutputs
%
% trnOutputs(1) : pump on/off signal
% trnOutputs(2) : sky temperature
%
% MKu, October 2004
% -----
```

```
% TRNSYS sets mFileErrorCode = 1 at the beginning of the M-File for error detection
```

```

% This file increments mFileErrorCode at different places. If an error occurs in the m-file the last successful step
will
% be indicated by mFileErrorCode, which is displayed in the TRNSYS error message
% At the very end, the m-file sets mFileErrorCode to 0 to indicate that everything was OK

```

```

mFileErrorCode = 100 % Beginning of the m-file

```

```

% --- Solar collector parameters-----
% -----

```

```

mFileErrorCode = 110 % After setting parameters

```

```

% --- Process Inputs -----
% -----

```

```

T_coll_out = trnInputs(1);
Tank_top_T = trnInputs(2);
Tank_bot_T = trnInputs(3);
Forcing_func = trnInputs(4);
Ambient_T = trnInputs(5);
T_dp=5;

```

```

mFileErrorCode = 120 % After processing inputs

```

```

% --- First call of the simulation: initial time step (no iterations) -----
% -----
% (note that Matlab is initialized before this at the info(7) = -1 call, but the m-file is not called)

```

```

if ( (trnInfo(7) == 0) & (trnTime-trnStartTime < 1e-6) )

```

```

    % This is the first call (Counter will be incremented later for this very first call)
    nCall = 0;

```

```

    % This is the first time step
    nStep = 1;

```

```

    % Initialize history of the variables for plotting at the end of the simulation
    nTimeSteps = (trnStopTime-trnStartTime)/trnTimeStep + 1;
    history.onoff = zeros(nTimeSteps,1);
    history.en = zeros(nTimeSteps,1);

```

```

    % No return, we will calculate the solar collector performance during this call
    mFileErrorCode = 130 % After initialization

```

```

end

```

```

% --- Very last call of the simulation (after the user clicks "OK"): Do nothing -----
% -----

```

```

if ( trnInfo(8) == -1 )

    mFileErrorCode = 1000;

    mFileErrorCode = 0; % Tell TRNSYS that we reached the end of the m-file without errors
    return

end

% --- Post convergence calls: store values -----
% -----

if (trnInfo(13) == 1)

    mFileErrorCode = 140; % Beginning of a post-convergence call

    history.onoff(nStep) = on_pump;
    history.en(nStep) = en_pump;
%   history.func(nStep) = Forcing_func;

    mFileErrorCode = 0; % Tell TRNSYS that we reached the end of the m-file without errors
    return % Do not update outputs at this call

end

% --- All iterative calls -----
% -----

% --- If this is a first call in the time step, increment counter ---

if ( trnInfo(7) == 0 )
    nStep = nStep+1;
end

% --- Get TRNSYS Inputs ---

nI = trnInfo(3); % For bookkeeping
nO = trnInfo(6); % For bookkeeping

T_coll_out = trnInputs(1);
Tank_top_T = trnInputs(2);
Tank_bot_T = trnInputs(3);
Forcing_func = trnInputs(4);
Ambient_T = trnInputs(5);

mFileErrorCode = 150; % After reading inputs

% --- Calculate solar collector performance ---
dis_pump = 0;
en_pump = 1;

```

```

on_pump = 1;

if Tank_bot_T > 60
    dis_pump == 1;
else
    dis_pump == 0;
end

if T_coll_out > 97
    dis_pump == 1;
else
    dis_pump == 0;
end

if nStep == 1
    if (Tank_bot_T < 55) && (T_coll_out < 97)
        en_pump = 1;
    else
        en_pump = 0;
    end
end

if en_pump == 1
    if (T_coll_out - Tank_bot_T) > 7 % 7*1.8
        on_pump = 1*Forcing_func;
    else
        on_pump = 0;
    end
else
    on_pump = 0;
end

if history.onoff(nStep-1) > 0
    if (T_coll_out - Tank_bot_T) > 0%3
        on_pump = 1*Forcing_func;
    else
        on_pump = 0;
    end
end

sky_T = 0.0552*(Ambient_T+273.15)^1.5-273.15;

% --- Set outputs ---
trnOutputs(1) = on_pump;
trnOutputs(2) = sky_T;

mFileErrorCode = 0; % Tell TRNSYS that we reached the end of the m-file without errors
return

```

APPENDIX B. Single-Glaze Collector TYPE 244–Fortran Code

```
      SUBROUTINE TYPE244 (TIME,XIN,OUT,T,DTDT,PAR,INFO,ICNTRL,*)
C*****
C Object: a
C Simulation Studio Model: Type244
C
C Author: b
C Editor: d
C Date:      January 2010 last modified: January 2010
C
C
C ***
C *** Model Parameters
C ***
C          Collector length      m [0.;+Inf]
C          Collector width       m [0.;+Inf]
C          Absorber plate thickness m [0.;+Inf]
C          Conductivity of absorber material kJ/hr.m.K [0.;+Inf]
C          Number of tubes       - [1;+Inf]
C          Inner tube diameter    m [0.;+Inf]
C          Outer tube diameter    m [0.;+Inf]
C          Bond resistance        h.m2.K/kJ [0.;+Inf]
C          Fluid specific heat    kJ/kg.K [0.0;+Inf]
C          Absorptance of the absorber plate Fraction [0.;1.]
C          Emissivity of the absorber plate Fraction [0.;1.]
C          Top loss mode- [1;1]
C          Number of identical covers - [0;+Inf]
C          Index of refraction of cover material - [0.;+Inf]
C          Extinction coefficient, thickness product - [0.;1.]
C          Emissivity of the glass Fraction [0.;1.]
C          Plate spacing m [0.;+Inf]
C          Glass spacing m [0.;+Inf]
C
C ***
C *** Model Inputs
C ***
C          Inlet temperature      C [-Inf;+Inf]
C          Inlet flow rate kg/hr [0.0;+Inf]
C          Ambient temperature    C [-Inf;+Inf]
C          Sky temperature        C [-Inf;+Inf]
C          Wind velocity m/s [0.;+Inf]
C          Incident solar radiation kJ/hr.m^2 [0.0;+Inf]
C          Total horizontal radiation kJ/hr.m^2 [0.0;+Inf]
C          Horizontal diffuse radiation kJ/hr.m^2 [0.0;+Inf]
C          Ground reflectance Fraction [0.0;1.0]
```

```

C          Incidence angle      degrees [-360;+360]
C          Collector slope      degrees [-360;+360]
C          Back heat loss coefficient    kJ/hr.m^2.K [0.;+Inf]
C          Edge heat loss coefficient    kJ/hr.m^2.K [0.;+Inf]
C          Fluid heat transfer coefficient - [0.;+Inf]
C          Atmospheric pressure atm [0.;+Inf]

```

```
C ***
```

```
C *** Model Outputs
```

```
C ***
```

```

C          Temperature at outlet C [-Inf;+Inf]
C          Flow rate at outlet    kg/hr [0.0;+Inf]
C          Useful energy gain    kJ/hr [0.0;+Inf]
C          Collector F'    - [-Inf;+Inf]
C          Collector FR    - [-Inf;+Inf]
C          Collector top losses  kJ/hr [-Inf;+Inf]
C          Collector back losses kJ/hr [-Inf;+Inf]
C          Collector edge losses kJ/hr [-Inf;+Inf]
C          Mean fluid temperature    C [-Inf;+Inf]
C          Plate temperature    C [-Inf;+Inf]
C          Incidence angle modifier  - [-Inf;+Inf]
C          Overall heat loss coefficient kJ/hr.m^2.K [-Inf;+Inf]
C          RHO DIFFUSE OUT - [-Inf;+Inf]
C          TAU ALPHA OUT  - [-Inf;+Inf]
C          First glass temperature    C [-Inf;+Inf]
C          Second glass temperature   C [-Inf;+Inf]

```

```
C ***
```

```
C *** Model Derivatives
```

```
C ***
```

```
C (Comments and routine interface generated by TRNSYS Studio)
```

```
C*****
```

```

C  TRNSYS access functions (allow to access TIME etc.)
C  USE TrnsysConstants
C  USE TrnsysFunctions

```

```
C-----
```

```
----
```

```

C  REQUIRED BY THE MULTI-DLL VERSION OF TRNSYS
C  !DEC$ATTRIBUTES DLLEXPORT :: TYPE244                                !SET THE
C  CORRECT TYPE NUMBER HERE

```

```
C-----
```

```
----
```

```

C-----
----
C  TRNSYS DECLARATIONS
    IMPLICIT NONE          !REQUIRES THE USER TO DEFINE ALL VARIABLES
    BEFORE USING THEM

        DOUBLE PRECISION XIN !THE ARRAY FROM WHICH THE INPUTS TO THIS
    TYPE WILL BE RETRIEVED
        DOUBLE PRECISION OUT !THE ARRAY WHICH WILL BE USED TO STORE THE
    OUTPUTS FROM THIS TYPE
        DOUBLE PRECISION TIME      !THE CURRENT SIMULATION TIME - YOU
    MAY USE THIS VARIABLE BUT DO NOT SET IT!
        DOUBLE PRECISION PAR !THE ARRAY FROM WHICH THE PARAMETERS
    FOR THIS TYPE WILL BE RETRIEVED
        DOUBLE PRECISION STORED !THE STORAGE ARRAY FOR HOLDING
    VARIABLES FROM TIMESTEP TO TIMESTEP
        DOUBLE PRECISION T          !AN ARRAY CONTAINING THE RESULTS
    FROM THE DIFFERENTIAL EQUATION SOLVER
        DOUBLE PRECISION DTD T      !AN ARRAY CONTAINING THE
    DERIVATIVES TO BE PASSED TO THE DIFF.EQ. SOLVER
        DOUBLE PRECISION TIME0,TFINAL,DELT
        INTEGER*4 INFO(15)          !THE INFO ARRAY STORES AND PASSES
    VALUABLE INFORMATION TO AND FROM THIS TYPE
        INTEGER*4 NP,NI,NOUT,ND     !VARIABLES FOR THE MAXIMUM NUMBER
    OF PARAMETERS,INPUTS,OUTPUTS AND DERIVATIVES
        INTEGER*4 NPAR,NIN,NDER     !VARIABLES FOR THE CORRECT NUMBER
    OF PARAMETERS,INPUTS,OUTPUTS AND DERIVATIVES
        INTEGER*4 IUNIT,ITYPE      !THE UNIT NUMBER AND TYPE NUMBER FOR THIS
    COMPONENT
        INTEGER*4 ICNTRL            !AN ARRAY FOR HOLDING VALUES OF
    CONTROL FUNCTIONS WITH THE NEW SOLVER
        INTEGER*4 NSTORED          !THE NUMBER OF VARIABLES THAT WILL
    BE PASSED INTO AND OUT OF STORAGE
        CHARACTER*3 OCHECK         !AN ARRAY TO BE FILLED WITH THE
    CORRECT VARIABLE TYPES FOR THE OUTPUTS
        CHARACTER*3 YCHECK        !AN ARRAY TO BE FILLED WITH THE
    CORRECT VARIABLE TYPES FOR THE INPUTS
C-----
----

C-----
----
C  USER DECLARATIONS - SET THE MAXIMUM NUMBER OF PARAMETERS (NP),
    INPUTS (NI),
C  OUTPUTS (NOUT), AND DERIVATIVES (ND) THAT MAY BE SUPPLIED FOR THIS
    TYPE

```

```

PARAMETER (NP=18,NI=16,NOUT=16,ND=0,NSTORED=0)
C-----
----

C-----
----
C  REQUIRED TRNSYS DIMENSIONS
  DIMENSION XIN(NI),OUT(NOUT),PAR(NP),YCHECK(NI),OCHECK(NOUT),
    1  STORED(NSTORED),T(ND),DTDT(ND)
  INTEGER NITEMS
C-----
----
C-----
----
C  ADD DECLARATIONS AND DEFINITIONS FOR THE USER-VARIABLES HERE

C  PARAMETERS
  DOUBLE PRECISION
RDCONV,PI,LENGTH,WIDTH,THICK_ABSORBER,K_ABSORBER,
  1  DIA_TUBE_I,DIA_TUBE_O,R_BOND,CP_FLUID,ABS_PLATE,EMISS_PLATE,
  1
REFR_INDEX,KL_COVER,RHO_DIFFUSE,TAU_ALPHA_N,TAU_ALPHA,M,X,FR,
  1  T_FLUID_IN,FLOW_IN,T_AMB,T_SKY,WINDSPEED,GT,GH,GDH,RHO_GROUND,
  1
ANGLE_INC,SLOPE,U_BACK,U_EDGES,H_FLUID,U_TOP,U_L,AREA,W,XKAT,
  1
EFFSKY,EFFGND,COSSLOPE,FSKY,FGND,GDSKY,GDGND,XKATDS,XKATDG,
  1  XKATB,T_FLUID_OUT,T_PLATE_MEAN,H_CONV,H_RAD,H_RADIATION,T_K,
  1  T_FLUID_MEAN,TMC,TAC,F,C,STF1,STF2,F_PRIME,QU,Q_TOP,Q_BACK,
  1  Q_EDGES,FPP,T_FLUID_OUT_OLD,P_ATM,P_KPA,T_GLASS1,T_GLASS2,
  1
T_GLASS1_OLD,T_GLASS2_OLD,AIRPROPS,EMISS_GLASS,HR_PC1,HR_C1C2,
  1
HR_C2A,RADCOEPP,RADCOEPA,H_RAD_GRAY,K_VISC,THERM_COND,PRAND_N,
  1
T_PG1,T_G1G2,RAYLEIGH_PG1,RAYLEIGH_G1G2,RAYLEIGH_NUM,DETA_TPG1,
  1  DETA_TG1G2,DIS_PG1,DIS_G1G2,NUSSELT_PG1,NUSSELT_G1G2,
  1  H_CONV_PG1,H_CONV_G1G2,NUSSELT_NUM,H_CONVECTION,HR_C1A,
  1  T_PLATE_MEAN_OLD,U_TOP2,FLAG
  INTEGER N_TUBES,ICOUNT,MODE_U,N_COVERS
  CHARACTER(LEN=MAXMESSAGELENGTH)::MESSAGE1,MESSAGE2
  DIMENSION AIRPROPS(5)
C-----
----

```

C RETRIEVE THE CURRENT VALUES OF THE INPUTS TO THIS MODEL FROM THE XIN ARRAY IN SEQUENTIAL ORDER

C Inlet_temperature=XIN(1)
C Inlet_flow_rate=XIN(2)
C Ambient_temperature=XIN(3)
C Sky_temperature=XIN(4)
C Wind_velocity=XIN(5)
C Incident_solar_radiation=XIN(6)
C Total_horizontal_radiation=XIN(7)
C Horizontal_diffuse_radiation=XIN(8)
C Ground_reflectance=XIN(9)
C Incidence_angle=XIN(10)
C Collector_slope=XIN(11)
C Back_heat_loss_coefficient=XIN(12)
C Edge_heat_loss_coefficient=XIN(13)
C Fluid_heat_transfer_coefficient=XIN(14)
C Atmospheric_pressure=XIN(15)
 IUNIT=INFO(1)
 ITYPE=INFO(2)

C-----

C-----

C DATA STATEMENTS
 DATA RDCONV/0.017453292/
 DATA MESSAGE1/'An illegal overall heat transfer coefficient has been calculated by the model. Please check the entering information carefully.'/

 DATA MESSAGE2/'Unable to find a stable solution for the mean plate temperature.'/

C-----

C GET GLOBAL TRNSYS SIMULATION VARIABLES
 TIME0=getSimulationStartTime()
 TFINAL=getSimulationStopTime()
 DELT=getSimulationTimeStep()

C-----

C-----

```

C  SET THE VERSION INFORMATION FOR TRNSYS
  IF(INFO(7).EQ.-2) THEN
    INFO(12)=16
    RETURN 1
  ENDIF
C-----
----
C-----
----
C  DO ALL THE VERY LAST CALL OF THE SIMULATION MANIPULATIONS HERE
  IF (INFO(8).EQ.-1) THEN
    RETURN 1
  ENDIF
C-----
----
C-----
----
C  PERFORM ANY 'AFTER-ITERATION' MANIPULATIONS THAT ARE REQUIRED
  HERE
C  e.g. save variables to storage array for the next timestep
  IF (INFO(13).GT.0) THEN
    NITEMS=0
C    STORED(1)=... (if NITEMS > 0)
C    CALL setStorageVars(STORED,NITEMS,INFO)
    RETURN 1
  ENDIF
C
C-----
----
C-----
----
C  DO ALL THE VERY FIRST CALL OF THE SIMULATION MANIPULATIONS HERE
  IF (INFO(7).EQ.-1) THEN

C    SET SOME INFO ARRAY VARIABLES TO TELL THE TRNSYS ENGINE HOW
  THIS TYPE IS TO WORK
    INFO(6)=NOUT
    INFO(9)=1
    INFO(10)=0 !STORAGE FOR VERSION 16 HAS BEEN CHANGED

C    SET THE REQUIRED NUMBER OF INPUTS, PARAMETERS AND DERIVATIVES
  THAT THE USER SHOULD SUPPLY IN THE INPUT FILE

```

C IN SOME CASES, THE NUMBER OF VARIABLES MAY DEPEND ON THE VALUE OF PARAMETERS TO THIS MODEL....

```
NIN=NI
  NPAR=NP
  NDER=ND
```

C SET THE REQUIRED NUMBER OF INPUTS BASED ON THE MODE FOR THE TOP LOSSES

```
  MODE_U=JFIX(PAR(12)+0.5)
  IF(MODE_U.LT.1) CALL TYPECK(-4,INFO,0,12,0)
  IF(MODE_U.GT.2) CALL TYPECK(-4,INFO,0,12,0)
```

```
  IF(MODE_U.EQ.1) THEN
    NIN=15
  ELSE
    NIN=16
  ENDIF
```

C CALL THE TYPE CHECK SUBROUTINE TO COMPARE WHAT THIS COMPONENT REQUIRES TO WHAT IS SUPPLIED IN

```
C THE TRNSYS INPUT FILE
  CALL TYPECK(1,INFO,NIN,NPAR,NDER)
```

C SET THE YCHECK AND OCHECK ARRAYS TO CONTAIN THE CORRECT VARIABLE TYPES FOR THE INPUTS AND OUTPUTS

```
  DATA YCHECK/'TE1','MF1','TE1','TE1','VE1','IR1','IR1','IR1',
    1 'DM1','DG1','DG1','HT1','HT1','HT1','PR4','HT1'/
  DATA OCHECK/'TE1','MF1','PW1','DM1','DM1','PW1','PW1','PW1',
    1 'TE1','TE1','DM1','HT1','DM1','DM1','TE1','TE1'/
```

C CALL THE RCHECK SUBROUTINE TO SET THE CORRECT INPUT AND OUTPUT TYPES FOR THIS COMPONENT

```
C CALL RCHECK(INFO,YCHECK,OCHECK)
```

C SET THE NUMBER OF STORAGE SPOTS NEEDED FOR THIS COMPONENT
NITEMS=0

```
C CALL setStorageSize(NITEMS,INFO)
```

C RETURN TO THE CALLING PROGRAM
RETURN 1

```
  ENDIF
```

```
C-----
----
```

```

C-----
----
C DO ALL OF THE INITIAL TIMESTEP MANIPULATIONS HERE - THERE ARE NO
ITERATIONS AT THE INITIAL TIME
  IF (TIME .LT. (getSimulationStartTime() +
    .getSimulationTimeStep()/2.D0)) THEN

C   SET THE UNIT NUMBER FOR FUTURE CALLS
  IUNIT=INFO(1)
  ITYPE=INFO(2)

C   READ IN THE VALUES OF THE PARAMETERS IN SEQUENTIAL ORDER
  LENGTH=PAR(1)
    WIDTH=PAR(2)
    THICK_ABSORBER=PAR(3)
    K_ABSORBER=PAR(4)
    N_TUBES=JFIX(PAR(5)+0.5)
    DIA_TUBE_I=PAR(6)
    DIA_TUBE_O=PAR(7)
    R_BOND=PAR(8)
    CP_FLUID=PAR(9)
    ABS_PLATE=PAR(10)
    EMISS_PLATE=PAR(11)
    MODE_U=JFIX(PAR(12)+0.5)
    N_COVERS=JFIX(PAR(13)+0.5)
    REFR_INDEX=PAR(14)
  KL_COVER=PAR(15)
    EMISS_GLASS=PAR(16)
  DIS_PG1=PAR(17)
    DIS_G1G2=PAR(18)

C   CHECK THE PARAMETERS FOR PROBLEMS AND RETURN FROM THE
SUBROUTINE IF AN ERROR IS FOUND
  IF(LENGTH.LE.0.) CALL TYPECK(-4,INFO,0,1,0)
  IF(WIDTH.LE.0.) CALL TYPECK(-4,INFO,0,2,0)
  IF(THICK_ABSORBER.LE.0.) CALL TYPECK(-4,INFO,0,3,0)
  IF(K_ABSORBER.LE.0.) CALL TYPECK(-4,INFO,0,4,0)
  IF(N_TUBES.LT.1) CALL TYPECK(-4,INFO,0,5,0)
  IF(DIA_TUBE_I.LE.0.) CALL TYPECK(-4,INFO,0,6,0)
  IF(DIA_TUBE_O.LE.0.) CALL TYPECK(-4,INFO,0,7,0)
  IF(DIA_TUBE_O*DBLE(N_TUBES).GT.WIDTH)
    1 CALL TYPECK(-4,INFO,0,7,0)
  IF(DIA_TUBE_O.LE.DIA_TUBE_I) CALL TYPECK(-4,INFO,0,7,0)
  IF(R_BOND.LT.0.) CALL TYPECK(-4,INFO,0,8,0)
  IF(CP_FLUID.LE.0.) CALL TYPECK(-4,INFO,0,9,0)
  IF(ABS_PLATE.LE.0.) CALL TYPECK(-4,INFO,0,10,0)

```

```

IF(ABS_PLATE.GT.1.) CALL TYPECK(-4,INFO,0,10,0)
IF(EMISS_PLATE.LT.0.) CALL TYPECK(-4,INFO,0,11,0)
IF(EMISS_PLATE.GT.1.) CALL TYPECK(-4,INFO,0,11,0)
IF(N_COVERS.LT.0.) CALL TYPECK(-4,INFO,0,13,0)
IF(REFR_INDEX.LE.0.) CALL TYPECK(-4,INFO,0,14,0)
IF(KL_COVER.LT.0.) CALL TYPECK(-4,INFO,0,15,0)

C   SET THE TRANSMITTANCE-ABSORPTANCE PRODUCT AT NORMAL
INCIDENCE AND THE REFLECTANCE OF THE COVER
C   TO DIFFUSE RADIATION
      RHO_DIFFUSE=-1.
      TAU_ALPHA_N=TAU_ALPHA(N_COVERS,0.D0,KL_COVER,REFR_INDEX,
C   TAU_ALPHA_N=TAU_ALPHA(N_COVERS,45.,KL_COVER,REFR_INDEX,
      1 ABS_PLATE,RHO_DIFFUSE)

C   CHECK THE PARAMETERS FOR PROBLEMS AND RETURN FROM THE
SUBROUTINE IF AN ERROR IS FOUND
C   IF(...) CALL TYPECK(-4,INFO,0,"BAD PARAMETER #",0)

C   PERFORM ANY REQUIRED CALCULATIONS TO SET THE INITIAL VALUES OF
THE OUTPUTS HERE
C   PERFORM ANY REQUIRED CALCULATIONS TO SET THE INITIAL VALUES OF
THE OUTPUTS HERE
      OUT(1)=XIN(1)
      OUT(2:8)=0.
      OUT(9)=XIN(1)
      OUT(10)=XIN(1)
      OUT(11:12)=0.
      OUT(13)=RHO_DIFFUSE
      OUT(14)=TAU_ALPHA_N
      OUT(15)=0.
      OUT(16)=0.

C   PERFORM ANY REQUIRED CALCULATIONS TO SET THE INITIAL STORAGE
VARIABLES HERE
      NITEMS=0
C   STORED(1)=...

C   PUT THE STORED ARRAY IN THE GLOBAL STORED ARRAY
C   CALL setStorageVars(STORED,NITEMS,INFO)

C   RETURN TO THE CALLING PROGRAM
      RETURN 1

ENDIF

```

```

C-----
----

C-----
----
C   *** ITS AN ITERATIVE CALL TO THIS COMPONENT ***
C-----
----

C-----
----
C   RE-READ THE PARAMETERS IF ANOTHER UNIT OF THIS TYPE HAS BEEN
CALLED
    IF(INFO(1).NE.IUNIT) THEN

C   RESET THE UNIT NUMBER
        IUNIT=INFO(1)
        ITYPE=INFO(2)

C   READ IN THE VALUES OF THE PARAMETERS IN SEQUENTIAL ORDER
    LENGTH=PAR(1)
        WIDTH=PAR(2)
        THICK_ABSORBER=PAR(3)
        K_ABSORBER=PAR(4)
        N_TUBES=JFIX(PAR(5)+0.5)
        DIA_TUBE_I=PAR(6)
        DIA_TUBE_O=PAR(7)
        R_BOND=PAR(8)
        CP_FLUID=PAR(9)
        ABS_PLATE=PAR(10)
        EMISS_PLATE=PAR(11)
        MODE_U=JFIX(PAR(12)+0.5)
        N_COVERS=JFIX(PAR(13)+0.5)
        REFR_INDEX=PAR(14)
        KL_COVER=PAR(15)
        EMISS_GLASS=PAR(16)
        DIS_PG1=PAR(17)
        DIS_G1G2=PAR(18)

    ENDIF

C-----
----

C-----
----

```

C RETRIEVE THE CURRENT VALUES OF THE INPUTS TO THIS MODEL FROM THE
XIN ARRAY IN SEQUENTIAL ORDER

```
T_FLUID_IN=XIN(1)
  FLOW_IN=XIN(2)
  T_AMB=XIN(3)
  T_SKY=XIN(4)
  WINDSPEED=XIN(5)
GT=XIN(6)
GH=XIN(7)
GDH=XIN(8)
RHO_GROUND=XIN(9)
ANGLE_INC=XIN(10)
SLOPE=XIN(11)
U_BACK=XIN(12)
U_EDGES=XIN(13)
H_FLUID=XIN(14)
  P_ATM=XIN(15)
```

```
IF(MODE_U.GT.1) THEN
  U_TOP=XIN(16)
  ELSE
    U_TOP=0.
  ENDIF
```

C-----

C-----

C CHECK THE INPUTS FOR PROBLEMS

```
IF(FLOW_IN.LT.0.) CALL TYPECK(-3,INFO,2,0,0)
IF(WINDSPEED.LT.0.) CALL TYPECK(-3,INFO,5,0,0)
IF(GT.LT.0.) CALL TYPECK(-3,INFO,6,0,0)
IF(GH.LT.0.) CALL TYPECK(-3,INFO,7,0,0)
IF(GDH.LT.0.) CALL TYPECK(-3,INFO,8,0,0)
IF(RHO_GROUND.LT.0.) CALL TYPECK(-3,INFO,9,0,0)
IF(RHO_GROUND.GT.1.) CALL TYPECK(-3,INFO,9,0,0)
IF(U_BACK.LT.0.) CALL TYPECK(-3,INFO,12,0,0)
IF(U_EDGES.LT.0.) CALL TYPECK(-3,INFO,13,0,0)
IF(H_FLUID.LE.0.) CALL TYPECK(-3,INFO,14,0,0)
IF(P_ATM.LE.0.) CALL TYPECK(-3,INFO,15,0,0)
IF(P_ATM.GT.5.) CALL TYPECK(-3,INFO,15,0,0)
IF(U_TOP.LT.0.) CALL TYPECK(-3,INFO,16,0,0)
  IF(ERRORFOUND()) RETURN 1
```

C-----

```

C-----
----
C  RETRIEVE THE VALUES IN THE STORAGE ARRAY FOR THIS ITERATION
C  NITEMS=
C    CALL getStorageVars(STORED,NITEMS,INFO)
C  STORED(1)=
C-----
----
C-----
----
C  CHECK THE INPUTS FOR PROBLEMS
C  IF(...) CALL TYPECK(-3,INFO,'BAD INPUT #',0,0)
C    IF(IERROR.GT.0) RETURN 1
C-----
----
C-----
----
C  *** PERFORM ALL THE CALCULATION HERE FOR THIS MODEL. ***
C-----
----

C          ADD YOUR COMPONENT EQUATIONS HERE; BASICALLY THE
EQUATIONS THAT WILL
C          CALCULATE THE OUTPUTS BASED ON THE PARAMETERS AND THE
INPUTS.    REFER TO
C          CHAPTER 3 OF THE TRNSYS VOLUME 1 MANUAL FOR DETAILED
INFORMATION ON
C          WRITING TRNSYS COMPONENTS.

C  SET PI
  PI=4*DATAN(1.D0)

C  CALCULATE THE AREA OF THE COLLECTOR
  AREA=LENGTH*WIDTH

C  CALCULATE THE TUBE-TO-TUBE DISTANCE
  W=WIDTH/DBLE(N_TUBES)

C  RETRIEVE THE TRANSMITTANCE ABSORPTANCE PRODUCT AT NORMAL
INCIDENCE AND THE REFLECTANCE TO DIFFUSE
  RHO_DIFFUSE=OUT(13)
  TAU_ALPHA_N=OUT(14)

C  GET THE INCIDENCE ANGLE MODIFIER

```

```

IF(N_COVERS.LT.1) THEN
    XKAT=1.

    ELSE

C    USE THE RELATIONS OF BRANDEMUEHL TO GET THE EFFECTIVE INCIDENCE
    ANGLES FOR DIFFUSE RADIATION
    EFFSKY=59.68-0.1388*SLOPE+0.001497*SLOPE*SLOPE
    EFFGND=90.-0.5788*SLOPE+0.002693*SLOPE*SLOPE
    COSSLOPE=DCOS(SLOPE*RDCONV)
    FSKY=(1.+COSSLOPE)/2.
    FGND=(1.-COSSLOPE)/2.
    GDSKY=FSKY*GDH
    GDGND=RHO_GROUND*FGND*GH

C    USE THE TAU_ALPHA FUNCTION FOR THE COMPONENT IAM VALUES

XKATDS=TAU_ALPHA(N_COVERS,EFFSKY,KL_COVER,REFR_INDEX,ABS_PLATE,
    1    RHO_DIFFUSE)/TAU_ALPHA_N

XKATDG=TAU_ALPHA(N_COVERS,EFFGND,KL_COVER,REFR_INDEX,ABS_PLATE,
    1    RHO_DIFFUSE)/TAU_ALPHA_N
XKATB=TAU_ALPHA(N_COVERS,ANGLE_INC,KL_COVER,REFR_INDEX,
    1    ABS_PLATE,RHO_DIFFUSE)/TAU_ALPHA_N

C    CALCULATE THE OVERALL IAM
    IF(GT.GT.0.) THEN
        XKAT=(XKATB*(GT-GDSKY-
        GDGND)+XKATDS*GDSKY+XKATDG*GDGND)/GT
    ELSE
        XKAT=0.
    ENDIF
    ENDIF

C    GUESS AN OUTPUT TEMPERATURE
    T_FLUID_OUT=T_FLUID_IN

C    GUESS THE MEAN PLATE ND MEAN FLUID TEMPERATURES
    T_PLATE_MEAN=(T_FLUID_IN+T_FLUID_OUT)/2.
    T_FLUID_MEAN=(T_FLUID_IN+T_FLUID_OUT)/2.

C    GUESS THE GLASS1 TEMPERATURES
    T_GLASS1=T_PLATE_MEAN-10.

C    INITIALIZE A FEW VARIABLES
    ICOUNT=1

```

```
T_FLUID_OUT_OLD=T_FLUID_OUT
T_GLASS1_OLD=T_GLASS1
```

```
C SET THE TOP LOSS COEFFICIENT
100 IF(MODE_U.EQ.1) THEN
```

```
C SET THE TOP LOSS FROM CONVECTION AND RADIATION
IF(N_COVERS.LT.0.5) THEN
```

```
    P_KPA=P_ATM*101.325
    T_K=T_AMB+273.15
    CALL WINDCOEF(WINDSPEED,LENGTH,WIDTH,T_K,P_KPA,H_CONV)
    H_CONV=H_CONV*3.6 !CONVERT W/M2/K TO KJ/H/M2.K
```

```
    H_RAD=H_RADIATION(T_PLATE_MEAN,T_SKY,EMISS_PLATE)
    U_TOP=H_CONV+H_RAD
```

```
C USE KLEIN'S TOP LOSS CORRELATION
```

```
    ELSE
    LENGTH=PAR(1)
    WIDTH=PAR(2)
    THICK_ABSORBER=PAR(3)
    K_ABSORBER=PAR(4)
    N_TUBES=JFIX(PAR(5)+0.5)
    DIA_TUBE_I=PAR(6)
    DIA_TUBE_O=PAR(7)
    R_BOND=PAR(8)
    CP_FLUID=PAR(9)
    ABS_PLATE=PAR(10)
    EMISS_PLATE=PAR(11)
    MODE_U=JFIX(PAR(12)+0.5)
    N_COVERS=JFIX(PAR(13)+0.5)
    REFR_INDEX=PAR(14)
    KL_COVER=PAR(15)
    EMISS_GLASS=PAR(16)
    DIS_PG1=PAR(17)
    DIS_G1G2=PAR(18)
```

```
T_FLUID_IN=XIN(1)
FLOW_IN=XIN(2)
T_AMB=XIN(3)
T_SKY=XIN(4)
WINDSPEED=XIN(5)
GT=XIN(6)
GH=XIN(7)
GDH=XIN(8)
```

```

RHO_GROUND=XIN(9)
ANGLE_INC=XIN(10)
SLOPE=XIN(11)
U_BACK=XIN(12)
U_EDGES=XIN(13)
H_FLUID=XIN(14)
  P_ATM=XIN(15)

```

```

C   SET THE MEAN FLUID TEMPERATURE

```

```

      P_KPA=P_ATM*101.325
      T_K=T_AMB+273.15

```

```

IF (GT.GE.50.) THEN

```

```

CALL WINDCOEF(WINDSPEED,LENGTH,WIDTH,T_K,P_KPA,H_CONV)

```

```

1   HR_PC1=H_RAD_GRAY(T_PLATE_MEAN,T_GLASS1,EMISS_PLATE,
      EMISS_GLASS)/3.6

```

```

      HR_C1A=H_RADIATION(T_GLASS1,T_SKY,EMISS_GLASS)/3.6

```

```

      T_PG1=(T_PLATE_MEAN+T_GLASS1)/2.+273.15
      DELTA_TPG1=DABS(T_PLATE_MEAN-T_GLASS1)

```

```

      CALL AIRPROP(T_PG1,P_KPA,AIRPROPS)
      K_VISC=AIRPROPS(2)
      THERM_COND=AIRPROPS(4)
      PRAND_N=AIRPROPS(3)

```

```

1   RAYLEIGH_PG1=RAYLEIGH_NUM(T_PG1,DELTA_TPG1,DIS_PG1,K_VISC,
      PRAND_N)

```

```

      NUSSELT_PG1=NUSSELT_NUM(RAYLEIGH_PG1,SLOPE)
      H_CONV_PG1=H_CONVECTION(NUSSELT_PG1,THERM_COND,DIS_PG1)

```

```

      U_TOP=1./(H_CONV_PG1+HR_PC1)+1./(H_CONV+HR_C1A)
      U_TOP=1./U_TOP

```

```

1   T_GLASS1=T_PLATE_MEAN-U_TOP*(T_PLATE_MEAN-T_AMB)/
      (H_CONV_PG1+HR_PC1)

```

```

      U_TOP=U_TOP*3.6
      FLAG=EMISS_GLASS

```

```

ELSE

```

```

      FLAG=EMISS_GLASS
ENDIF

```

```

ENDIF

ELSE
  U_TOP=XIN(16)

ENDIF

C SET THE OVERALL LOSS COEFFICIENT
U_L=U_TOP+U_BACK+U_EDGES
  IF(U_L.LE.0.) THEN
    CALL MESSAGES(-1,MESSAGE1,'FATAL',IUNIT,ITYPE)
    RETURN 1
  ENDIF

C SET SOME REQUIRED VARIABLES
M=(U_L/K_ABSORBER/THICK_ABSORBER)**0.5
  F=DTANH((M*(W-DIA_TUBE_O)/2.))/(M*(W-DIA_TUBE_O)/2.)
X=1./(U_L*(DIA_TUBE_O+(W-DIA_TUBE_O)*F))+R_BOND+
  1 1./PI/DIA_TUBE_I/H_FLUID

C SET THE COLLECTOR EFFICIENCY FACTOR
  F_PRIME=1./U_L/W/X

C CALCULATE THE COLLECTOR HEAT REMOVAL FACTOR
IF(FLOW_IN.LE.0.) THEN
  FR=0.
ELSE
  FR=FLOW_IN*CP_FLUID/AREA/U_L*(1.-DEXP(-AREA*U_L*F_PRIME/
  1 FLOW_IN/CP_FLUID))
ENDIF

C CALCULATE THE COLLECTOR USEFUL ENERGY GAIN
QU=AREA*FR*(GT*TAU_ALPHA_N*XKAT-U_L*(T_FLUID_IN-T_AMB))

C CALCULATE THE COLLECTOR OUTLET TEMPERATURE
IF (FLOW_IN.LE.0.) THEN

  T_FLUID_OUT=GT*XKAT*TAU_ALPHA_N/U_L+T_AMB

  T_PLATE_MEAN=T_FLUID_OUT
  T_FLUID_MEAN=T_FLUID_OUT

C IF ((T_PLATE_MEAN-T_AMB).LE.0.) THEN
  IF (GT.LE.50.) THEN
    T_PLATE_MEAN_OLD=T_PLATE_MEAN

```

```

        P_KPA=P_ATM*101.325
        T_K=T_AMB+273.15
        CALL WINDCOEF(WINDSPEED,LENGTH,WIDTH,T_K,P_KPA,H_CONV)
150   T_PLATE_MEAN=T_AMB-EMISS_GLASS*5.67D-8*((T_PLATE_MEAN+273.15)
1     **4-(T_SKY+273.15)**4)/H_CONV
        IF (DABS(T_PLATE_MEAN-T_PLATE_MEAN_OLD).GT.0.001) THEN
            T_PLATE_MEAN_OLD=T_PLATE_MEAN
            GOTO 150
        ENDIF

        H_CONV=H_CONV*3.6
        T_GLASS1=T_PLATE_MEAN

        T_FLUID_OUT=(T_PLATE_MEAN+T_AMB)/2.
        T_FLUID_MEAN=T_PLATE_MEAN

        Q_TOP=AREA*H_CONV*(T_AMB-T_GLASS1)
        Q_BACK=AREA*U_BACK*(T_PLATE_MEAN-T_AMB)
        Q_EDGES=AREA*U_EDGES*(T_PLATE_MEAN-T_AMB)
        ENDIF

    ELSE
        T_FLUID_OUT=T_FLUID_IN+QU/FLOW_IN/CP_FLUID
        FPP=FR/F_PRIME
        T_FLUID_MEAN=T_FLUID_IN+QU/AREA*(1.-FPP)/FR/U_L
        T_PLATE_MEAN=T_FLUID_IN+QU/AREA*(1.-FR)/FR/U_L

        Q_TOP=AREA*U_TOP*(T_PLATE_MEAN-T_AMB)
        Q_BACK=AREA*U_BACK*(T_PLATE_MEAN-T_AMB)
        Q_EDGES=AREA*U_EDGES*(T_PLATE_MEAN-T_AMB)

    ENDIF

C   SEE IF CONVERGENCE HAS BEEN REACHED
    IF((ICOUNT.LT.200).AND.(DABS(T_FLUID_OUT_OLD-T_FLUID_OUT
1   ).GT.0.001).AND.(DABS(T_GLASS1_OLD-T_GLASS1).GT.0.001)) THEN
        ICOUNT=ICOUNT+1
        T_FLUID_OUT_OLD=T_FLUID_OUT
        T_GLASS1_OLD=T_GLASS1
        GOTO 100
    ENDIF

C   WARN THE USER IF CONVERGENCE HAS NOT BEEN OBTAINED
    IF(ICOUNT.GE.50) THEN
        CALL MESSAGES(-1,MESSAGE2,'WARNING',IUNIT,ITYPE)
    ENDIF

```

```

C-----
----

C-----
----

C-----
----

C  SET THE STORAGE ARRAY AT THE END OF THIS ITERATION IF NECESSARY
C  NITEMS=
C  STORED(1)=
C    CALL setStorageVars(STORED,NITEMS,INFO)
C-----
----

C-----
----

C  REPORT ANY PROBLEMS THAT HAVE BEEN FOUND USING CALLS LIKE THIS:
C  CALL MESSAGES(-1,'put your message here','MESSAGE',IUNIT,ITYPE)
C  CALL MESSAGES(-1,'put your message here','WARNING',IUNIT,ITYPE)
C  CALL MESSAGES(-1,'put your message here','SEVERE',IUNIT,ITYPE)
C  CALL MESSAGES(-1,'put your message here','FATAL',IUNIT,ITYPE)
C-----
----

C-----
----

C  SET THE OUTPUTS FROM THIS MODEL IN SEQUENTIAL ORDER AND GET OUT

OUT(1)=T_FLUID_OUT
OUT(2)=FLOW_IN
OUT(3)=QU
  OUT(4)=F_PRIME
  OUT(5)=FR
  OUT(6)=Q_TOP
  OUT(7)=Q_BACK
  OUT(8)=Q_EDGES
  OUT(9)=T_FLUID_MEAN
  OUT(10)=T_PLATE_MEAN
  OUT(11)=XKAT
  OUT(12)=U_L
  OUT(13)=RHO_DIFFUSE
  OUT(14)=TAU_ALPHA_N
  OUT(15)=T_GLASS1
  OUT(16)=FLAG

```

```
C-----  
----  
C  EVERYTHING IS DONE - RETURN FROM THIS SUBROUTINE AND MOVE ON  
  RETURN 1  
  END  
C-----  
----
```


APPENDIX C. Double-Glaze Collector TYPE 242–Fortran Code

```
SUBROUTINE TYPE242 (TIME,XIN,OUT,T,DTDT,PAR,INFO,ICNTRL,*)
C*****
C Object: a
C Simulation Studio Model: Type242
C
C Author: b
C Editor: d
C Date:      January 2010 last modified: January 2010
C
C
C ***
C *** Model Parameters
C ***
C          Collector length      m [0.;+Inf]
C          Collector width       m [0.;+Inf]
C          Absorber plate thickness m [0.;+Inf]
C          Conductivity of absorber material kJ/hr.m.K [0.;+Inf]
C          Number of tubes       - [1;+Inf]
C          Inner tube diameter    m [0.;+Inf]
C          Outer tube diameter    m [0.;+Inf]
C          Bond resistance        h.m2.K/kJ [0.;+Inf]
C          Fluid specific heat    kJ/kg.K [0.0;+Inf]
C          Absorptance of the absorber plate Fraction [0.;1.]
C          Emissivity of the absorber plate Fraction [0.;1.]
C          Top loss mode- [1;1]
C          Number of identical covers - [0;+Inf]
C          Index of refraction of cover material - [0.;+Inf]
C          Extinction coefficient, thickness product - [0.;1.]
C          Emissivity of the glass Fraction [0.;1.]
C          Plate spacing m [0.;+Inf]
C          Glass spacing m [0.;+Inf]
C
C ***
C *** Model Inputs
C ***
C          Inlet temperature      C [-Inf;+Inf]
C          Inlet flow rate kg/hr [0.0;+Inf]
C          Ambient temperature    C [-Inf;+Inf]
C          Sky temperature        C [-Inf;+Inf]
C          Wind velocity m/s [0.;+Inf]
C          Incident solar radiation kJ/hr.m^2 [0.0;+Inf]
C          Total horizontal radiation kJ/hr.m^2 [0.0;+Inf]
C          Horizontal diffuse radiation kJ/hr.m^2 [0.0;+Inf]
C          Ground reflectance Fraction [0.0;1.0]
```

```

C          Incidence angle      degrees [-360;+360]
C          Collector slope      degrees [-360;+360]
C          Back heat loss coefficient    kJ/hr.m^2.K [0.;+Inf]
C          Edge heat loss coefficient    kJ/hr.m^2.K [0.;+Inf]
C          Fluid heat transfer coefficient - [0.;+Inf]
C          Atmospheric pressure atm [0.;+Inf]

```

```
C ***
```

```
C *** Model Outputs
```

```
C ***
```

```

C          Temperature at outlet C [-Inf;+Inf]
C          Flow rate at outlet    kg/hr [0.0;+Inf]
C          Useful energy gain    kJ/hr [0.0;+Inf]
C          Collector F'    - [-Inf;+Inf]
C          Collector FR    - [-Inf;+Inf]
C          Collector top losses  kJ/hr [-Inf;+Inf]
C          Collector back losses kJ/hr [-Inf;+Inf]
C          Collector edge losses kJ/hr [-Inf;+Inf]
C          Mean fluid temperature    C [-Inf;+Inf]
C          Plate temperature    C [-Inf;+Inf]
C          Incidence angle modifier  - [-Inf;+Inf]
C          Overall heat loss coefficient kJ/hr.m^2.K [-Inf;+Inf]
C          RHO DIFFUSE OUT - [-Inf;+Inf]
C          TAU ALPHA OUT  - [-Inf;+Inf]
C          First glass temperature    C [-Inf;+Inf]
C          Second glass temperature   C [-Inf;+Inf]

```

```
C ***
```

```
C *** Model Derivatives
```

```
C ***
```

```
C (Comments and routine interface generated by TRNSYS Studio)
```

```
C*****
```

```

C  TRNSYS access functions (allow to access TIME etc.)
C  USE TrnsysConstants
C  USE TrnsysFunctions

```

```
C-----
```

```
----
```

```

C  REQUIRED BY THE MULTI-DLL VERSION OF TRNSYS
C  !DEC$ATTRIBUTES DLLEXPORT :: TYPE242                                !SET THE
C  CORRECT TYPE NUMBER HERE

```

```
C-----
```

```
----
```

```

C-----
----
C  TRNSYS DECLARATIONS
    IMPLICIT NONE          !REQUIRES THE USER TO DEFINE ALL VARIABLES
    BEFORE USING THEM

        DOUBLE PRECISION XIN !THE ARRAY FROM WHICH THE INPUTS TO THIS
    TYPE WILL BE RETRIEVED
        DOUBLE PRECISION OUT !THE ARRAY WHICH WILL BE USED TO STORE THE
    OUTPUTS FROM THIS TYPE
        DOUBLE PRECISION TIME      !THE CURRENT SIMULATION TIME - YOU
    MAY USE THIS VARIABLE BUT DO NOT SET IT!
        DOUBLE PRECISION PAR !THE ARRAY FROM WHICH THE PARAMETERS
    FOR THIS TYPE WILL BE RETRIEVED
        DOUBLE PRECISION STORED !THE STORAGE ARRAY FOR HOLDING
    VARIABLES FROM TIMESTEP TO TIMESTEP
        DOUBLE PRECISION T          !AN ARRAY CONTAINING THE RESULTS
    FROM THE DIFFERENTIAL EQUATION SOLVER
        DOUBLE PRECISION DTD T      !AN ARRAY CONTAINING THE
    DERIVATIVES TO BE PASSED TO THE DIFF.EQ. SOLVER
        DOUBLE PRECISION TIME0,TFINAL,DELT
        INTEGER*4 INFO(15)          !THE INFO ARRAY STORES AND PASSES
    VALUABLE INFORMATION TO AND FROM THIS TYPE
        INTEGER*4 NP,NI,NOUT,ND     !VARIABLES FOR THE MAXIMUM NUMBER
    OF PARAMETERS,INPUTS,OUTPUTS AND DERIVATIVES
        INTEGER*4 NPAR,NIN,NDER     !VARIABLES FOR THE CORRECT NUMBER
    OF PARAMETERS,INPUTS,OUTPUTS AND DERIVATIVES
        INTEGER*4 IUNIT,ITYPE !THE UNIT NUMBER AND TYPE NUMBER FOR THIS
    COMPONENT
        INTEGER*4 ICNTRL            !AN ARRAY FOR HOLDING VALUES OF
    CONTROL FUNCTIONS WITH THE NEW SOLVER
        INTEGER*4 NSTORED          !THE NUMBER OF VARIABLES THAT WILL
    BE PASSED INTO AND OUT OF STORAGE
        CHARACTER*3 OCHECK         !AN ARRAY TO BE FILLED WITH THE
    CORRECT VARIABLE TYPES FOR THE OUTPUTS
        CHARACTER*3 YCHECK         !AN ARRAY TO BE FILLED WITH THE
    CORRECT VARIABLE TYPES FOR THE INPUTS
C-----
----

C-----
----
C  USER DECLARATIONS - SET THE MAXIMUM NUMBER OF PARAMETERS (NP),
    INPUTS (NI),
C  OUTPUTS (NOUT), AND DERIVATIVES (ND) THAT MAY BE SUPPLIED FOR THIS
    TYPE

```

```

PARAMETER (NP=18,NI=16,NOUT=16,ND=0,NSTORED=0)
C-----
----

C-----
----
C  REQUIRED TRNSYS DIMENSIONS
  DIMENSION XIN(NI),OUT(NOUT),PAR(NP),YCHECK(NI),OCHECK(NOUT),
    1  STORED(NSTORED),T(ND),DTDT(ND)
  INTEGER NITEMS
C-----
----
C-----
----
C  ADD DECLARATIONS AND DEFINITIONS FOR THE USER-VARIABLES HERE

C  PARAMETERS
  DOUBLE PRECISION
RDCONV,PI,LENGTH,WIDTH,THICK_ABSORBER,K_ABSORBER,
  1  DIA_TUBE_I,DIA_TUBE_O,R_BOND,CP_FLUID,ABS_PLATE,EMISS_PLATE,
  1
REFR_INDEX,KL_COVER,RHO_DIFFUSE,TAU_ALPHA_N,TAU_ALPHA,M,X,FR,
  1  T_FLUID_IN,FLOW_IN,T_AMB,T_SKY,WINDSPEED,GT,GH,GDH,RHO_GROUND,
  1
ANGLE_INC,SLOPE,U_BACK,U_EDGES,H_FLUID,U_TOP,U_L,AREA,W,XKAT,
  1
EFFSKY,EFFGND,COSSLOPE,FSKY,FGND,GDSKY,GDGND,XKATDS,XKATDG,
  1  XKATB,T_FLUID_OUT,T_PLATE_MEAN,H_CONV,H_RAD,H_RADIATION,T_K,
  1  T_FLUID_MEAN,TMC,TAC,F,C,STF1,STF2,F_PRIME,QU,Q_TOP,Q_BACK,
  1  Q_EDGES,FPP,T_FLUID_OUT_OLD,P_ATM,P_KPA,T_GLASS1,T_GLASS2,
  1
T_GLASS1_OLD,T_GLASS2_OLD,AIRPROPS,EMISS_GLASS,HR_PC1,HR_C1C2,
  1
HR_C2A,RADCOEPP,RADCOEPA,H_RAD_GRAY,K_VISC,THERM_COND,PRAND_N,
  1
T_PG1,T_G1G2,RAYLEIGH_PG1,RAYLEIGH_G1G2,RAYLEIGH_NUM,DETA_TPG1,
  1  DETA_TG1G2,DIS_PG1,DIS_G1G2,NUSSELT_PG1,NUSSELT_G1G2,
  1  H_CONV_PG1,H_CONV_G1G2,NUSSELT_NUM,H_CONVECTION,
  1  T_PLATE_MEAN_OLD,U_TOP2
  INTEGER N_TUBES,ICOUNT,MODE_U,N_COVERS
  CHARACTER(LEN=MAXMESSAGELENGTH)::MESSAGE1,MESSAGE2
  DIMENSION AIRPROPS(5)
    IUNIT=INFO(1)
    ITYPE=INFO(2)

```

C-----

C-----

```
C DATA STATEMENTS
  DATA RDCONV/0.017453292/
    DATA MESSAGE1/'An illegal overall heat transfer coefficient has be
    1en calculated by the model. Please check the entering information
    1 carefully.'/
    DATA MESSAGE2/'Unable to find a stable solution for the mean plate
    1 temperature.'/
```

C-----

C-----

```
C GET GLOBAL TRNSYS SIMULATION VARIABLES
  TIME0=getSimulationStartTime()
  TFINAL=getSimulationStopTime()
  DELT=getSimulationTimeStep()
```

C-----

C-----

```
C SET THE VERSION INFORMATION FOR TRNSYS
  IF(INFO(7).EQ.-2) THEN
    INFO(12)=16
    RETURN 1
  ENDIF
```

C-----

C-----

```
C DO ALL THE VERY LAST CALL OF THE SIMULATION MANIPULATIONS HERE
  IF (INFO(8).EQ.-1) THEN
    RETURN 1
  ENDIF
```

C-----

C-----

```

C PERFORM ANY 'AFTER-ITERATION' MANIPULATIONS THAT ARE REQUIRED
HERE
C e.g. save variables to storage array for the next timestep
  IF (INFO(13).GT.0) THEN
    NITEMS=0
C     STORED(1)=... (if NITEMS > 0)
C     CALL setStorageVars(STORED,NITEMS,INFO)
    RETURN 1
  ENDIF

C
C-----
----

C-----
----

C DO ALL THE VERY FIRST CALL OF THE SIMULATION MANIPULATIONS HERE
  IF (INFO(7).EQ.-1) THEN

C   SET SOME INFO ARRAY VARIABLES TO TELL THE TRNSYS ENGINE HOW
THIS TYPE IS TO WORK
  INFO(6)=NOUT
  INFO(9)=1
  INFO(10)=0 !STORAGE FOR VERSION 16 HAS BEEN CHANGED

C   SET THE REQUIRED NUMBER OF INPUTS, PARAMETERS AND DERIVATIVES
  THAT THE USER SHOULD SUPPLY IN THE INPUT FILE
C   IN SOME CASES, THE NUMBER OF VARIABLES MAY DEPEND ON THE VALUE
OF PARAMETERS TO THIS MODEL....
  NIN=NI
  NPAR=NP
  NDER=ND

C   SET THE REQUIRED NUMBER OF INPUTS BASED ON THE MODE FOR THE TOP
LOSSES
  MODE_U=JFIX(PAR(12)+0.5)
  IF(MODE_U.LT.1) CALL TYPECK(-4,INFO,0,12,0)
  IF(MODE_U.GT.2) CALL TYPECK(-4,INFO,0,12,0)

  IF(MODE_U.EQ.1) THEN
    NIN=15
  ELSE
    NIN=16
  ENDIF

```

```

C   CALL THE TYPE CHECK SUBROUTINE TO COMPARE WHAT THIS
COMPONENT REQUIRES TO WHAT IS SUPPLIED IN
C   THE TRNSYS INPUT FILE
      CALL TYPECK(1,INFO,NIN,NPAR,NDER)

C   SET THE YCHECK AND OCHECK ARRAYS TO CONTAIN THE CORRECT
VARIABLE TYPES FOR THE INPUTS AND OUTPUTS
      DATA YCHECK/'TE1','MF1','TE1','TE1','VE1','IR1','IR1','IR1',
1      'DM1','DG1','DG1','HT1','HT1','HT1','PR4','HT1'/
      DATA OCHECK/'TE1','MF1','PW1','DM1','DM1','PW1','PW1','PW1',
1      'TE1','TE1','DM1','HT1','DM1','DM1','TE1','TE1'/

C   CALL THE RCHECK SUBROUTINE TO SET THE CORRECT INPUT AND OUTPUT
TYPES FOR THIS COMPONENT
C   CALL RCHECK(INFO,YCHECK,OCHECK)

C   SET THE NUMBER OF STORAGE SPOTS NEEDED FOR THIS COMPONENT
NITEMS=0
C   CALL setStorageSize(NITEMS,INFO)

C   RETURN TO THE CALLING PROGRAM
RETURN 1

      ENDIF

C-----
----

C-----
----

C   DO ALL OF THE INITIAL TIMESTEP MANIPULATIONS HERE - THERE ARE NO
ITERATIONS AT THE INTIAL TIME
      IF (TIME .LT. (getSimulationStartTime() +
. getSimulationTimeStep()/2.D0)) THEN

C   SET THE UNIT NUMBER FOR FUTURE CALLS
      IUNIT=INFO(1)
      ITYPE=INFO(2)

C   READ IN THE VALUES OF THE PARAMETERS IN SEQUENTIAL ORDER
      LENGTH=PAR(1)
      WIDTH=PAR(2)
      THICK_ABSORBER=PAR(3)
      K_ABSORBER=PAR(4)
      N_TUBES=JFIX(PAR(5)+0.5)
      DIA_TUBE_I=PAR(6)
      DIA_TUBE_O=PAR(7)

```

```

R_BOND=PAR(8)
CP_FLUID=PAR(9)
ABS_PLATE=PAR(10)
EMISS_PLATE=PAR(11)
MODE_U=JFIX(PAR(12)+0.5)
N_COVERS=JFIX(PAR(13)+0.5)
REFR_INDEX=PAR(14)
KL_COVER=PAR(15)
  EMISS_GLASS=PAR(16)
DIS_PG1=PAR(17)
  DIS_G1G2=PAR(18)

```

C CHECK THE PARAMETERS FOR PROBLEMS AND RETURN FROM THE SUBROUTINE IF AN ERROR IS FOUND

```

IF(LENGTH.LE.0.) CALL TYPECK(-4,INFO,0,1,0)
IF(WIDTH.LE.0.) CALL TYPECK(-4,INFO,0,2,0)
IF(THICK_ABSORBER.LE.0.) CALL TYPECK(-4,INFO,0,3,0)
IF(K_ABSORBER.LE.0.) CALL TYPECK(-4,INFO,0,4,0)
IF(N_TUBES.LT.1) CALL TYPECK(-4,INFO,0,5,0)
IF(DIA_TUBE_I.LE.0.) CALL TYPECK(-4,INFO,0,6,0)
IF(DIA_TUBE_O.LE.0.) CALL TYPECK(-4,INFO,0,7,0)
IF(DIA_TUBE_O*DBLE(N_TUBES).GT.WIDTH)
  1 CALL TYPECK(-4,INFO,0,7,0)
IF(DIA_TUBE_O.LE.DIA_TUBE_I) CALL TYPECK(-4,INFO,0,7,0)
IF(R_BOND.LT.0.) CALL TYPECK(-4,INFO,0,8,0)
IF(CP_FLUID.LE.0.) CALL TYPECK(-4,INFO,0,9,0)
IF(ABS_PLATE.LE.0.) CALL TYPECK(-4,INFO,0,10,0)
IF(ABS_PLATE.GT.1.) CALL TYPECK(-4,INFO,0,10,0)
IF(EMISS_PLATE.LT.0.) CALL TYPECK(-4,INFO,0,11,0)
IF(EMISS_PLATE.GT.1.) CALL TYPECK(-4,INFO,0,11,0)
IF(N_COVERS.LT.0) CALL TYPECK(-4,INFO,0,13,0)
IF(REFR_INDEX.LE.0.) CALL TYPECK(-4,INFO,0,14,0)
IF(KL_COVER.LT.0.) CALL TYPECK(-4,INFO,0,15,0)

```

C SET THE TRANSMITTANCE-ABSORPTANCE PRODUCT AT NORMAL INCIDENCE AND THE REFLECTANCE OF THE COVER

C TO DIFFUSE RADIATION

```

RHO_DIFFUSE=-1.

```

```

TAU_ALPHA_N=TAU_ALPHA(N_COVERS,0.D0,KL_COVER,REFR_INDEX,
C   TAU_ALPHA_N=TAU_ALPHA(N_COVERS,45.,KL_COVER,REFR_INDEX,
  1   ABS_PLATE,RHO_DIFFUSE)

```

C CHECK THE PARAMETERS FOR PROBLEMS AND RETURN FROM THE SUBROUTINE IF AN ERROR IS FOUND

```

C   IF(...) CALL TYPECK(-4,INFO,0,"BAD PARAMETER #",0)

```

```

C   PERFORM ANY REQUIRED CALCULATIONS TO SET THE INITIAL VALUES OF
THE OUTPUTS HERE
C   PERFORM ANY REQUIRED CALCULATIONS TO SET THE INITIAL VALUES OF
THE OUTPUTS HERE
    OUT(1)=XIN(1)
    OUT(2:8)=0.
        OUT(9)=XIN(1)
        OUT(10)=XIN(1)
        OUT(11:12)=0.
        OUT(13)=RHO_DIFFUSE
        OUT(14)=TAU_ALPHA_N
        OUT(15)=0.
        OUT(16)=0.

C   PERFORM ANY REQUIRED CALCULATIONS TO SET THE INITIAL STORAGE
VARIABLES HERE
    NITEMS=0
C   STORED(1)=...

C   PUT THE STORED ARRAY IN THE GLOBAL STORED ARRAY
C   CALL setStorageVars(STORED,NITEMS,INFO)

C   RETURN TO THE CALLING PROGRAM
    RETURN 1

ENDIF
C-----
----

C-----
----

C   *** ITS AN ITERATIVE CALL TO THIS COMPONENT ***
C-----
----

C-----
----

C   RE-READ THE PARAMETERS IF ANOTHER UNIT OF THIS TYPE HAS BEEN
CALLED
    IF(INFO(1).NE.IUNIT) THEN

C   RESET THE UNIT NUMBER
        IUNIT=INFO(1)
        ITYPE=INFO(2)

C   READ IN THE VALUES OF THE PARAMETERS IN SEQUENTIAL ORDER

```

```

LENGTH=PAR(1)
  WIDTH=PAR(2)
  THICK_ABSORBER=PAR(3)
  K_ABSORBER=PAR(4)
  N_TUBES=JFIX(PAR(5)+0.5)
  DIA_TUBE_I=PAR(6)
  DIA_TUBE_O=PAR(7)
  R_BOND=PAR(8)
  CP_FLUID=PAR(9)
  ABS_PLATE=PAR(10)
  EMISS_PLATE=PAR(11)
  MODE_U=JFIX(PAR(12)+0.5)
  N_COVERS=JFIX(PAR(13)+0.5)
  REFR_INDEX=PAR(14)
  KL_COVER=PAR(15)
  EMISS_GLASS=PAR(16)
  DIS_PG1=PAR(17)
  DIS_G1G2=PAR(18)

```

```

ENDIF

```

```

C-----
----

```

```

C-----
----

```

```

C RETRIEVE THE CURRENT VALUES OF THE INPUTS TO THIS MODEL FROM THE
XIN ARRAY IN SEQUENTIAL ORDER

```

```

  T_FLUID_IN=XIN(1)
  FLOW_IN=XIN(2)
  T_AMB=XIN(3)
  T_SKY=XIN(4)
  WINDSPEED=XIN(5)
  GT=XIN(6)
  GH=XIN(7)
  GDH=XIN(8)
  RHO_GROUND=XIN(9)
  ANGLE_INC=XIN(10)
  SLOPE=XIN(11)
  U_BACK=XIN(12)
  U_EDGES=XIN(13)
  H_FLUID=XIN(14)
  P_ATM=XIN(15)

```

```

IF(MODE_U.GT.1) THEN
  U_TOP=XIN(16)
ELSE

```

```

        U_TOP=0.
    ENDIF
C-----
----

C-----
----

C CHECK THE INPUTS FOR PROBLEMS
  IF(FLOW_IN.LT.0.) CALL TYPECK(-3,INFO,2,0,0)
  IF(WINDSPEED.LT.0.) CALL TYPECK(-3,INFO,5,0,0)
  IF(GT.LT.0.) CALL TYPECK(-3,INFO,6,0,0)
  IF(GH.LT.0.) CALL TYPECK(-3,INFO,7,0,0)
  IF(GDH.LT.0.) CALL TYPECK(-3,INFO,8,0,0)
  IF(RHO_GROUND.LT.0.) CALL TYPECK(-3,INFO,9,0,0)
  IF(RHO_GROUND.GT.1.) CALL TYPECK(-3,INFO,9,0,0)
  IF(U_BACK.LT.0.) CALL TYPECK(-3,INFO,12,0,0)
  IF(U_EDGES.LT.0.) CALL TYPECK(-3,INFO,13,0,0)
  IF(H_FLUID.LE.0.) CALL TYPECK(-3,INFO,14,0,0)
  IF(P_ATM.LE.0.) CALL TYPECK(-3,INFO,15,0,0)
  IF(P_ATM.GT.5.) CALL TYPECK(-3,INFO,15,0,0)
  IF(U_TOP.LT.0.) CALL TYPECK(-3,INFO,16,0,0)
    IF(ERRORFOUND()) RETURN 1
C-----
----

C-----
----

C RETRIEVE THE VALUES IN THE STORAGE ARRAY FOR THIS ITERATION
C NITEMS=
C   CALL getStorageVars(STORED,NITEMS,INFO)
C   STORED(1)=
C-----
----

C-----
----

C CHECK THE INPUTS FOR PROBLEMS
C   IF(...) CALL TYPECK(-3,INFO,'BAD INPUT #',0,0)
C   IF(IERROR.GT.0) RETURN 1
C-----
----

C-----
----

C *** PERFORM ALL THE CALCULATION HERE FOR THIS MODEL. ***
C-----
----

```

```

C          ADD YOUR COMPONENT EQUATIONS HERE; BASICALLY THE
EQUATIONS THAT WILL
C          CALCULATE THE OUTPUTS BASED ON THE PARAMETERS AND THE
INPUTS.    REFER TO
C          CHAPTER 3 OF THE TRNSYS VOLUME 1 MANUAL FOR DETAILED
INFORMATION ON
C          WRITING TRNSYS COMPONENTS.

C  SET PI
PI=4*DATAN(1.D0)

C  CALCULATE THE AREA OF THE COLLECTOR
AREA=LENGTH*WIDTH

C  CALCULATE THE TUBE-TO-TUBE DISTANCE
W=WIDTH/DBLE(N_TUBES)

C  RETRIEVE THE TRANSMITTANCE ABSORPTANCE PRODUCT AT NORMAL
INCIDENCE AND THE REFLECTANCE TO DIFFUSE
RHO_DIFFUSE=OUT(13)
TAU_ALPHA_N=OUT(14)

C  GET THE INCIDENCE ANGLE MODIFIER
IF(N_COVERS.LT.1) THEN
    XKAT=1.

    ELSE

C  USE THE RELATIONS OF BRANDEMUEHL TO GET THE EFFECTIVE INCIDENCE
ANGLES FOR DIFFUSE RADIATION
EFFSKY=59.68-0.1388*SLOPE+0.001497*SLOPE*SLOPE
EFFGND=90.-0.5788*SLOPE+0.002693*SLOPE*SLOPE
COSSLOPE=DCOS(SLOPE*RDCONV)
FSKY=(1.+COSSLOPE)/2.
FGND=(1.-COSSLOPE)/2.
GDSKY=FSKY*GDH
GDGND=RHO_GROUND*FGND*GH

C  USE THE TAU_ALPHA FUNCTION FOR THE COMPONENT IAM VALUES
XKATDS=TAU_ALPHA(N_COVERS,EFFSKY,KL_COVER,REFR_INDEX,ABS_PLATE,
1  RHO_DIFFUSE)/TAU_ALPHA_N
XKATDG=TAU_ALPHA(N_COVERS,EFFGND,KL_COVER,REFR_INDEX,ABS_PLATE,

```

```

1  RHO_DIFFUSE)/TAU_ALPHA_N
XKATB=TAU_ALPHA(N_COVERS,ANGLE_INC,KL_COVER,REFR_INDEX,
1  ABS_PLATE,RHO_DIFFUSE)/TAU_ALPHA_N

C  CALCULATE THE OVERALL IAM
IF(GT.GT.0.) THEN
  XKAT=(XKATB*(GT-GDSKY-
GDGND)+XKATDS*GDSKY+XKATDG*GDGND)/GT
  ELSE
  XKAT=0.
  ENDIF
ENDIF

C  GUESS AN OUTPUT TEMPERATURE
T_FLUID_OUT=T_FLUID_IN

C  GUESS THE MEAN PLATE AND MEAN FLUID TEMPERATURES
T_PLATE_MEAN=(T_FLUID_IN+T_FLUID_OUT)/2.
C  T_PLATE_MEAN=100.
T_FLUID_MEAN=(T_FLUID_IN+T_FLUID_OUT)/2.

C  GUESS THE GLASS1 AND GLASS2 TEMPERATURES
T_GLASS1=T_PLATE_MEAN-5.
T_GLASS2=T_PLATE_MEAN-10.

C  INITIALIZE A FEW VARIABLES
ICOUNT=1
T_FLUID_OUT_OLD=T_FLUID_OUT
T_GLASS1_OLD=T_GLASS1
T_GLASS2_OLD=T_GLASS2

C  SET THE TOP LOSS COEFFICIENT
100 IF(MODE_U.EQ.1) THEN

C  SET THE TOP LOSS FROM CONVECTION AND RADIATION
IF(N_COVERS.LT.1) THEN

  P_KPA=P_ATM*101.325
  T_K=T_AMB+273.15
  CALL WINDCOEF(WINDSPEED,LENGTH,WIDTH,T_K,P_KPA,H_CONV)
  H_CONV=H_CONV*3.6 !CONVERT W/M2/K TO KJ/H/M2.K

  H_RAD=H_RADIATION(T_PLATE_MEAN,T_SKY,EMISS_PLATE)
  U_TOP=H_CONV+H_RAD

C  USE KLEIN'S TOP LOSS CORRELATION

```

```

ELSE

LENGTH=PAR(1)
WIDTH=PAR(2)
THICK_ABSORBER=PAR(3)
K_ABSORBER=PAR(4)
N_TUBES=JFIX(PAR(5)+0.5)
DIA_TUBE_I=PAR(6)
DIA_TUBE_O=PAR(7)
R_BOND=PAR(8)
CP_FLUID=PAR(9)
ABS_PLATE=PAR(10)
EMISS_PLATE=PAR(11)
MODE_U=JFIX(PAR(12)+0.5)
N_COVERS=JFIX(PAR(13)+0.5)
REFR_INDEX=PAR(14)
KL_COVER=PAR(15)
EMISS_GLASS=PAR(16)
DIS_PG1=PAR(17)
DIS_G1G2=PAR(18)

T_FLUID_IN=XIN(1)
FLOW_IN=XIN(2)
T_AMB=XIN(3)
T_SKY=XIN(4)
WINDSPEED=XIN(5)
GT=XIN(6)
GH=XIN(7)
GDH=XIN(8)
RHO_GROUND=XIN(9)
ANGLE_INC=XIN(10)
SLOPE=XIN(11)
U_BACK=XIN(12)
U_EDGES=XIN(13)
H_FLUID=XIN(14)
P_ATM=XIN(15)

C    SET THE MEAN FLUID TEMPERATURE
      P_KPA=P_ATM*101.325
      T_K=T_AMB+273.15

      IF (GT.GE.50.) THEN
        CALL WINDCOEF(WINDSPEED,LENGTH,WIDTH,T_K,P_KPA,H_CONV)

      HR_PC1=H_RAD_GRAY(T_PLATE_MEAN,T_GLASS1,EMISS_PLATE,
1      EMISS_GLASS)/3.6

```

```

HR_C1C2=H_RAD_GRAY(T_GLASS1,T_GLASS2,EMISS_GLASS,
1      EMISS_GLASS)/3.6
HR_C2A=H_RADIATION(T_GLASS2,T_SKY,EMISS_GLASS)*
1      DABS(T_GLASS2-T_SKY)/DABS(T_GLASS2-T_AMB+1.D-3)/3.6

      T_PG1=(T_PLATE_MEAN+T_GLASS1)/2.+273.15
      T_G1G2=(T_GLASS1+T_GLASS2)/2.+273.15
      DELTA_TPG1=DABS(T_PLATE_MEAN-T_GLASS1)
      DELTA_TG1G2=DABS(T_GLASS1-T_GLASS2)

      CALL AIRPROP(T_PG1,P_KPA,AIRPROPS)
      K_VISC=AIRPROPS(2)
      THERM_COND=AIRPROPS(4)
      PRAND_N=AIRPROPS(3)

      RAYLEIGH_PG1=RAYLEIGH_NUM(T_PG1,DELTA_TPG1,DIS_PG1,K_VISC,
1      PRAND_N)
      NUSSELT_PG1=NUSSELT_NUM(RAYLEIGH_PG1,SLOPE)
      H_CONV_PG1=H_CONVECTION(NUSSELT_PG1,THERM_COND,DIS_PG1)

      CALL AIRPROP(T_G1G2,P_KPA,AIRPROPS)
      K_VISC=AIRPROPS(2)
      THERM_COND=AIRPROPS(4)
      PRAND_N=AIRPROPS(3)

      RAYLEIGH_G1G2=RAYLEIGH_NUM(T_G1G2,DELTA_TG1G2,DIS_G1G2,
1      K_VISC,PRAND_N)
      NUSSELT_G1G2=NUSSELT_NUM(RAYLEIGH_G1G2,SLOPE)

H_CONV_G1G2=H_CONVECTION(NUSSELT_G1G2,THERM_COND,DIS_G1G2)

      U_TOP=1/(H_CONV_PG1+HR_PC1)+1/(H_CONV_G1G2+HR_C1C2)+
1      1/(H_CONV+HR_C2A+1.D-3)
      U_TOP=1/U_TOP

      T_GLASS1=T_PLATE_MEAN-U_TOP*(T_PLATE_MEAN-T_AMB)/
1      (H_CONV_PG1+HR_PC1)
      T_GLASS2=T_GLASS1-U_TOP*(T_PLATE_MEAN-T_AMB+1.D-3)/
1      (H_CONV_G1G2+HR_C1C2)

      U_TOP=U_TOP*3.6
ENDIF

      ENDIF

      ELSE

```

```

    U_TOP=XIN(16)

    ENDIF

C  SET THE OVERALL LOSS COEFFICIENT
U_L=U_TOP+U_BACK+U_EDGES
  IF(U_L.LE.0.) THEN
    CALL MESSAGES(-1,MESSAGE1,'FATAL',IUNIT,ITYPE)
    RETURN 1
  ENDIF

C  SET SOME REQUIRED VARIABLES
M=(U_L/K_ABSORBER/THICK_ABSORBER)**0.5
  F=DTANH((M*(W-DIA_TUBE_O)/2.))/(M*(W-DIA_TUBE_O)/2.)
X=1./(U_L*(DIA_TUBE_O+(W-DIA_TUBE_O)*F))+R_BOND+
  1  1./PI/DIA_TUBE_I/H_FLUID

C  SET THE COLLECTOR EFFICIENCY FACTOR
  F_PRIME=1./U_L/W/X

C  CALCULATE THE COLLECTOR HEAT REMOVAL FACTOR
IF(FLOW_IN.LE.0.) THEN
  FR=0.
ELSE
  FR=FLOW_IN*CP_FLUID/AREA/U_L*(1.-DEXP(-AREA*U_L*F_PRIME/
  1  FLOW_IN/CP_FLUID))
ENDIF

C  CALCULATE THE COLLECTOR USEFUL ENERGY GAIN
QU=AREA*FR*(GT*TAU_ALPHA_N*XKAT-U_L*(T_FLUID_IN-T_AMB))

C  CALCULATE THE COLLECTOR OUTLET TEMPERATURE
IF (FLOW_IN.LE.0.) THEN

  T_FLUID_OUT=GT*XKAT*TAU_ALPHA_N/U_L+T_AMB

  T_PLATE_MEAN=T_FLUID_OUT
  T_FLUID_MEAN=T_FLUID_OUT

C  IF ((T_PLATE_MEAN-T_AMB).LE.0.) THEN
  IF (GT.LE.50.) THEN
    T_PLATE_MEAN_OLD=T_PLATE_MEAN

    P_KPA=P_ATM*101.325
    T_K=T_AMB+273.15
    CALL WINDCOEF(WINDSPEED,LENGTH,WIDTH,T_K,P_KPA,H_CONV)

```

```

150   T_PLATE_MEAN=T_AMB-EMISS_GLASS*5.67D-8*((T_PLATE_MEAN+273.15)
1     **4-(T_SKY+273.15)**4)/H_CONV
      IF (DABS(T_PLATE_MEAN-T_PLATE_MEAN_OLD).GT.0.001) THEN
          T_PLATE_MEAN_OLD=T_PLATE_MEAN
          GOTO 150
      ENDIF

      H_CONV=H_CONV*3.6
      T_GLASS1=T_PLATE_MEAN
      T_GLASS2=T_PLATE_MEAN

      T_FLUID_OUT=(T_PLATE_MEAN+T_AMB)/2.
      T_FLUID_MEAN=T_PLATE_MEAN

      Q_TOP=AREA*H_CONV*(T_AMB-T_GLASS2)
      Q_BACK=AREA*U_BACK*(T_PLATE_MEAN-T_AMB)
      Q_EDGES=AREA*U_EDGES*(T_PLATE_MEAN-T_AMB)
      ENDIF

      ELSE
          T_FLUID_OUT=T_FLUID_IN+QU/FLOW_IN/CP_FLUID
          FPP=FR/F_PRIME
          T_FLUID_MEAN=T_FLUID_IN+QU/AREA*(1.-FPP)/FR/U_L
          T_PLATE_MEAN=T_FLUID_IN+QU/AREA*(1.-FR)/FR/U_L

          Q_TOP=AREA*U_TOP*(T_PLATE_MEAN-T_AMB)
          Q_BACK=AREA*U_BACK*(T_PLATE_MEAN-T_AMB)
          Q_EDGES=AREA*U_EDGES*(T_PLATE_MEAN-T_AMB)

      ENDIF

C   SEE IF CONVERGENCE HAS BEEN REACHED
IF((ICOUNT.LT.200).AND.(DABS(T_FLUID_OUT_OLD-T_FLUID_OUT
1  ).GT.0.001).AND.(DABS(T_GLASS1_OLD-T_GLASS1).GT.0.001).
1  AND.(DABS(T_GLASS2_OLD-T_GLASS2).GT.0.001)) THEN
      ICOUNT=ICOUNT+1
      T_FLUID_OUT_OLD=T_FLUID_OUT
      T_GLASS1_OLD=T_GLASS1
      T_GLASS2_OLD=T_GLASS2
      GOTO 100
  ENDIF

C   WARN THE USER IF CONVERGENCE HAS NOT BEEN OBTAINED
IF(ICOUNT.GE.50) THEN
      CALL MESSAGES(-1,MESSAGE2,'WARNING',IUNIT,ITYPE)
  ENDIF

```

```

C-----
----

C-----
----

C-----
----

C  SET THE STORAGE ARRAY AT THE END OF THIS ITERATION IF NECESSARY
C  NITEMS=
C  STORED(1)=
C    CALL setStorageVars(STORED,NITEMS,INFO)
C-----
----

C-----
----

C  REPORT ANY PROBLEMS THAT HAVE BEEN FOUND USING CALLS LIKE THIS:
C  CALL MESSAGES(-1,'put your message here','MESSAGE',IUNIT,ITYPE)
C  CALL MESSAGES(-1,'put your message here','WARNING',IUNIT,ITYPE)
C  CALL MESSAGES(-1,'put your message here','SEVERE',IUNIT,ITYPE)
C  CALL MESSAGES(-1,'put your message here','FATAL',IUNIT,ITYPE)
C-----
----

C-----
----

C  SET THE OUTPUTS FROM THIS MODEL IN SEQUENTIAL ORDER AND GET OUT

OUT(1)=T_FLUID_OUT
OUT(2)=FLOW_IN
OUT(3)=QU
  OUT(4)=F_PRIME
  OUT(5)=FR
  OUT(6)=Q_TOP
  OUT(7)=Q_BACK
  OUT(8)=Q_EDGES
  OUT(9)=T_FLUID_MEAN
  OUT(10)=T_PLATE_MEAN
  OUT(11)=XKAT
  OUT(12)=U_L
  OUT(13)=RHO_DIFFUSE
  OUT(14)=TAU_ALPHA_N
  OUT(15)=T_GLASS1
  OUT(16)=T_GLASS2

```

```
C-----  
----  
C  EVERYTHING IS DONE - RETURN FROM THIS SUBROUTINE AND MOVE ON  
  RETURN 1  
  END  
C-----  
----
```


DISTRIBUTION

Internal distribution:

1 MS0899 Technical Library 9536 (*electronic copy*)

